

**Analysis of long term groundwater dispersal of  
contaminants from proposed Jabiluka Mine  
tailings repositories**

**Jabiluka Technical Review**

**Groundwater Hydrology**

**Report prepared for the Supervising Scientist**

**March 1999**

**Dr F Kalf** B.Sc, M App Sc, Ph D, Cert Eng Hyd

**Prof C Dudgeon** M E, Ph D ,CP Eng, MIE Aust, MASCE

# Contents

Executive Summary	viii
1 Introduction	1
1.1 Background	1
1.2 Brief and objectives	1
2 Methodology and approach	1
3 Topography, drainage and climate	2
4 Hydrogeology	2
4.1 Geology	2
4.2 Groundwater system	3
4.3 Groundwater quality	5
4.4 Groundwater – flow directions and dynamics	7
5 Proposed tailings repositories	8
5.1 Previous proposals	8
5.2 Proposed silo storage bank	8
5.3 Mine void storage	8
6 Tailings characteristics	8
6.1 Comparison with Ranger Mine tailings	8
6.2 Proposed paste disposal and properties	8
6.3 Potential contaminants	9
6.4 Mobilisation of potential contaminants	11
7 Analysis of contaminant movement	12
7.1 General principles	12
8 Modelling approach	14
8.1 General	14
8.2 The hybrid model	14
8.3 Contaminant characteristics	15
9 Groundwater flow system – numerical 2D model	16
9.1 Model mesh and boundary conditions	17
10 Solute transport – analytical model	18
10.1 Description	18
10.2 Model assumptions	18

10.3 Monte-Carlo simulation	18
11 Summary and discussion of results	21
11.1 General comments	21
11.2 Discussion of specific findings	22
12 Potential for contamination of the wetlands	23
13 Conclusions	24
14 Recommendations	27
References	28
Figures	30
Appendix A Domenico-Palciauskas-Robins Analytical Solute Transport Equation	57

## Tables

Table 1  $K_d$  Distribution coefficient (mL/g) values from batch experiments (Moody 1982)

Table 2 Range of estimated retardation factors for uranium in the non-weathered Kombolgie and Cahill formations

Table 3 Range of estimated retardation factors for Radium 226 in the non-weathered Kombolgie and Cahill formations

Table 4 Parameter ranges used in the Monte Carlo analysis for non-reactive transport

Table 5 Additional parameters for uranium transport

Table 6 Additional parameters for Radium 226 transport

## Figures

Figure 1 Site area key features and model section A-B-C

Figure 2 Site topography and key features

Figure 3 Model section A-B-C – hydrogeological units surface and sub surface features

Figure 4 Advection-Dispersion-Retardation

Figure 5 Model finite element mesh section A-B-C and boundary conditions

Figure 6 Steady state heads – section A-B-C

Figure 7 Groundwater flow through silo bank and assumed source plane

Figure 8 Groundwater flow – mine void and assumed source plane

Figure 9a Non-reactive contaminant – Monte-Carlo simulations relative concentrations – silo bank – 255 realizations

Figure 9b Non-reactive contaminant – Monte-Carlo simulations median relative concentration – silo bank - 255 realizations

Figure 9c Non-reactive contaminant – Monte-Carlo simulations median relative concentration – silo bank – 500 realizations

Figure 9d Non-reactive contaminant – Monte-Carlo simulations median relative concentration – silo bank – 1000 realizations

Figure 9e Non-reactive contaminant Monte-Carlo simulations relative concentration – silo bank – source plane decay – 255 realizations

Figure 10a Uranium Monte-Carlo simulations relative concentrations silo bank – 255 realizations

Figure 10b Uranium Monte-Carlo simulations median relative concentrations silo bank – 255 realizations

Figure 11a Radium 226 Monte-Carlo simulations relative concentrations silo bank – 255 realizations

Figure 11b Radium 226 Monte-Carlo simulations median relative concentration – silo bank – 255 realizations

Figure 12a Non-reactive contaminant – Monte-Carlo simulations relative concentrations – mine void fill - 255 realizations

Figure 12b Non-reactive Ccontaminant – Monte-Carlo simulations median relative concentrations – mine void fill – 255 realizations

Figure 13a Uranium contaminant – Monte-Carlo simulations – relative concentrations – mine void fill - 255 realizations

Figure 13b Uranium contaminant – Monte-Carlo simulations – median relative concentrations – mine void fill – 255 realizations

Figure 14a Radium 226 contaminant uranium Monte-Carlo simulations – normalized C/Co median concentration – 500 realizations

Figure 14b Radium 226 contaminant – Monte-Carlo simulations – median relative concentrations – mine void fill – 255 Realizations

# Appendices

## Appendix A

Domenico-Palciauskas-Robins Analytical Solute Transport Equation

Figure A-1 Analytical model migration geometry and spreading directions

## Appendix B

Simulation of leaching of non-reactive and radionuclide contaminants from proposed Jabiluka silo banks.

### Figures

- Figure B-1 Silo/Aquifer Head and Velocity Vectors  
Ks=0.001(m/d); Ka=0.01(m/d) – Gradient 0.03-Steady State
- Figure B-2 Silo/Aquifer Head and Velocity Vectors  
Ks=1e-5(m/d); Ka=0.01(m/d) – Gradient 0.03-Steady State
- Figure B-3a Silo/Aquifer Concentration % – non-reactive contaminant  
Ks=1e-4(m/d); Ka=0.01(m/d) – Gradient –Pa=5%; Ps=10%; 200 yrs
- Figure B-3b Concentration % Profile – Row 25 – non-reactive – 200 yrs
- Figure B-3c Concentration % Profile – Col 36 - non-reactive – 200 yrs
- Figure B-4a Silo/Aquifer Concentration % – non-reactive contaminant  
Ks=1e-5(m/d); Ka=0.01(m/d) – Gradient –0.03 -Pa=5%; Ps=10%; 200 yrs
- Figure B-4b Concentration % Profile –Row 25 – non-reactive – 200 yrs
- Figure B-4c Concentration % Profile –Col 36 – non-reactive – 200 yrs
- Figure B-5a Silo/Aquifer Concentration % – non-reactive contaminant  
Ks=1e-4(m/d); Ka=0.01(m/d) – Gradient –0.03 -Pa=5%; Ps=10%; 200 yrs
- Figure B-5b Concentration % Profile –Row 1 – non-reactive – 200 yrs
- Figure B-5c Concentration % Profile – non-reactive – Col 66 – 200 yrs
- Figure B-6a Silo/Aquifer Concentration % – non-reactive contaminant
- Figure B-6b Concentration % Profile –Row 1 – non-reactive – 200 yrs
- Figure B-6c Concentration % Profile –Col 66 – non-reactive – 200 yrs
- Figure B-7a Silo/Aquifer Concentration % – Uranium  
Ks=1e-4(m/d); Ka=0.01(m/d) – Gradient –0.03 - Pa=5%; Ps=10% - 1000 yrs; Rf=21
- Figure B-7b Concentration % Profile – Row 1 – Uranium – 1000 yrs – Rf=21
- Figure B-7c Concentration % Profile – Column 66 – Uranium – 1000 yrs – Rf=21
- Figure B-8a Silo/Aquifer Concentration % – Radium 226  
Ks=1e-4(m/d); Ka=0.01(m/d) - Gradient 0.03 -Pa=5%; Ps=10% - 1000 yrs;  
Rf=200a;100s

- Figure B-8b Concentration % Profile – Row 1 – Radium 226-1000 yrs; Rf=201a,101s
- Figure B-8c Concentration % Profile – Col66 – Radium 226-1000 yrs-Rf=201a,101s
- Figure B-9 Assumed Fault/Fracture Zone
- Figure B-10a Silo/Aquifer Concentration % – non-reactive contaminant  
 $K_s=1e-4(m/d)$ ;  $K_a=0.01(m/d)$  - Gradient 0.03 -  $P_a=5\%$ ;  $P_s=10\%$  - 200 yrs-Fault  
 $K_f=0.5m/day$
- Figure B-10b Concentration % Profile – Row 1 – non-reactive 200 yrs with Fault
- Figure B-10c Concentration % Profile – Col 66 – non-reactive 200 yrs with Fault
- Figure B-10d Concentration % Profile – Row 30 – non-reactive 200 yrs fault opposite
- Figure B-11a Silo/Aquifer Concentration % – Uranium  
 $K_s=1e-4(m/d)$ ;  $K_a=0.01(m/d)$  - Gradient 0.03 -  $P_a=5\%$ ;  $P_s=10\%$  - 1000 yrs-Fault  
 $K_f=0.5m/day$ ;  $R_f=21$
- Figure B-11b Concentration % Profile – Row 1 – Uranium – 1000 yrs with Fault
- Figure B-11c Concentration % Profile – Col 66 – Uranium – 1000 yrs with Fault
- Figure B-11d Concentration % Profile – Row 30 – Uranium – 1000 yrs with Fault
- Figure B-12a Silo/Aquifer Concentration % – non-reactive contaminant  
 $K_s=1e-3(m/d)$ ;  $K_a=0.01(m/d)$  - Gradient 0.03- $P_a=5\%$ ;  $P_s=10\%$ -200 yrs
- Figure B-12b Concentration % Profile – Row 1 – non-reactive – 200 yrs
- Figure B-12c Concentration % Profile – Col 66 – non-reactive – 200 yrs

# Executive Summary

The Jabiluka project area lies within a 73 km<sup>2</sup> mining lease near the edge of Kakadu National Park, a World Heritage area of approximately 19 800 km<sup>2</sup>. Existing approvals require all tailings to be disposed of underground. The current proposal is to add cement to the partially dewatered tailings to form a paste which would be deposited and allowed to set in the underground mine voids and specially excavated underground silos.

Fears have been expressed that the park will suffer long term adverse effects as a result of the mining operation. Contamination of groundwater is one possibility to be considered.

This report describes and gives the results of an investigation into the movement of the potential contaminants magnesium sulphate, manganese, radium and uranium from mine tailings by groundwater flow towards the park after disposal of tailings underground in the mine voids and silos. The proposed silos would be constructed to hold the balance of the tailings which could not be accommodated in the mine workings. The tops of the silos would be approximately 100 m below ground surface. Tailings stored in mine voids would have an even greater average cover, with a minimum of approximately 90 m.

Groundwater flow in the vicinity of the mine is topographically controlled. A relatively high mean annual rainfall of about 1500 mm, which occurs mainly in the annual Wet seasons, and relatively low permeability of the sandstone hills surrounding the mine site maintain, high water table levels in the hills. Both surface water and groundwater drainage is from the hills towards the major valleys which run approximately east and west from the surface water divide which is located near the mine site. Groundwater flow in both of these directions eventually reaches the Magela floodplain in Kakadu National Park. The westward flow towards the floodplain follows the general line of Mine Valley. The eastward flow must turn north to follow the course of Swift Creek and flow further before it can reach the floodplain.

Groundwater flow and consequent contaminant transport from the mine site towards the Magela floodplain has been modelled to predict the concentrations of contaminants to be expected along the flow paths. The availability of data on aquifer properties and the nature of the drainage pattern led to the use of a two dimensional finite element numerical model of flow along the paths described above. A three dimensional numerical solute transport model applied in a single layer was used to predict relative concentrations along the flow paths of contaminants leached from the tailings repositories. An analytical contaminant transport model was used in conjunction with a numerical model to determine the effects of advection, dispersion and retardation on contaminant movement away from the tailings storages. Monte Carlo simulations were used to determine concentration profiles over a range of relevant variables. The hybrid model was run for the equivalent of 1 000 years in the case of radium and uranium and 200 years for other contaminants.

Predicted median relative contaminant concentration versus distance curves for flow east from the tailings silos can be seen in figure 9d for non-reactive contaminants, figure 10b for uranium and figure 11b and 11d for radium 226. Corresponding results for flow west from the mine voids repository can be seen in figures 12b, 13b, 14b and 14d. The distances to negligible concentration are greater to the west than to the east because of higher permeability west of the mine and consequent higher velocity groundwater flow in that direction. However, it will be seen that even after 1 000 years the median predicted concentration of uranium 200 m west of the source is negligible. The range of concentration versus distance curves resulting from the Monte Carlo simulations can be seen in figures 9a, 10a, 11a and 11c for movement of non-reactive contaminants, uranium and radium 226

respectively for movement east from the silos. Corresponding figures for movement west of the mine voids storage are 12a, 13a, 14a and 14c.

Extreme curves of very low probability show that east of the mine no significant concentration of any contaminant is likely beyond a few hundred metres for radioactive contaminants and one kilometre for non-reactive contaminants.

The results indicate that west of the mine it is possible, although improbable, that significant concentrations of uranium and radium could occur in groundwater about one kilometre from the mine. For non-reactive contaminants such as magnesium sulphate, the distance could be several kilometres. However, in this case the contaminated groundwater would be entering an area of known poor water quality and could not be considered to have a significant adverse effect on the water quality.

Weak upward components of groundwater flow are indicated both east and west of the mine. It is considered that any such flow which reaches the shallow alluvial or weathered rock zone will be diluted and flushed away by the annual surficial Wet season flows.

The overall conclusion is that underground storage of tailings will not have any significant adverse effect on Kakadu Park as a result of leaching by groundwater of contaminants from the tailings provided a permeability of  $10^{-4}$  m/day of the set tailings paste is achieved. A target of  $10^{-5}$  m/day would be preferable.

# 1 Introduction

## 1.1 Background

Energy Resources Australia (ERA) is proposing to mine a uranium deposit at Jabiluka in the Northern Territory, Australia. The proposed Jabiluka mine site is about 230 km east of Darwin and 20 km north of the existing Ranger Uranium Mine. It is situated within a 73 km<sup>2</sup> mineral lease near the edge of, but surrounded by, the Kakadu National Park (fig 1). The mine will be underground and accessed by a decline from the surface. The area to be occupied by the mine facilities is 27 ha (0.27 km<sup>2</sup>).

ERA is currently proposing to mine and mill the ore at Jabiluka. This option, known as the Jabiluka Mill Alternative (JMA), will involve storage of mill tailings in deep sub-surface repositories. These repositories are to include the voids created during mining of the orebody and about 180 specially constructed vertical cylindrical silos, 20 m in diameter, up to 135 m long (vertically), situated with their tops about 100 m below ground level.

## 1.2 Brief and objectives

As a result of the UNESCO World Heritage Committee Delegation to Australia and its recommendations, various aspects of the JMA are to be reviewed by a team of experts. In January 1999 the Supervising Scientist, requested specific studies be completed regarding groundwater issues at the site. These issues concern the possible dispersal of contaminants from the proposed buried tailings in the repositories into the surrounding groundwater system. Specifically the issues that needed to be addressed were:

The likely extent of movement from the tailings repositories of magnesium sulphate, manganese, radium and uranium.

The effect on contaminant mobility and, as a consequence, on possible surface water contamination, of adding cement to the tailings to form a paste designed to solidify in the repositories.

Quantification of contaminant concentrations for extreme situations (ie a major fracture or fault intersecting a silo or filled mining stope), and the probability of such a condition.

Assessment of the effects of spatial location (eg in schist or sandstone) and elevation of tailings storage silos on possible surface water contamination.

Providing predicted contaminant concentration values for water between the mine and the adjacent Magela floodplain to be used for toxicological risk assessment to be completed by others.

## 2 Methodology and approach

Given the limited available data and time, the approach used in this report to address these issues has been pragmatic. Where possible, use is made of existing information on aquifer and contaminant characteristics, but where this information is lacking we have used data available in the literature. Both analytical and numerical models have been used in a hybrid approach in conjunction with a stochastic method (Monte Carlo simulation) to determine the leaching characteristics and range of possible contaminant movement, and where possible, we have erred on the side of conservatism.

Whilst the assessment in this report provides a better understanding of the leaching mechanism and attempts to answer the issues raised, we believe that the material presented can only be considered as a ‘first pass’. Thus, this report should therefore be viewed as a screening analysis in its scope. It is clear that more detailed data need to be obtained and, specifically, more complete regional numerical model setups need to be established to reproduce as far as possible the actual field situation both in the entire silo bank area and the tailings filled orebody void.

To verify assumptions that have been made in this report, laboratory and possibly field studies need to be carried out on the physical properties and the adsorption/precipitation and leaching characteristics of the proposed tailings paste material. Paste set, strength, plasticity, porosity, permeability and contaminant fixation/mobility of pastes made from uranium ore tailings need investigation. It is understood that some of this work will be carried out on behalf of ERA in the near future.

Further recommendations on all of these aspects are provided later in the report.

### **3 Topography, drainage and climate**

The Jabiluka mine site is situated in hilly terrain surrounded by undulating to flat terrain along the Magela floodplain with elevations ranging between several metres along the floodplain to 160 m AHD (1160 m Mine RL)<sup>1</sup>. The hilly terrain forms an approximate north-south broad ridge which includes the Jabiluka outlier and northern outcrop. The ridge is intersected in an east-west direction by numerous drainage gullies/creeks situated on either side of the topographic divide (fig 1). The top of the ore-body is located below a broad, shallow valley, known as Mine Valley, carved from the surrounding quartz sandstone (fig 2). Surface water drainage in Mine Valley is towards the Magela floodplain, which lies about 1.5 km to the west of the topographic divide which separates Mine Valley from the Swift Creek catchment.

On the eastern side of the divide, surface water flows eastward towards Swift Creek which joins the Magela floodplain several kilometers north of the orebody (fig 1).

The region is subject to annual Wet and Dry seasons. It has an average yearly rainfall of about 1500 mm. Monthly average rainfall increases steadily from near zero in September to a peak in January/February (approximately 370 mm in each month) and decreases rapidly to near zero again in June.

## **4 Hydrogeology**

### **4.1 Geology**

The detailed geology of the area is described in the Jabiluka Project EIS (Kinhill & ERAES 1998).

In summary, the Jabiluka orebody No 2 to be mined is contained within the Cahill Formation which is mostly schist but includes some carbonate. To the west, the Cahill formation underlies the Magela floodplain and forms the bedrock which dips east and south beneath the overlying Kombolgie Formation.

---

<sup>1</sup> In this report all elevations referred to are Mine RL's unless stated otherwise. Mine RL is obtained by adding 1000 m to the AHD values.

The Kombolgie Formation is comprised mainly of quartz sandstone with a little siltstone and forms the broad north-south topographic ridge across the site and terrain further east. Most of the sandstone is better described as quartzite because of the deposition of secondary silica, although some relatively friable layers do occur. The intergranular porosity is very low and the groundwater flow at the mine site is restricted mainly to the joint and fracture system. Inspection of the decline being constructed to gain access to the orebody showed appreciable groundwater inflow only at one fracture zone. Most of the other joints were dry.

Along the Magela floodplain, clays (generally dark organic overlying grey), silts and sandy alluvial sediments overlie the Cahill Formation. The bedrock in contact with the sediments is weathered.

Immediately east and west of the topographic divide the weathered bedrock in the lower drainage valley slopes is overlain by sands and silts. Drilling has revealed that weathered bedrock can occur up to 50 m below ground surface.

Strongly developed lineaments comprising joints/fracture systems in the sandstone are evident from aerial photographs of the Jabiluka outlier and the elevated sandstone outcrop north of orebody No 2. These structures strike at 60 to 80 degrees with another less dominant set at 350 degrees. The structural lineaments are less well defined in Mine Valley; however, it is possible that Mine Valley may have formed along zones of rock weakness created initially in the past by one or a number of these structures that have now been filled in with weathered material.

Other structural features include the Hegge fault that dissects the orebody and a pegmatite dyke that crosses the western part of the ore-body (fig 2).

## **4.2 Groundwater system**

### **4.2.1 Sub-surface water-bearing zones**

A hydrogeological section based on that given by Milnes et al (1998) is shown in figure 3. The orientation and extent of this section is given in figure 1 (shown as A-B-C). The section extends from the Magela floodplain in the west across the site through the orebody, the topographic ridge, Swift Creek, and then north until it reaches a branch of the Magela floodplain.

Note that the orebody and tailings silos shown in figure 3 are included to show approximately their locations in the section. The tops of the orebody and silos should not be scaled from the figure. The orebody height varies greatly on either side of the section being used to represent the two dimensional flow and the height drawn is between the upper RL of approximately 958 and lower limits, some undetermined. Under the existing mine plan ore will be extracted down to RL 650 m. The current proposal for the silos is for their tops to be at about the top of the RL 955 mine level so they are shown at approximately RL 960.

There are four main sub-surface water-bearing zones with essentially different hydraulic characteristics within this section at Jabiluka. They include:

- A shallow sandy aquifer overlying weathered bedrock in Mine Valley and east of the topographic divide.
- A weathered bedrock aquifer.
- A deeper fractured rock aquifer.
- Floodplain non-indurated sediments.

The shallow aquifer is contained within topographic valley catchments carved into the surrounding Kombolgie Sandstone to the west (ie Mine Valley) and to the east (Swift Creek and its tributaries). According to Foley, this aquifer is comprised of sands and silts up to about 13 m in thickness (ERAES 1998).

Beneath this aquifer lies the weathered bedrock which extends down tens of metres below the upper aquifer within the drainage valleys.

The deeper aquifer comprises essentially fractured Kombolgie quartz sandstone over most of the area and schists and carbonates of the Cahill Formation further west.

The Magela floodplain sediments consist largely of organic clays and silts with prior stream channels of sand and silt.

#### **4.2.2 Permeability**

Seven holes were drilled in the Mine Valley area west of the topographic and groundwater divide (fig 2). These holes were percussion drilled to below the contact between the sandstone and underlying schist, and then diamond drilled to their respective total depths (AGC-Woodward Clyde 1993). Recorded airlift yields were in the range 5 to 30 kL/day (0.06 L/sec to 0.35 L/sec), although bore T132V recorded 120 kL/day (1.4 L/sec). The main water bearing zones encountered were at the contact between the Cahill Formation schists and Kombolgie sandstone and in the lower sections of the sandstone. The report indicates a transmissivity of 1 m<sup>2</sup>/day at bore T132V, whilst at Bore V120V the transmissivity is given in the range 0.01 to 0.1 m<sup>2</sup>/day. Foley (ERAES 1998) has estimated the permeability for the sandstone/schist to be in the range 0.017 to 0.1 m/day in this area.

Drilling in Mine Valley in 1996 also indicated transmissive zones in the shallow carbonates in the Cahill Formation further west, with one bore having a transmissivity of 8 m<sup>2</sup>/day (hole V081V). Hole U111V also encountered carbonates and was tested at 280 m<sup>3</sup>/day giving a transmissivity of 5 m<sup>2</sup>/day, (ERAES 1998). These carbonates lie between the Jabiluka No 1 and No 2 orebody (fig 2). Foley (ERAES 1998) has estimated permeability from these results to be in the range 0.08 to 0.2 m/day in the carbonate/schist.

East of the divide, seven bores drilled to 15 m above the schist and sandstone contact gave only minor water airlift flows. These were too small to be measured accurately (AGC-Woodward Clyde 1993).

From a number of bores constructed east of the divide Foley (ERAES 1998) has reported yields of between 0.5 to 1.5 L/sec from the weathered shallow aquifer between the mine portal and Swift Creek with corresponding permeabilities in the range 10<sup>-3</sup> m/day to 1.2 m/day. The report indicates permeabilities in the range 3 x 10<sup>-2</sup> m/day to 3 x 10<sup>-4</sup> m/day for the lower sections of the Kombolgie Sandstone in this area.

A 30 m wide pegmatite dyke which crosses the western part of the orebody and dips 80 degrees to the east is referred to in the ERA report (ERAES 1998), but no specific hydraulic testing has been conducted on it. However the report does indicate that testing in bore U111V demonstrated partial boundary effects in observation bores on the opposite side of the dyke.

#### **4.2.3 Porosity**

There is no specific data on porosity on the fractured rocks at the proposed Jabiluka site. However, comparisons can be made with other site areas in the literature with similar rock types to obtain a possible range of values that can be used in this study.

DeWeist (1966) for example indicates porosities in weathered igneous and metamorphic fractured rock of up to 35%, and suggests porosity of non-weathered fractured rock in the range 2% to 10%. Freeze (1979) notes non-fractured samples of igneous and metamorphic rock have porosities rarely greater than 2%. He quotes a fractured weathered or brecciated Yakima basalt having a permeability of  $10^{-4}$  to 1 m/day having a porosity of 10%. A tabulated list of porosities in Spitz and Moreno (1996) indicates porosity in fractured dolomite in the range 7% to 18% and fractured granite in the range 2% to 8%.

The quoted values of porosity for sandstone in these references generally have high values at the top end of the ranges. However, at Jabiluka these higher values are probably not relevant except at shallower depths where weathering is extensive. Diamond drill cores inspected at the Jabiluka site showed that at depth there is little weathering and few open fractures. There is no doubt that the large scale jointing evident on the land surface and in the decline under construction will persist at depth. There will also be smaller scale fractures. However the evidence points to the fractures being tightly closed at depth. For the most part, at depth, the sandstone is highly silicified with virtually no inter-granular porosity or permeability. Overall, the evidence indicates that the sandstone has relatively low bulk porosity and permeability.

In the absence of further data on the Jabiluka sandstone and schist, bulk effective porosities are conservatively estimated to be in the range 0.5% to 5% for fractured rock at depth, and up to 10% for weathered rock<sup>2</sup>.

### 4.3 Groundwater quality

Deutscher et al (1980) have described the broad geochemistry of the Jabiluka area. In their investigation during the 1976 and 1978 Dry seasons, 17 exploration holes were drilled in the vicinity of the Jabiluka No 1 and 2 ore bodies. These holes penetrated both the Kombolgie Formation sandstone and underlying Cahill Formation schists and were logged for Eh-pH and conductivity at 5 metre intervals to a depth of 195 metres below ground surface. In addition 47 water samples were also collected and analyzed from both exploration bores and auger holes constructed on the Magela floodplain and at two nearby billabongs. All samples were reportedly collected 'just below the watertable'. The general location of the groups of boreholes in which water levels and/or water quality have been measured are shown in figure 2. It will be observed that they are in three groups. One is west of the mine site in the Magela floodplain, another is at the orebody, and the third is east of the orebody near the site of the mine's surface facilities in the Swift Creek catchment. Several holes mentioned specifically in the text are marked (eg V081V).

For the 17 exploration holes drilled, analysis indicated that beyond a depth of 5 m from the surface, conductivity was in the range 620 to 680  $\mu\text{S}/\text{cm}$ , pH was between 7.1 and 7.6 and Eh was between +60 and +150 mV. The authors of the paper note that there was virtually no variation between each of these parameters in the Kombolgie Sandstone and the underlying Cahill Formation schists.

---

<sup>2</sup> Effective porosity should be used to calculate the linear groundwater flow velocity rather than drainable porosity (specific yield) which would give an overestimation in travel distance of contaminants. This is so since all of the groundwater in connected fractures or pores (except dead ends) contributes to the movement rather than only that water which is drainable.

Of the 47 shallow water samples, those taken above the Jabiluka ore bodies 1 and 2 had very low concentrations of chloride, sulphate and silica whilst some samples had higher bicarbonate content. Chloride content was in the range 6 to 20 mg/L, sulphate less than 14 mg/L; silica in the range 5 to 12 mg/L and bicarbonate 50 mg/L to 223 mg/L.

On the floodplain shallow water samples from augured holes (locations shown in fig 2) showed greater ion concentrations. Deutscher et al (1980) summarize the samples characteristics as follows:

- A large proportion of samples contained high concentrations of sulphate (>1000 mg/L).
- High sulphate concentrations (range: 1500 to 6854 mg/L) were usually accompanied by low pH (3 to 4) and a high concentration of  $\text{Fe}^{2+}$  (200 to 700 mg/L).
- All samples with high sulphate contained higher concentrations of the major ions calcium, magnesium, sodium and potassium.
- No samples had high ion content without a corresponding high sulphate content.

Water samples were also analyzed for concentrations of the trace elements uranium, copper, lead, zinc and cadmium. Exploration holes near and above the ore bodies had low concentrations of these elements with the highest uranium concentration found to be 0.003 mg/L.

In the floodplain, concentrations of uranium were also low with only two samples exceeding 0.01 mg/L. The paper's authors express surprise at these low concentrations since, as noted by them, United States uranium deposits in Colorado have associated groundwater uranium concentrations in excess of 0.1 mg/L, and for a Western Australian example uranium concentrations in the groundwater near uranium deposits are typically in the range 0.02 to 0.08 mg/L.

In general, higher concentrations of the other trace elements were found in the Magela floodplain groundwater, (Zn >0.1 mg/L; Pb >0.2 mg/L; Cd and Cu <0.05 mg/L).

Energy Resources Australia (ERAES 1998) provide groundwater quality results from samples obtained from eight geotechnical boreholes (OB97/1, 2, 3, 4D, 4S, 5, 6 and 7). These holes were constructed east of the divide within a proposed tailings storage area (concept now abandoned) and proposed excavated pit area (concept now shelved). Hole depth ranged from 3.3 metres (OB97/1) to 55.6 metres (OB97/4D). All holes were drilled through the alluvium into weathered sandstone (Kombolgie Formation) except for the 3.3 m bore which was in alluvial sand overlying weathered sandstone. Acidic groundwater with a pH range of 4.5 to 5.0 and low conductivity in the range 17 to 20  $\mu\text{S}/\text{cm}$  was found in the shallow bores OB97/1 and 97/2 (10 m deep). In bores OB97/6 and OB97/4S the pH was in the range 6.6 to 7.3 and conductivity in the range 100 to 200  $\mu\text{S}/\text{cm}$ . The deeper bore OB97/4D had a pH of 7.5 and conductivity in the range 300 to 350  $\mu\text{S}/\text{cm}$ .

Additional groundwater quality data is available from Kilborn-MWP (1976) for samples collected in 1976, Pancontinental (1981) for samples collected in 1978 and 1979 and ERA for samples collected in 1992, 1993, 1996 in the Mine Valley area. All data are listed in ERAES (1998) tables 3 to 8. These tables are consistent with concentrations reported in the previous findings. The additional information given for the period 1992/96 includes manganese concentrations that were found to be in the range 0.03 to 3.5 mg/L with an average of around 0.3 to 0.4 mg/L. Also uranium concentrations are reported to be in the range 0.2  $\mu\text{g}/\text{L}$  (Bore V081V) to 132  $\mu\text{g}/\text{L}$  (Bore T132V) and radium 226 in the range <2

mBq/L (Bore W135V) to 1078 mBq/L (Bore T132V). Both these bores are within the boundary of the orebody No 2 whilst Bore V081V lies outside of the orebody.

In summary, measured values of groundwater quality at Jabiluka can be separated into two distinct groups. The first group includes groundwater within the fractured bedrock and overlying weathered zone beneath and immediately adjacent to the ridge and extending to Swift Creek in the east. The second group includes groundwater beneath the Magela floodplain. The first group is characterized by low salinity, having very low to low chloride, sulphate, silica and neutral to slightly alkaline pH, with no major change in the chemical characteristics noted between the underlying Kombolgie and Cahill formation groundwater. The second group is characterized by having overall higher overall ionic content, high sulphate and iron and low pH. Overall, concentrations of naturally occurring radionuclides are low.

It is considered that chemical characteristics of the first group can be largely attributed to flushing action through high levels of Wet season recharge along the topographic ridge and the relatively inert sandstone.

For the second group, the chemical characteristics are largely due to decay of organic matter and oxidation of pyrite and seasonal floodwater fluctuations along the floodplain creating alternating reducing and oxidising conditions. It should be noted that acid sulphate soils occur extensively in the floodplain. Their significance is discussed by East et al (1992).

The occurrence of low concentrations of radionuclides in groundwater at this site compared to other sites elsewhere in Australia and the US is probably also due to Wet season groundwater dilution which is high compared to that which would occur in arid climates at these other sites.

## **4.4 Groundwater – flow directions and dynamics**

### **4.4.1 Recharge and potentiometric surface**

Recharge of the groundwater system is through direct infiltration of rainfall and through infiltration from local natural depression storages filled by runoff from the ridge. Both shallow and deeper groundwater originates from the overlying shallow aquifers with percolation of groundwater into the weathered zone and then preferentially along higher permeability zones into the deeper fractured rock aquifer. Because of the lower permeability of the underlying weathered zone and fractured bedrock, vertical flow is somewhat impeded, with predominant flow in a horizontal direction along the more permeable shallow aquifer. Nevertheless, the similar low salinity groundwater found in the fractured bedrock would suggest continual flushing with water recharged during annual Wet seasons.

Bore water levels (ERAES 1998) show that groundwater flows to the east and west away from the Jabiluka Mine Valley topographic ridge. On the western side of the ridge groundwater flows west towards the Magela floodplain, whilst to the east it flows towards Swift Creek. Potentiometric heads in the deeper aquifer in the vicinity of the divide are reported to be lower than those in the shallow aquifer, indicating a downward component in the hydraulic gradient in this area (ERAES 1998).

Based on accepted hydrogeological principles, groundwater flowing to the west would have the potential to join groundwater flowing in a northerly direction beneath the Magela floodplain, whilst groundwater flowing to the east would tend to flow in a northerly direction once it reaches the Swift Creek catchment (fig 1, 2). Milnes et al (1998) support this conceptual model of the flow system.

## **5 Proposed tailings repositories**

### **5.1 Previous proposals**

The initial proposal for storing tailings involved construction of an above ground tailings storage to the east of the divide. Subsequently two sub-surface disposal pits, respectively 100m and 180m deep, were proposed to take excess tailings material that could not be accommodated within the mine voids. However, Waite et al (1998) expressed reservations about the suitability of the site for the pits.

ERA have now proposed the construction of sub-surface tailings silo storages to meet the current approval condition that all tailings must be stored in underground repositories.

### **5.2 Proposed silo storage bank**

The proposed silo bank area is shown outlined in figures 2 and 3. About 180 vertical silos, 20 m in diameter are to be spaced at 30 m centres and extend from RL 955 m mine level down to about RL 820 m. Each silo is to be filled with a tailings paste prepared from partially de-watered tailings and cement.

### **5.3 Mine void storage**

The primary tailings repository will be the excavated stopes in the mining zone of Jabiluka orebody No 2. Longhole open stoping mining is usually carried out with alternate removal of rectangular stopes in a checkerboard pattern. The mining sequence would probably include filling each alternate stope prior to the removal of each adjacent stope.

## **6 Tailings characteristics**

### **6.1 Comparison with Ranger Mine tailings**

Although tailings have yet to be produced at Jabiluka, it is expected that when they are they will be similar to those produced at the nearby Ranger mine. The host rock for the uranium in both cases is Cahill formation schist which can be expected to mill in a similar manner at the two processing plants. Laboratory and field testing by the CSIRO (Richards et al 1989) of the properties of tailings in the Ranger tailings pond yielded extensive data on physical and chemical properties.

The Ranger tailings were not deposited as a paste. However, the measured permeabilities can be taken as a guide to those likely to apply to uncemented Jabiluka tailings. Appropriate testing to determine an optimal paste mix should allow a permeability lower than that of uncemented tailings to be achieved. Pore water chemistry will be affected by the addition of cement. Again, appropriate paste mix design should prevent contaminants being leached as easily from the set paste as it would be from uncemented tailings.

Paste and pore water properties assumed in the analysis during this investigation take into account the measured properties of the Ranger tailings.

### **6.2 Proposed paste disposal and properties**

As noted above, the current proposal is to dispose of the mill tailings at Jabiluka as a paste material in underground repositories.

The paste material will comprise a dense, low permeability, viscous mixture of tailings and water having the consistency of 'wet cement', with low segregation properties (Cincilla et al 1997). It is common to add a percentage (3 to 6%) of cement to bind the tailings into a solid mass, thereby improving the strength and reducing the permeability. A cement content of 1% to 4% is envisaged by ERA in this case. A review of the technology has been prepared recently by Waite et al (1998), although this is currently being reassessed as part of a research project.

Although the paste material would be of low permeability there is currently no specific data available on the probable range of magnitude of the permeability of the cured tailings paste. Waite et al (1998) have indicated uncertainty of the magnitude of permeability reduction which could be accomplished by the addition of cement to the paste if it is placed under water.

It has been suggested (Kinhill/ERAES 1998 – page 4–38 of Jabiluka Mill Alternative, Public Environment Report) that the permeability of a non-cured paste (no added cement) may be at least half an order of magnitude (ie 5 times) lower than that of conventionally deposited tailings. Tailings normally have a permeability in the range  $10^{-2}$  m/day to  $10^{-3}$  m/day (about  $10^{-7}$  m/sec to about  $10^{-8}$  m/sec) if the effects of overburden pressure are not included (Richards et al 1989). The permeability of a paste without added cement could be expected to be somewhat lower than this range.

It is noted in the Jabiluka EIS that adding 4% cement to the paste decreases the permeability from  $10^{-7}$  m/sec to  $10^{-10}$  m/sec (ie from about  $10^{-2}$  m/day to about  $10^{-5}$  m/day). However, it is not known from where these values were obtained or derived.

Given that saturated permeability of the host sandstone rock is generally in the range  $10^2$  to  $10^4$  m/day it is possible that the permeability of the paste could therefore be up to two orders of magnitude less than the average permeability of the host bedrock.

Both Milne et al (1998) and Waite et al (1998) note that there is no quantitative data available on the leaching characteristics of uranium tailings pastes under buried saturated conditions. In particular, the mass flux rates and adsorption behaviour of specific contaminants from this material in contact with flowing groundwater are unknown. Conservative estimates have been used in the modelling. ERA is currently investigating tailings paste properties. This will allow the modelling to be refined in the future.

The absence of specific permeability data and leaching characteristics of the paste material has been highlighted by both Milnes et al (1998) and Waite et al (1998).

The possibility of acid occurrence/formation within the paste because of sulphate in the process water and the sulphide content of the tailings has been reviewed. It has been concluded that sulphate acidity will be neutralised by the cement content of the paste material if sufficient cement is added (DLPE 1998). However, tests to examine the setting properties of the paste and its long term chemical stability are considered essential to verification of permeability assumptions made in the analysis of groundwater flow and dispersion of contaminants described in this report.

### **6.3 Potential contaminants**

Potential contaminants to be addressed in this report are magnesium sulphate, manganese, uranium and radium (specifically radium 226).

### **6.3.1 Magnesium sulphate**

This compound is one of the main contaminants to be contained in the tailings waste material. Waite et al (1998) have indicated up to 50 000 mg/L of sulphate in the process water at Ranger, and tailings water with typical concentration of 20 000 mg/L sulphate. It is not known at present what the concentration might be in either the silo or mine fill paste or the adsorption characteristics, if any, of this chemical within this material. In general, it would be expected that both sulphate and magnesium would have low adsorption characteristics.

### **6.3.2 Manganese**

The Ranger process water contains 2440 mg/L of manganese but the tailings pore water generally contains less than 1000 mg/L. Similarly high levels could be expected in the Jabiluka process water but, after neutralisation and processing tailings to form a paste, the concentration of manganese in Jabiluka tailings pore water is unlikely to exceed 500 mg/L. Adsorption of manganese is known to occur. However it is complicated by redox reactions that affect aqueous species and transformations, and the formation of manganese compounds of different oxidation states (EPRI 1984). It would be expected that manganese would have moderately high adsorption characteristics in the aquifer. No data are available on the adsorption characteristics of manganese in the tailings paste material.

### **6.3.3 Uranium**

Uranium concentrations in the Ranger tailings water had a concentration of 500–1000 µg/L up to 1988 (AGC 1989). ERA has quoted (pers comm) 1 mg/L or 10 Bq/L for the Ranger tailings pore water. For the richer Jabiluka ore, the concentrations in tailings could be expected to be about 50% higher. No data are currently available about the adsorption characteristics of uranium within the paste material.

### **6.3.4 Radium 226**

Radium 226 is one of the decay products of Uranium 238 having the longest half life (1600 years) of all the radium isotopes. The decay of Radium 226 in turn results in Radon (Rn 222), an inert gas that has a half-life of 3.82 days and can be carried by groundwater.

Radium 226 is also known to be capable of being transported by groundwater and its mobility has been extensively studied near the Jabiluka project area at the Ranger Uranium tailings storage (Martin & Akber 1996). This study reported a five-fold increase from 50 mBq/L to 250 mBq/L in radium 226 concentration over a period of ten years in one bore (OB11A) located approximately 150 m to 200 m down gradient from edge of the stored tailings. In a second bore (OB13A) at about the same distance, a two-fold increase was noted during the available record, although concentrations fluctuated and subsequently decreased to 1983 values in 1993. Other bores (OB 16, OB 15) either showed no increase in water levels, or fluctuating water levels with no overall increase in levels. During the 1983 to 1993 period the Radium 226 concentration in the tailings varied from 30,000 mBq/L to 20,000 mBq/L respectively.

Using detailed radium isotope ratio analysis Martin and Akber (1996) concluded that the variation in radium 226 concentration down gradient in the observation bores were due to two processes:

- Desorption of available radium from adsorption sites caused by the increase in other cations (eg Mg and Ca) in solution, the increase in radium being a contribution from the aquifer and not due to transport from the tailings dam.

- Formation of a barite phase with co-precipitation of radium.

That is, the fluctuations were not due to radium transport processes, which, although present, were being masked by the geochemical adsorption/desorption.

No data are currently available on the adsorption characteristics or concentrations of radium 226 in the tailings.

## **6.4 Mobilisation of potential contaminants**

### **6.4.1 Leaching potential-silo bank**

Under buried conditions and with cured paste permeability likely to be similar to or lower than the fracture permeability of a large portion of the host rock, groundwater will preferentially flow around the silos. Even if the bulk permeability values are similar, each cylinder of paste will block off fractures acting as preferential groundwater flow paths and much of the water will be diverted around the cylinder. The length(s) of the diversion path(s) and the consequent increase in head loss and reduction of flow through the silo bank as a whole will depend on connections within the fracture network. If the permeability of the paste is less than the bulk permeability of the surrounding rock the effect will be correspondingly greater. Under both conditions the mass flux of contaminants emanating from the silos would be much lower than if the groundwater flowed directly through the matrix of the silo tailings. The permeability of the paste and the adsorption characteristics of the contaminant in the paste and the surrounding fractured rock would control concentrations within the flowing groundwater. Specifically, the adsorption characteristics of the contaminant in the tailings paste will determine the paste pore water concentrations and the permeability of this material will control the rate of leaching.

Lowering the permeability of the tailings paste will decrease proportionally the leaching rate of the resulting tailings paste pore water. In this report the effect of both adsorption and paste permeability in a single and group of silos is examined using a numerical flow and solute transport model. This work is described in detail in Appendix B.

### **6.4.2 Leaching potential mine void fill**

The comments made regarding the adsorption and leaching characteristics of the silos also apply to the mine void tailings. However, there are probably some differences regarding the uniformity of the placement of the mine void tailings compared to those in the silos where placement conditions can be better controlled. This could result in voids or fissures which would allow greater groundwater throughflow. Also the structural integrity of the paste material in the filled stope(s) after curing is less certain than that of paste in the cylinders. The fill in the stopes will be used for structural support and rock movement could cause cracking or more serious failures. Whether any fissures are likely to develop during blasting/excavation of adjacent stope(s) or as a consequence of longer term ground movements will depend on the strength and plasticity of the set paste. Any cracks that do develop will allow a greater level of throughflow. Conversely, the higher cement content of the paste in the stopes will act to reduce the hydraulic conductivity of the matrix.

## 7 Analysis of contaminant movement

### 7.1 General principles

#### 7.1.1 Advection-dispersion-retardation

Essentially three processes control the movement of a contaminant in the sub-surface. The first of these is advection that potentially moves or transports the contaminant with the velocity of the surrounding groundwater in a sharp concentration front (fig 4). Advection is the Darcy velocity divided by the effective porosity and therefore is larger than the Darcy velocity. As the effective porosity<sup>3</sup> decreases, the advective velocity increases for a given Darcy velocity and vice-versa. Advective velocity is usually referred to as linear or pore velocity.

Dispersion, on the other hand, can spread the contaminant in three different co-ordinate directions due to variations in groundwater velocity caused by local permeability differences within the sub-surface strata or rock mass. The parameter describing the degree to which the contaminant will spread in any of the three primary directions is dispersivity, which has the dimension metres. Higher values of dispersivity will cause greater spreading and consequently lower concentrations with increasing distance from the source and vice-versa.

Retardation is a broad term encompassing adsorption, precipitation/dissolution and other complex ion exchange reactions. In its most fundamental sense it can have the effect of retarding or slowing the velocity of the contaminant relative to the flowing groundwater. It is generally recognised that the concept of retardation is a simplification, but it is often necessary to invoke it given the limited hydrochemical data and uncertainty about the chemical reactions and conditions that may occur in the sub-surface. Despite this, it has been shown to describe quite well contaminant plume movement at sites subjected to very detailed monitoring. Use of this concept greatly simplifies the contaminant modelling process.

Adsorption is commonly viewed as the process where contaminant adheres to the surface of the porous medium or rock mass due to a number of different mechanisms. Adsorption is usually quantified by a measure of the amount of contaminant mass held by the rock or porous medium compared to the contaminant mass in the flowing groundwater. The relationship between the amount of a solute held by the rock and that remaining in solution in the groundwater is called an isotherm.

#### *Distribution Co-efficient $K_d$*

The simplest isotherm<sup>4</sup> is the distribution co-efficient where the contaminant mass on the rock or porous matrix is given by:

$$S_m = K_d C \quad (1)$$

where  $K_d$  is the distribution coefficient [ $L^3/M$ ];  $S_m$  is the mass of the contaminant adsorbed or precipitated on the solids of the matrix per unit bulk dry mass of the media [ $M/M$ ] and  $C$  is the contaminant concentration [ $M/L^3$ ].

---

<sup>3</sup> Effective porosity is smaller than (total) porosity as it excludes dead end pores or structures that are not connected. Effective porosity is larger than drainable porosity (ie specific yield) and much larger than storage co-efficient.

<sup>4</sup> Not strictly an isotherm but a constant.

In fractured rocks  $K_d$  is better defined as  $K_a [L]$  which is the mass of contaminant on the rock surface per unit area of the rock divided by the contaminant concentration within a fracture (Freeze & Cherry 1979).

An important assumption made in the derivation of Equation (1) is that there is infinite capacity of the media to adsorb the contaminant. This assumption is reasonable for low concentrations.

Equation (1) is the equation most often used in solute transport simulations. It is a linear relationship and is the only relationship that can be included in commonly available analytical models.

#### *Freundlich Isotherm*

This non-linear isotherm allows for decreases in the capacity to adsorb contaminant as the concentration increases and is given by (EPRI 1984):

$$S_m = K_f C^{1/N} \quad (2)$$

where  $K_f$  and  $N$  are constants. When  $N=1$  then  $K_f$  is the same as the distribution co-efficient constant  $K_d$  above.

#### *Langmuir Isotherm*

This isotherm limits the adsorption to a maximum value as concentration increases and is given by (EPRI 1984):

$$S_m = K_L A_m C / (1 + K_L C) \quad (3)$$

where  $K_L$  is the Langmuir adsorption constant and  $A_m$  is the maximum adsorption capacity of the matrix.

Whilst non-linear isotherms can be incorporated into the numerical models used in this study, their use could not be justified in this case because of the limited data available.

#### *Retardation Factor*

Using Equation (1) to describe the retardation process, the retardation factor  $R_f$  can be expressed as:

$$R_f = 1 + \rho_b K_d / n \quad (4)$$

where  $\rho_b$  is the bulk density of the aquifer and  $n$  is the effective porosity.

The contaminant velocity is therefore given by  $v_c = v_L / R_f$  where  $v_c$  is the contaminant velocity and  $v_L$  the linear (pore) velocity and  $v_L = v_D / n$  where  $v_D$  is the Darcy velocity.

In a uniform fracture the retardation factor is given by  $R_f = 1 + AK_d$  where  $A$  is the surface area to void space (volume) ratio [1/L] (Freeze & Cherry 1979). For a planar fracture  $A = 2/b$  where  $b$  is the aperture width.

### **7.1.2 Radioactive decay**

Radioactive decay is given by the decay constant:

$$\lambda = \text{Ln}(2) / t_{1/2} \quad (5)$$

where  $t_{1/2}$  is the half life [T].

### **7.1.3 Dilution**

Dilution normally refers to reduction of concentration by mixing of water containing a substance (eg a contaminant) with water of lower concentration entering the flow system

from another source. In this respect it differs from dispersion in that dispersion is caused by velocity variations in the aquifer alone and simply distributes the contaminant more widely throughout the system.

In the Jabiluka mine area, dilution would involve mixing of deep groundwater carrying contaminants leached from the stored tailings with groundwater of more recent origin. This recently recharged water has travelled only through the relatively inert surface layer of soil and rock and is thus less contaminated than the deeper flowing water.

## **8 Modelling approach**

### **8.1 General**

Groundwater flow and contaminant transport are complex three dimensional processes. Metalliferous mining usually involves fractured rock aquifers with the fractures providing the main flow paths for the groundwater which has the potential to transport contaminants away from the mine area. The scale of the fracture network is usually small compared with that of the region of interest in potential contamination so a fractured rock aquifer can be represented as an equivalent porous medium on a regional scale. Only exceptional geological features such as major faults need to be accounted for separately as flow conduits.

Geological conditions at Jabiluka meet the above modelling scale criterion. However, the data available to describe the hydraulic characteristics of the aquifer do not justify a fully three dimensional model to represent flow and contaminant transport. In most cases of mining the available data are less than desirable. In this case ERA has particular difficulties to overcome because of restrictions on access to areas from which data are required.

Data are available to allow modelling of flow along the main flow paths and potential contaminant transport routes east and west from the mine towards the Magela floodplain in Kakadu National Park. Consequently, modelling has been carried out to first determine flow velocities in these directions and then to estimate the transport of contaminants from tailings repositories to and along these paths. The overall model can be described as hybrid. Details are given below and in Appendices A and B.

### **8.2 The hybrid model**

As indicated in the previous section, a hybrid modelling approach has been used in this investigation. The models used include:

1. A two dimensional (2D) section finite element model (SEEP/W) of section A-B-C to determine flow directions, head distributions and the range of Darcy velocities along a section parallel to the groundwater flow lines extending west then north and east then north of the Mine Valley topographic divide (figure 1 – section A-B-C).
2. A three dimensional (3D) numerical solute transport model (MODFLOW-SURFACT) applied to a single representative 1 metre thick horizontal layer of flow through and around a repository to determine the leaching concentrations from the tailings paste material for use as the source concentrations in the analytical model (an analysis of this work is described in Appendix B).
3. An analytical contaminant transport model (Appendix A) to determine concentrations due to advection, dispersion in three co-ordinate directions and retardation. This model uses as input the range of velocities determined from 1 above and source concentrations

determined from 2 above. This model has been combined with Monte Carlo simulations to determine concentration profiles for a large number of different parameter values within selected ranges.

The models have been chosen to provide levels of approximation which match that of the available data. The numerical solute transport leaching model and the numerical flow model provide data of appropriate accuracy to be entered into the analytical contaminant transport model.

Calculations of contaminant concentrations that may emanate from the tailings paste and the concentrations within the aquifer system have been expressed in relative or normalised form. Relative or normalised concentrations are fractions or percentages of the source concentrations whatever they may happen to be. The results in this report can therefore be used to determine absolute concentrations at downstream points for a range of source concentrations. Absolute concentration values that are based on Ranger mine data and the literature, and considered to be conservative, are given in section 12.1. These may be used to assess the impact of the tailings repositories on water quality in the Mine Valley and Swift Creek areas.

### **8.3 Contaminant characteristics**

#### **8.3.1 Magnesium sulphate**

In general sulphate is weakly retained on soils and most adsorption is associated with hydrated Al and Fe oxides (EPRI 1984). EPRI provides tables of values of Langmuir  $A_m$  and  $K_L$  and Freundlich  $K_f$  and  $1/N$  isotherm constants; however, these are for materials and soils that are not directly relevant to the current site. Nevertheless, they indicate low adsorption for various soils with  $K_f$  in the range 0.006 to 0.127 and  $1/N$  in the range 0.48 to 0.77. For some of the same soil types the reference gives  $A_m$  in the range 2.7 to 4.1 and  $K_L$  in the range 3.2 to 3.9.

EPRI indicate that sulphate adsorption increases somewhat at lower pH.

As a conservative estimate sulphate is treated as a non-reactive (ie no adsorption) contaminant in the solute transport analysis, that is it is assumed that  $K_d = 0$ .

#### **8.3.2 Manganese**

EPRI (1984) provide adsorption isotherm constants for manganese for various adsorbents and pH. These constants are not representative of the actual site conditions. For sand loam the values of  $A_m$  are 8.0 and 8.7 and corresponding values for  $K_L$  are 3.5 and 4.0. for pH of 5.2 and 6.7 respectively.

In the Ranger tailings dam concentrations of manganese in pore water have been measured as 140 mg/L near the bottom of the deposited tailings and 900mg/L near the top and in the supernatant liquid.

For Ranger uranium tailings solute transport modelling, a  $K_d$  value of 1.5 was used to match model and measured results (AGC 1989).

#### **8.3.3 Uranium**

Moody (1982) presents empirically derived distribution coefficient  $K_d$  values from batch experiments for selected radionuclides. Relevant values from these tables are shown in table 1. (See also Domenico & Schwartz 1990.)

**Table 1**  $K_d$  Distribution co-efficient (mL/g) values from batch experiments (Moody 1982)

Element	Host Environment			
	Salt	Basalt	Tuff	Granite
Uranium	1*	6*	4*	4*
Radium	5	50	200	50
Thorium5	50:1002**	500	500	500

\* No significant difference between values measured in oxidizing and reducing Eh.

\*\* First value for dome salt, second for bedded salt.

The table indicates that salinity, in particular high salinity, has a marked effect on reducing the  $K_d$  values and therefore the retardation factor. For uranium it reduces the  $K_d$  by a factor between 4 to 6 and radium by an order of magnitude or more.

Based on equation 4 the corresponding retardation factors for the sandstone and schists at Jabiluka using an average mass density of  $2.0 \text{ g/cm}^3$ , porosity in the range 2 to 10% and  $K_d$  in the range 1 to 6 mL/g are given in table 2.

**Table 2** Range of estimated retardation factors for uranium in the Kombolgie and Cahill formations

$K_d$ (mL/g)	Retardation Factor for Porosity 2%	Retardation Factor for Porosity 10%
1	100	20
6	600	120

### 8.3.4 Radium 226

Table 1 above provides estimates of  $K_d$  values for radium 226. Table 3 gives the corresponding calculated retardation factors.

**Table 3** Range of estimated retardation factors for Radium 226 in the Kombolgie and Cahill formations

$K_d$ (mL/g)	Retardation Factor for Porosity 2%	Retardation Factor for Porosity 10%
5	500	100
50	5000	1000

Note that in the above tables 2% has been used as the lowest effective porosity for comparison since lower values than this would give larger values of retardation factor. In this analysis we require conservative lower values of this factor.

## 9 Groundwater flow system – numerical 2D model

This section describes the set up and results of the 2D finite element model of section A-B-C (fig 1). This model was set up to determine groundwater flow directions, head distributions and the range of Darcy velocities within the section on the eastern and western side of the topographic divide.

<sup>5</sup> Although not included in the list of elements for this brief Thorium has a  $K_d$  value and therefore a retardation at least one order of magnitude (ie x 10) larger than radium 226 according to table 1

## 9.1 Model mesh and boundary conditions

Figure 5 shows the finite element mesh used within section A-B-C given in figure 3 for simulating the groundwater flow system<sup>6</sup>. The mesh comprises quadrilateral and triangular elements which both use secondary nodes and 9th and 3rd order integration respectively for higher accuracy.

To remove the 'no flow' edges of the model 'infinite' elements have been used that allow the model to behave as though the section is extended to a very large distance beyond each of these edges.

For simulating long-term response it is valid to consider the potentiometric surface to be at steady state since the influence of seasonal fluctuations on contaminant movement will tend cancel out below and above a mean potentiometric level. This approach is accepted practice in modelling studies. Also any variation in flow velocities due to fluctuating water levels will lie well within the range of velocities to be used in the analysis. To simulate steady state, constant heads at the elevation of the depicted potentiometric surface were set in the model. These are shown as red dots along this depicted surface.

### 9.1.1 Aquifer-aquitard properties

The model was set with a uniform permeability of  $10^{-2}$  m/day in the sandstone east of the divide and 0.05 m/day in the sandstone west of the divide. The carbonate/schist in the east was assigned a permeability of 0.2 m/day. Non-indurated alluvial sediments were assigned a permeability of 0.1 m/day and the floodplain sediments 0.01 m/day. Note that the results are not sensitive to the permeability of the non-indurated sediments.

### 9.1.2 Tailings repositories

For all simulations the fill in the mine void was assigned a uniform permeability of  $10^{-4}$  m/day.

No permeability changes were made in the area designated as silo bank since introducing a lower permeability here would violate the ability of the groundwater to flow in the third dimension around the silo repositories. In fact the groundwater velocities would be higher around the silo bank than elsewhere because of the smaller available area of flow cross-section (See also Appendix B).

### 9.1.3 Model assumptions

The model assumes that flow is along the planes of the section A-B-C and that long-term water level fluctuations will deviate around an average level represented by the potentiometric surface given by Milnes et al (1998). This surface is derived from measured water table levels.

The assumption is made that, on the scale simulated, the fracture system behaves as an equivalent porous medium.

The pegmatite dyke has not been given special properties in the section. If it is less fractured and permeable than the adjoining rocks it will act as a partial barrier to flow towards the west. Although pump testing has indicated that this could be the case to at least a limited extent, in the absence of adequate data this possibly beneficial effect of the dyke has been ignored, as has the possibility of any increase in upward flow component.

---

<sup>6</sup> The model used is the **SEEP/W** code developed by Geo-Slope International which is an internationally recognized 2D saturated/unsaturated groundwater flow model used in 70 countries throughout the world.

#### **9.1.4 Model results**

The results of the steady state simulation are presented in figure 6. The figure presents the computed hydraulic heads in terms of mine RL (m). Potentiometric heads are marked at the upper and lower ends of lines of constant head shown in the figure. The water table shown was set in the model at the temporally averaged value derived from field measurements.

The results indicate essentially horizontal flow with a slight upward component developing with distance from the topographic divide to the west. This is shown by deviation of constant head lines from the vertical, with the lower ends further to the west.

From the model results the Darcy velocities in the section adopted east of the divide are in the range  $5 \times 10^{-5}$  m/day to about  $5 \times 10^{-6}$  m/day whilst to the west the range was  $5 \times 10^{-4}$  m/day to  $5 \times 10^{-5}$  m/day.

It is evident from the flow pattern obtained by modelling that it would be better to site the tailings storage silos in the Magela sandstone east of the orebody than in the Cahill formation schist to the west. Any contaminant leached from the silos would have a much longer flow path to the Magela floodplain to the east. The groundwater flow velocities in this direction are also lower.

The silos should be constructed in sandstone which is not significantly weathered. The top level proposed for the silos appears to be suitable. Approval of the proposed level should await confirmation of the sandstone properties when the RL 955 m mine level is reached during mining.

## **10 Solute transport – analytical model**

### **10.1 Description**

Appendix A presents in detail the equations used in the analytical solute transport model including additional derivations for leaching and radioactive decay of the source concentration.

Figures 7 and 8 present the conceptual model of the representation of the source plane for the analytical model. The concentrations in the source plane are those derived from the leaching models described fully in Appendix B.

For all simulations, concentrations were computed along the axis of symmetry of the resulting plume, (ie through the center of the plume).

### **10.2 Model assumptions**

The transport model is based on an analytical solution to the advection-dispersion equation and therefore assumes uniform conditions throughout the flow field. It also assumes one co-ordinate direction for advection along the planes in section A-B-C and in three co-ordinate directions for dispersion.

### **10.3 Monte-Carlo simulation**

Monte Carlo simulation refers to the technique of repeatedly re-running the model, in this case the analytical transport model, using various model parameters selected randomly within a given range. Provided a sufficient number of computer runs is chosen, the results are an approximate representation of the results of all the possible combinations of the given parameters within each range.

No particular probability distribution of parameter values within each range of values was assumed in any of the simulations; all parameter values had equal probability of occurrence as determined by the random number generator. This approach is conservative.

Two sets of simulations were conducted. The first is representative of the silo bank east of the divide and the second is representative of the mine void fill west of the divide. The difference between these simulations is the size of the assumed source plane and the range of Darcy velocities determined from the section model.

Simulations were conducted using 255<sup>7</sup>, 500 and 1000 runs or realizations. It was found that there was little difference between each of these simulations so, for simplicity, subsequent runs were made with 255 realisations.

### 10.3.1 Simulation east – silo bank area

#### 10.3.1.1 Model parameters –non-reactive transport

Solute transport model parameters for non-reactive transport used in the Monte Carlo analysis are given in table 4. As explained in the previous section, A uniform distribution was assumed with an equal chance of any value in the given range<sup>8</sup>.

**Table 4** Parameter ranges used in the Monte Carlo analysis for non-reactive transport

Parameter		Range
Longitudinal Dispersivity	$\alpha_L$	1 m to 10 m
Transverse Dispersivity	$\alpha_T$	0.1 m to 1m
Vertical Dispersivity	$\alpha_V$	0.01 to 0.1 m
Darcy Velocity	$v_D$	$5 \times 10^{-5}$ m/day to $5 \times 10^{-6}$ m/day
Effective Porosity	$P_a$	0.005 to 0.10
Retardation	$R_f$	1 (constant)

In addition to the above a constant source plane of dimensions 600 m wide and 100 m high was used for all simulations.

Simulations were conducted over a period of 200 years with values calculated every 20 m from the source plane along the axis of symmetry of the plume.

#### 10.3.1.2 Results

The results of the simulations using 255 realizations are plotted in figure 9a in terms of normalized concentrations ( $C/C_{sp}$ ) where  $C_{sp}$  is the source plane concentration.

The curves show a wide scatter but the majority of the concentration curves are grouped together within 200 m from the source. A central measure of the entire grouping can be obtained by computing the median curve for all of the 255 curves plotted (fig 9b). This median was obtained by calculating the median value of each curve at the 20 m distance increments and plotting the result.

Figure 9c shows the median curve for 500 realizations while figure 9d shows the results for 1000 realizations.

<sup>7</sup> 255 was selected as this is the current limit on the number of Excel 97 spreadsheet plotted graphs allowed.

<sup>8</sup> It is known that some parameter values are probably normally or log normally distributed, however, at this stage no prior judgement was made and no information is available to invoke such distributions.

Figure 9e shows the concentrations including a leaching source decay for the same set of randomly generated parameters. The leaching characteristics were determined in the Appendix B simulations.

Note that while source concentrations are reduced, the inclusion of leaching has no effect on the concentration fronts away from the source. For all subsequent simulations a constant source concentration has therefore been assumed.

Figures 9a to 9e can be used with source plane concentrations obtained from both figures B5 and B6. They relate downstream concentrations to concentration at the source plane regardless of what that might be or what paste parameter values were used to calculate it. For this case of silo bank and non-reactive contaminant, two different paste permeabilities,  $K_s = 10^{-4}$  m/day and  $K_s = 10^{-5}$  m/day were used to produce the different source plane concentrations given in figures B5 and B6. Both concentrations can be introduced as  $C_{sp}$  in figures 9a to 9e.

#### 10.3.1.3 Model parameters – reactive transport

Reactive transport includes uranium and radium 226 and for these simulations the parameter ranges given in table 4 were used except for retardation and additional decay constants as follows:

**Table 5** Additional parameters for uranium transport

Parameter		Range
Retardation	Rf	20 (constant)
Decay Constant	$\lambda_u$	(negligible)

**Table 6** Additional parameters for Radium 226 transport

Parameter		Range
Retardation	Rf	100 (constant)
Decay Constant	$\lambda_u$	$1.186 \times 10^{-6}$ day <sup>-1</sup> (constant)

A simulation period of 1000 years was used for all simulations.

#### 10.3.1.4 Results

The results for these simulations are given in figures 10a, b for uranium and figures 11a, b for Radium 226. Note that in figure 11a, concentrations at the source (and in the aquifer) are reduced because of radioactive decay (radium 226 half life being 1600 years). Figures 11a,b assume a finite, non-replaceable radium concentration at the source. Figures 11c and d present the case where radium 226 derived from thorium 230 decay replaces the decayed radium at the source. Under these circumstances the radium source would remain constant.

Since similar values for  $K_d$  have been adopted for uranium and manganese, the results for uranium can be taken as indicative of those for manganese. The  $K_d$  value of 1.5 adopted for manganese on the basis of Ranger test results is a little higher than the value of 1 used for uranium, so adoption of the uranium curves for manganese transport is conservative.

### **10.3.2 Simulation west – mine void fill area**

#### *10.3.2.1 Model parameters –non-reactive transport*

Model parameters used were those in table 4 except that the Darcy velocities were in the range between  $5 \times 10^{-4}$  and  $5 \times 10^{-5}$  m/day. The source plane dimensions were also changed to 500 m width and 100 m depth.

#### *10.3.2.2 Results*

The results for 255 realizations are presented in figures 12a, b.

#### *10.3.2.3 Model Parameters – Reactive Transport*

Model parameters used were those in tables 4, 5 and 6 except that the Darcy velocities were set between  $5 \times 10^{-4}$  and  $5 \times 10^{-5}$  m/day.

#### *10.3.2.4 Results*

The results for 255 realizations are presented in figures 13a, b and 14a, b for uranium and radium respectively. Figures 14a,b assume a finite, non-replaceable radium concentration at the source. Figures 14c and d present the case where radium 226 derived from thorium 230 decay replaces the decayed radium at the source. Under these circumstances the radium source would remain constant.

As for flow from the silo bank area, the results for uranium can be taken as indicative of those for manganese since similar values for  $K_d$  have been adopted for these contaminants. Again, since the  $K_d$  value of 1.5 adopted for manganese on the basis of Ranger test results is a little higher than the value of 1 used for uranium, adoption of the uranium curves for manganese transport is conservative.

### **10.3.3 Application of figures 9 to 14**

Figures 9 to 14 can be used to assess the extent to which the selected contaminants will move towards the Magela floodplain for given source concentrations. Since downstream concentrations are given in relative terms, predictions of actual concentrations can be upgraded as more information becomes available on paste properties.

As noted previously in relation to figure 9, the Monte Carlo results for a specified case (in that case a bank of silos and non-reactive contaminant) can be applied to source plane concentrations regardless of the values of paste parameters used to derive them. Silo bank source plane concentrations relevant to figure 9 were calculated as percentages of paste pore water source concentrations  $C_0$  for two paste permeability  $K_s$  values,  $10^{-4}$  m/day and  $10^{-5}$  m/day (fig B5 and B6). Both sets of results can be used with the concentration ratios shown in figure 9.

## **11 Summary and discussion of results**

### **11.1 General comments**

Conservative estimates of Jabiluka tailings paste properties based on measured properties of tailings produced from very similar ore at Ranger and data from the literature can be used to convert the proportional (dimensionless) contaminant concentration figures determined by modelling to conservative estimates of actual concentrations. In the following discussion, such values have been introduced where relevant.

The conservative value used for expected paste permeability is  $10^{-4}$  m/day, although it should be possible to achieve  $10^{-5}$  m/day. Poor placement techniques in backfilling mine voids might

possibly increase the effective bulk permeability to  $10^{-3}$  m/day so this figure has also been introduced to demonstrate the consequences if this were to happen.

Maximum tailings pore water concentrations of the four potential contaminants which have been studied in this investigation are estimated from Ranger tailings data to be:

sulphate	20 000 mg/L
magnesium	5 000 mg/L
manganese	500 mg/L
uranium	15 Bq/L
radium	15 Bq/L

Reduced concentrations at selected distances east of the silos and west of the mine backfill can be estimated by applying the ratios and percentages shown in the graphs to the source concentrations given above.

## 11.2 Discussion of specific findings

Numerical model simulations conducted to determine leaching behaviour over time of an individual silo and a group of silos (Appendix B) indicate that it would be desirable to achieve a target paste permeability of  $10^{-5}$  m/day if possible, and not to exceed a permeability of  $10^{-4}$  m/day. Simulations show that with a paste permeability of  $10^{-4}$  m/day leaching of non-reactive contaminants would create a concentration generally less than 12% of the source concentration immediately down-gradient of the silos. Dispersion would reduce this concentration further in a down-gradient direction.

Preliminary calculations of the leaching concentrations from the mine void fill indicate that concentrations immediately down-gradient of the source would most likely be less than 5% of the source concentration for a paste permeability of  $10^{-5}$  m/day and less than 30% for a paste permeability of  $10^{-4}$  m/day. For a paste permeability of  $10^{-3}$  m/day, the immediate down-gradient concentrations could be 80% or more.

Analysis conducted using a finite element section flow model, combined with Monte Carlo simulations using numerical and analytical solute transport models has provided estimates of normalized concentrations with respect to distance, for possible ranges of key aquifer and contaminant parameter values. The flow model confirms that possible pathways around or through the tailings filled orebody void will be directed towards the bedrock beneath the Magela floodplain to the west whilst flow around and through the silo bank will follow an easterly course. The model indicates essentially horizontal flow with a slight upward component through the underlying bedrock.

The modelling results show that over a period of 200 years the non-reactive contaminant fronts from the silos would migrate a probable distance of less than 200 m in a easterly direction. Beyond this distance concentrations would be negligible. The maximum computed distance (of very low probability) for this case is 800 m.

The simulations conducted for uranium over a period of 1000 years indicate that contaminant fronts from the silos with a paste permeability of  $10^{-4}$  m/day would migrate a probable distance of less than 50 m in an easterly direction. the maximum computed distance (of very low probability) for this case is less than 300 m. For the same period, the radium 226 fronts from the mine void fill would migrate a probable distance of less than 15 m in a easterly direction with a maximum distance (of very low probability) of less than 100 m.

Simulations conducted for a non-reactive contaminant emanating from the mine fill void indicates a probable contaminant migration distance in a westerly direction of 500 m after 200 years although greater migration distances are possible. However, the large migration distances indicated in the Monte Carlo simulations can largely be ignored because the gradients beneath the Magela floodplain would be much smaller than those assumed in the simulations. The groundwater would also be entering an area of already poor water quality so would not have a significantly deleterious effect on the environment.

For the silos with a paste permeability of  $10^{-4}$  m/day, uranium migration (to negligible concentrations) could extend a probable distance of 200 m in a westerly direction over a period of 1000 years. The maximum computed distance (of very low probability) for negligible concentrations in this case is 1200 m. For the same period the radium 226 concentration fronts from the mine void fill would migrate a probable distance of less than 50 m in a westerly direction. A maximum migration distance to negligible concentrations (of very low probability) of 500 m is indicated.

Based on the results of leaching and dispersion-advection simulations it is evident that sulphate will be the most mobile of all potential contaminants. Also it is evident that for the most probable situation over 200 years, concentrations will decrease to negligible concentrations over a distance of 200 m. For example should the concentration of sulphate in the silo be 20 000 mg/L, the concentrations immediately down-gradient of the silo would be less than 10% (or less than 2000 mg/L) and at 100 m the concentration would be a further 1% of this value (ie 20 mg/L). Concentrations of sulphate as well as being affected by dispersion will also be affected by dilution due to the influence of rainfall infiltration at shallow depths. Hence there would be a further dilution for that part of the plume extending upward into shallow alluvial or weathered rock aquifers. Overall, our conclusion is that there would be negligible potential for contamination of surface streams to the east. The probability of a continuous high permeability fracture system extending to the east over long distances is considered to be low. Even with a fracture system extending some one to two hundred metres, the final concentration due to both dispersion and dilution would be low and probably negligible compared to the high sulphate levels in the Magela floodplain created by natural oxidation processes. Similar arguments are valid for concentrations extending in a westerly direction from the mine filled void provided an adequately low bulk permeability ( $10^{-4}$  m/day or preferably less) for the mine void tailings paste can be achieved. However, we recommend that further complete numerical solute transport simulations be conducted for both the entire silo bank and mine void fill to confirm these predictions.

## **12 Potential for contamination of the wetlands**

The results of the simulations conducted, based on the assumptions made and data available, indicate that if a low permeability of the proposed tailings paste material can be achieved, it will reduce significantly the rate at which the available contaminant mass will leach from the repositories.

Simulations conducted for radionuclides uranium and radium 226 indicate that these contaminants are restricted in their movement and provided that adequate low permeability can be achieved in the tailings paste the concentrations will remain at background levels within the wetlands. This situation would also apply to manganese.

Sulphate will be the most mobile contaminant but concentrations emanating from the tailings paste by flowing groundwater would be reduced significantly provided tailings paste

permeability is equal to or preferably lower than  $10^{-4}$  m/day. Sulphate concentrations in the wetlands currently occur at high levels due to naturally occurring processes of oxidation of pyrite from the bedrock. Whilst the possibility exists of some sulphate reaching the floodplain to the west over a 200 year period the concentration levels could be expected to be below those that currently occur naturally in this area.

It is significant that sulphate levels in the Magela floodplain are substantially reduced by Wet season floodwaters through dilution.

The probability of occurrence of linear and continuous major fracture systems extending for kilometres is unlikely, and it is not considered that these structures would be sufficiently continuous to propagate contaminants beyond distances computed in this analysis.

## 13 Conclusions

1. Good quality groundwater occurs in the vicinity of the proposed Jabiluka minesite within fractured bedrock comprising Kombolgie Formation siliceous sandstone and Cahill Formation schists and carbonates, a weathered profile of variable thickness and sandy deposits elsewhere along drainage gullies. Poor quality groundwater occurs in organic silts, clays and sand across the Magela Creek floodplain.
2. Groundwater flow is controlled by topography and flows towards the east and west from the catchment divide formed by an approximate north-south ridge of Kombolgie sandstone which overlies the eastern edge of the Jabiluka orebody No 2. On the eastern side of the divide groundwater flows towards Swift Creek and then north to the Magela floodplain. On the western side of the divide groundwater flows directly towards the main branch of the Magela floodplain. Groundwater generally flows with higher velocity through the non-indurated sediments and weathered profile than the underlying fractured bedrock. The rock mass of schist and carbonate west of the orebody in the mine valley has overall higher permeability than the sandstone to the east. Hence groundwater velocities would tend to be higher in a westerly direction than in an easterly direction by, on average, one order of magnitude. Beneath the floodplain, particularly during the Wet season, groundwater velocities could be expected to be low due to the low hydraulic gradients that would occur in a northerly direction. It is possible, although not certain, that a reverse hydraulic gradient is established at the edge of the floodplain towards the mine site during Wet seasons.
3. Groundwater quality at Jabiluka can be separated into two distinct groups. The first group includes groundwater within the bedrock and overlying weathered zone beneath and immediately adjacent of the ridge. The second group includes groundwater beneath the Magela floodplain. The first group is characterized by low salinity, having very low to low chloride, sulphate, silica and neutral to slightly alkaline pH with no major change in the chemical characteristics noted between the underlying Kombolgie and Cahill formation groundwater. The second group is characterized by having overall higher overall ionic content, high sulphate and iron and low pH. Overall concentrations of naturally occurring radionuclides is low. The chemical differences between the two groups can be largely attributed to flushing action through Wet season recharge along the topographic ridge and the relatively inert sandstone leading to waters of the first group. The decay of organic matter, oxidation of pyrite leading to high sulphate concentrations and seasonal floodwater fluctuations along the floodplain is thought to be responsible for the chemical characteristics of the second group. The occurrence of low concentrations of

radionuclides in the groundwater compared to other sites elsewhere in Australia and the US is probably also due to Wet season groundwater dilution compared to arid climates at these other sites.

4. Overall the concept of tailings paste disposal at depth is a good one. However, there is currently little information available on the leaching characteristics of the proposed tailings paste disposal technology. This includes the ultimate permeability, curing characteristics under saturated conditions and release rates of the potential contaminants from the paste material. Consequently, it is not possible at this stage to verify the magnitude of absolute concentrations that would emanate from either the mining void tailings fill or bank of proposed disposal silos. However it is possible to determine the range of normalized concentrations, that is, fractions or percentages of the source concentration (whatever they may be) with distance from these sources. Using these results it would be possible to determine absolute concentrations when the source concentrations are known from these facilities or when they can be determined with greater confidence. At this time the best estimates of Jabiluka tailings paste properties can be derived from the results of tests on Ranger mine tailings adjusted for the effects of partial dewatering and addition of cement during paste production. They have been taken into account when selecting conservative values of parameters for modelling contaminant movement.
5. Numerical model simulations were conducted to determine leaching behaviour over time of individual and a group of silos, using conservative estimates of aquifer permeability. These simulations (Appendix B) indicate that it would be desirable to achieve a target paste permeability of  $10^{-5}$  m/day if possible, and not to exceed a permeability of  $10^{-4}$  m/day. This maximum would be similar to the permeability required for a clay liner in a landfill (ie  $10^{-9}$  m/sec) and should be achievable. Simulations show that with a paste permeability of  $10^{-4}$  m/day leaching of non-reactive contaminants would create a concentration generally less than 10% of the source concentration immediately down-gradient of the silos. Dispersion and dilution will reduce this concentration further in a down-gradient direction to an extent demonstrated by the regional scale modelling summarised below.
6. Preliminary calculations on the leaching concentrations from the mine void fill indicate that concentrations immediately down-gradient of the source would most likely be less than 5% for a paste permeability of  $10^{-5}$  m/day and 30% of the source concentration for a paste permeability of  $10^{-4}$  m/day. However, for a paste permeability of  $10^{-3}$  m/day the immediate down-gradient concentrations could be 80% or more.
7. An analysis conducted using a finite element section flow model, combined with Monte Carlo simulations using analytical solute transport models has provided estimates of normalized concentrations with respect to distance, for possible ranges in key aquifer and contaminant parameter values. The flow model confirms that possible pathways around or through the tailings filled orebody void will be potentially directed towards the bedrock beneath the Magela floodplain to the west whilst those through the silo bank will follow a potential westerly course. The model indicates essentially horizontal flow with a slight upward component through the underlying bedrock for the western flow path.
8. The modelling results show that over a period of 200 years the non-reactive contaminant fronts from the silos would migrate a probable distance of less than 200 m in a easterly direction to negligible concentrations. The maximum computed distance (of very low probability) for this case is 800 m.

9. The simulations conducted for uranium over a period of 1000 years indicate contaminant fronts from the silos with a paste permeability of  $10^{-4}$  m/day would migrate a probable distance of less than 50 m in an easterly direction to negligible concentrations. The maximum computed distance (of very low probability) for this case is less than 300 m. For the same period the radium 226 fronts from the mine void fill would migrate a probable distance of less than 15 m in a easterly direction to negligible concentrations with a maximum distance (of very low probability) of less than 100 m.
10. Simulations conducted for a non-reactive contaminant emanating from the mine fill void indicates a probable contaminant migration distance in a westerly direction of 500 m after 200 years although greater migration distances are shown to be possible for the assumed conditions. However, it is considered that the larger migration distances indicated in the simulations can be ignored because the gradients beneath the Magela floodplain would be much smaller than those assumed in the simulations.
11. For silo fill with a paste permeability of  $10^{-4}$  m/day, uranium migration (to negligible concentrations) could extend a probable distance of 200 m in a westerly direction over a period of 1000 years. The maximum computed distance (of very low probability) for negligible concentrations in this case is 1200 m. For the same period the radium 226 concentration fronts from the mine void fill would migrate a probable distance of less than 50 m in a westerly direction to negligible concentrations. A maximum migration distance to negligible concentrations (of very low probability) of 500 m is indicated.
12. Based on the results of leaching and dispersion-advection simulations it is evident that sulphate will be the most mobile of all potential contaminants. Also it is evident that for the most probable situation over 200 years concentrations will decrease to negligible concentrations over a distance of 200 m. For example should the concentration of sulphate in the silo be 20 000 mg/L then the concentrations immediately down-gradient of the silo would be less than 10% (or less than 2000 mg/L) and at 100 m the concentration would be a further 1% of this value (ie 20 mg/L). Concentrations of sulphate as well as being affected by dispersion will also be affected by dilution due to the influence of rainfall infiltration at shallow depth. Hence there would be further dilution for that part of the plume extending upward to shallow depth. Overall our conclusion is that there would be negligible potential for contamination of surface streams to the east. The probability of a continuous high permeability fracture system extending to the east over long distances is considered to be low. Even with a fracture system extending some one to two hundred metres the final concentration due to both dispersion and dilution would be low and, likely to be at negligible levels, compared to the high sulphate levels in the Magela floodplain created by natural oxidation processes. Similar arguments are valid for concentrations extending in a westerly direction from the mine filled void provided an adequate low bulk permeability ( $10^{-4}$  m/day or preferably less) for the mine void tailings paste can be achieved. However, we recommend that further complete numerical solute transport simulations be conducted of both the entire silo bank and mine void fill to confirm these predictions.
13. Groundwater flow patterns and velocities obtained by modelling indicate that the proposed tailings disposal silos should be sited in Kombolgje sandstone east of the orebody rather than in Cahill formation schist to the west. This would minimise the rate of movement of contaminants leached from the silos toward the Magela floodplain and provide the longest flow path. The sandstone excavated from the silos would also be more resistant to breakdown by weathering than the schist. The silos should be constructed in sandstone

which is not significantly weathered. The proposed top level appears to be suitable, but this should be confirmed when the sandstone is exposed during mining.

## **14 Recommendations**

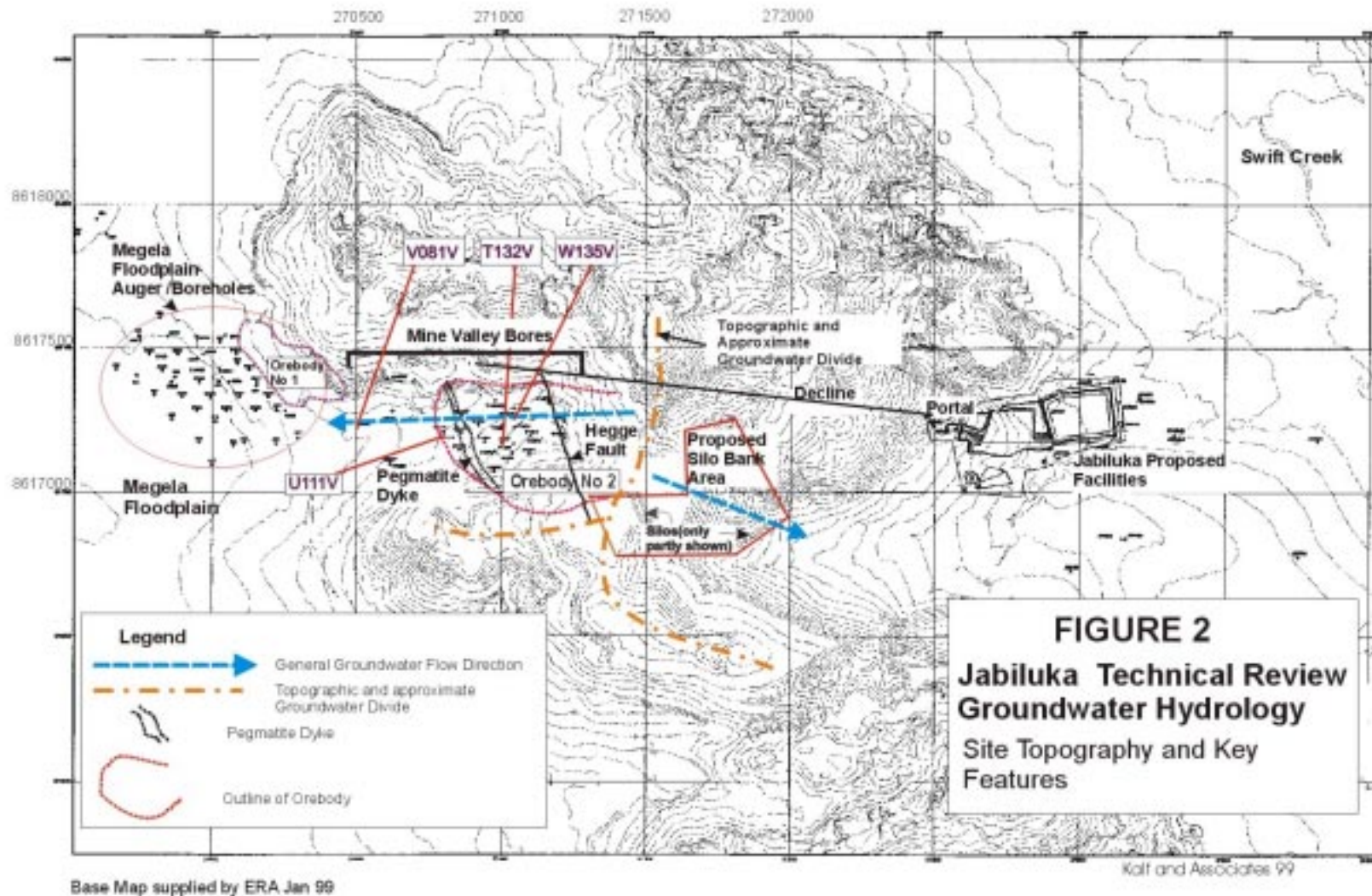
1. Better and more detailed hydrogeological cross-sections and maps need to be prepared for both the eastern and the western area at Jabiluka. These maps should be drawn accurately to scale and related to mine RL. The maps should show the relationship of the proposed mining stopes, carbonate/schist rocks, locations and depths of bore hydraulic data (projected into the section(s)), position, depth, and dip of known geological structures and weathered zones including the Magela floodplain area.
2. Laboratory permeability and leaching tests of uranium tailings pastes are considered necessary to confirm the validity of property values used in this investigation. Scaled down physical modelling (tank modelling) of accelerated flow around silos containing representative paste tailings would also be useful. The results could be calibrated against a numerical solute transport model to provide additional confidence in the predicted field situation.
3. Additional separate numerical model simulation of the entire silo bank and mine filled void is recommended. This could be initially done using a horizontal planar layer, similar to that described in this report. In due course full 3D models of both flow and solute transport should be used to attempt to reproduce as closely as possible the groundwater flow systems in the area. For example the influence of the pegmatite dyke on contaminant migrations needs to be assessed, in particular whether the dyke could create significant upward flow components into the shallow non-indurated sediments. Additional field test data would be required to set up such a model.

## References

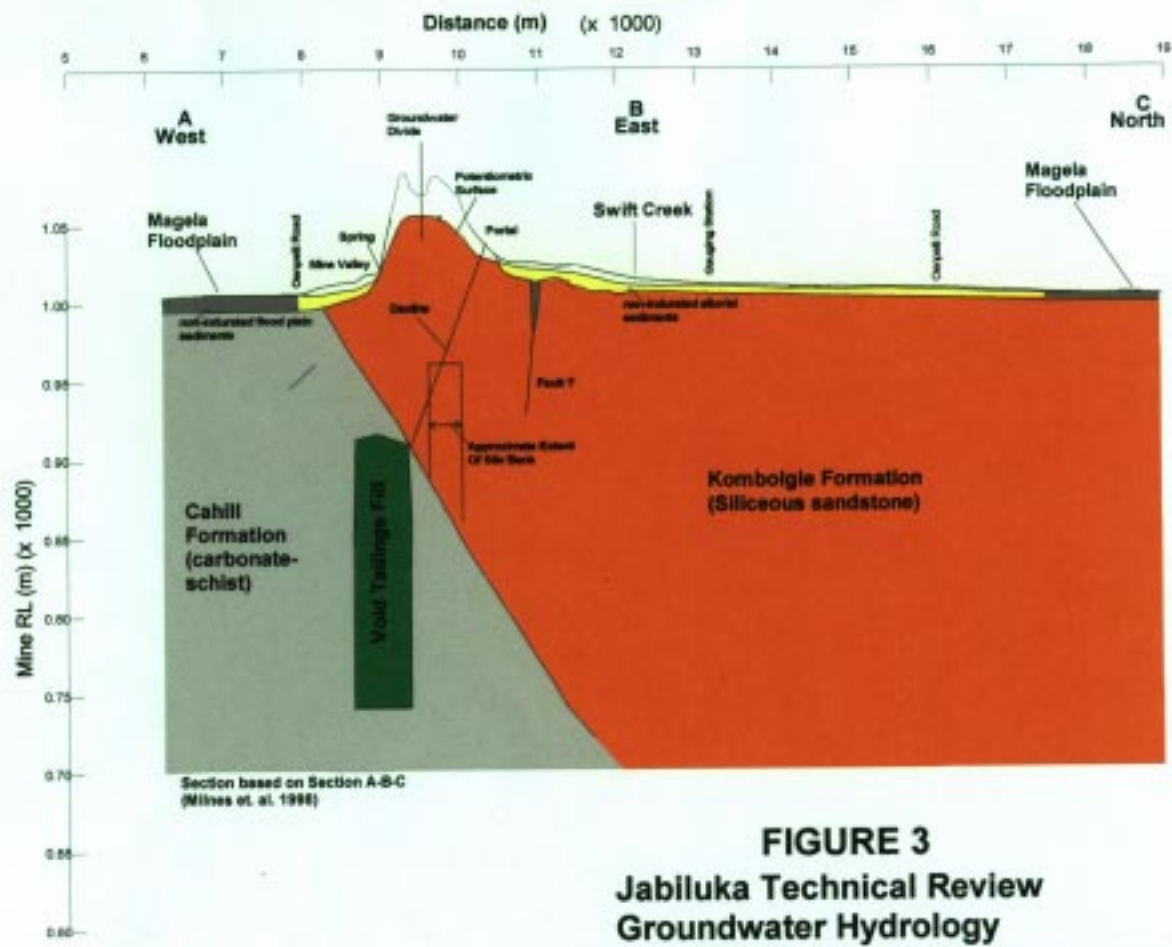
- AGC 1989. Tailings dam solute transport model Stage 1. Report for Ranger Uranium.
- AGC-Woodward Clyde 1993. Letter Report to ERA prepared by J Hall. 15 Jan 1993.
- Chiew F & Wang QJ 1999. Hydrological Analysis Relevant to Surface Water Storage at Jabiluka. Supervising Scientist for the Alligator Rivers Region, Report, Aust. Govt. Publishing Service, Canberra (in press).
- Cincilla WA, Landriault DA & Verburg R 1997. Application of paste technology to surface disposal of mineral waters. In Proceedings of the Fourth International Conference on *Tailings and mine waste*, AA Balkema, Rotterdam. 343–355.
- Department of Lands, Planning and Environment (DLPE) 1998. Jabiluka Mill Alternative-Public Environment Report- Environmental Assessment Report and Recommendations. Assessment Report 26. July
- Deutscher RL, Mann AW & Giblin A 1980. Groundwater Geochemistry in the vicinity of the Jabiluka Deposits. Proc of Int. Uranium Symposium on the Pine Creek Geosyncline.
- Deweist R 1966. Hydrogeology. John Wiley and Sons.
- Domenico PA & Schwartz FW 1990. Physical and chemical hydrogeology. John Wiley and Sons.
- East TJ, Noller B & I Willett 1992. Soil materials and their formation on the Magela Plain. In *Modern sedimentation and late quaternary evolution of the Magela Creek Plain*, ed RJ Wasson. Research report 6, Supervising Scientist for the Alligator Rivers Region, AGPS, Canberra.
- Energy Resources Australia Environmental Services – ERAES 1998. Jabiluka Project-Six Monthly Progress Report-The Minister for Resources and Energy- Additional Environmental Studies.
- Electric Power Research Institute (EPRI) 1984. Chemical Attenuation Rates, Coefficients, and Constants in Leachate Migration. Vol 1-A Critical Review.EA-3356 Research Project 2198-1. Research Reports Center Box 50490, Palo Alto CA 94303. Feb 1984.
- Freeze A & Cherry J 1979. Groundwater. Prentice-Hall.
- Kalf F 1999. Addition of Source Decay Modifications for the Domenico Solute Transport Equation. Kalf and Associates - Internal Report.
- Kilborn-MWP 1976. Groundwater Investigations for Jabiluka Orebody. Report to Pancontinental Mining Ltd.
- Kinhill & ERA Environmental Services 1998 The Jabiluka Project Draft Environmental Statement/Supplement to the Draft EIS/The Jabiluka Mill Alternative, Public Environment Report. CD-ROM, ERA 1998.
- Martin Paul & Akber Riaz A 1996. *Groundwater seepage from the Ranger uranium mine tailings dam: Radioisotopes of radium, thorium and actinium*. Supervising Scientist Report 106, Supervising Scientist, Canberra.
- Milnes AR, Hall J, Jackson A & Shirvington PJ 1998. Jabiluka Mill Alternative. Synopsis of Key Issues and Processes. Report prepared for Minister for Environment. August.

- Moody JB 1982. Radionuclide Migration/retardation. Research and Development Technology Status Report. Office of Nuclear Waste Isolation. Batelle Memorial Inst. ONWI-321.
- Pancontinental 1981. A Review of the Jabiluka Project Environmental Studies. Volume 2: Chemistry of Groundwaters of the Jabiluka Project Area.
- Richards BG, Peter P & Martin R 1989. Physical, Hydraulic and Geotechnical Properties of the Tailings in the Ranger No.1 Tailings Dam - Stage 1. CSIRO Division of Soils, Glen Osmond, S.A. Final Report to Ranger Uranium Mines.
- Spitz K & Moreno J 1996. A Practical Guide to Groundwater and Solute Transport Modeling. John Wiley and Sons.
- Waite JD, Dudgeon C & Fell R 1998. Review of Jabiluka Mine Alternative Tailings Management Proposal. Unisearch Report. No 35051. August 1998.





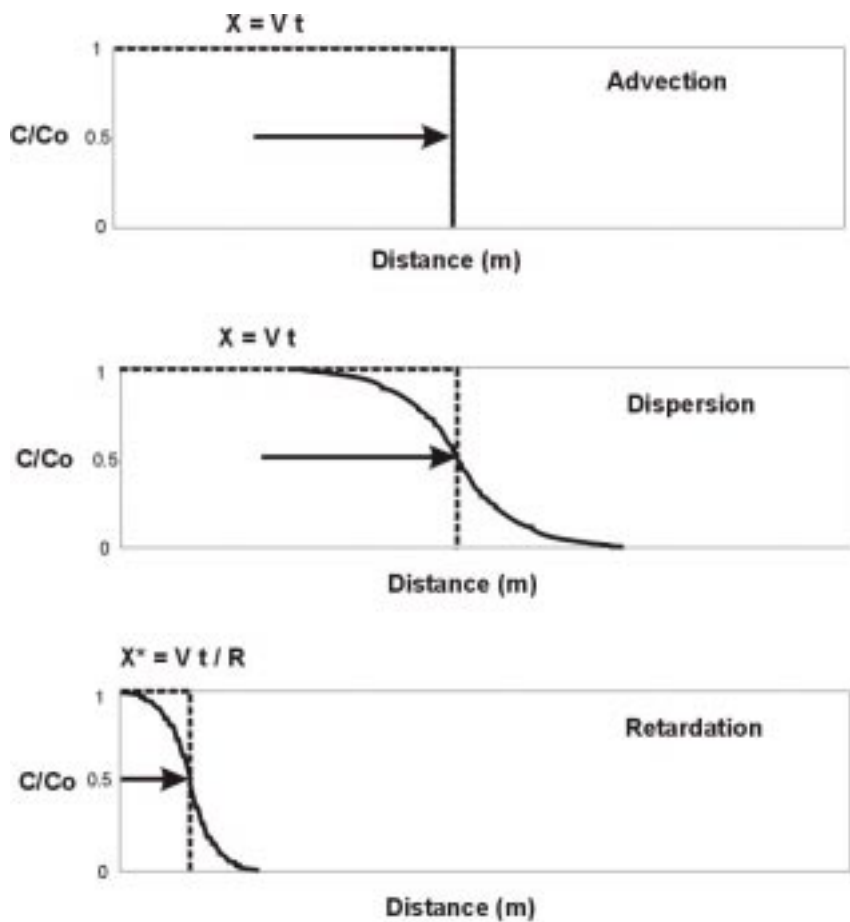




Section based on Section A-B-C  
(Milnes et al. 1996)

**FIGURE 3**  
**Jabiluka Technical Review**  
**Groundwater Hydrology**  
**Model Section A-B-C - Hydrogeological Units**  
**Surface and Sub-surface Features**

Kalf and Associates Feb 99



$V$  = Linear Velocity  
 $t$  = time  
 $X$  = Travel Distance  
 $R$  = Retardation  
 $C$  = Concentration at distance  
 $C_0$  = Source Concentration

**FIGURE 4**

Jabiluka Review  
 Groundwater Hydrology  
 Advection-Dispersion  
 -Retardation

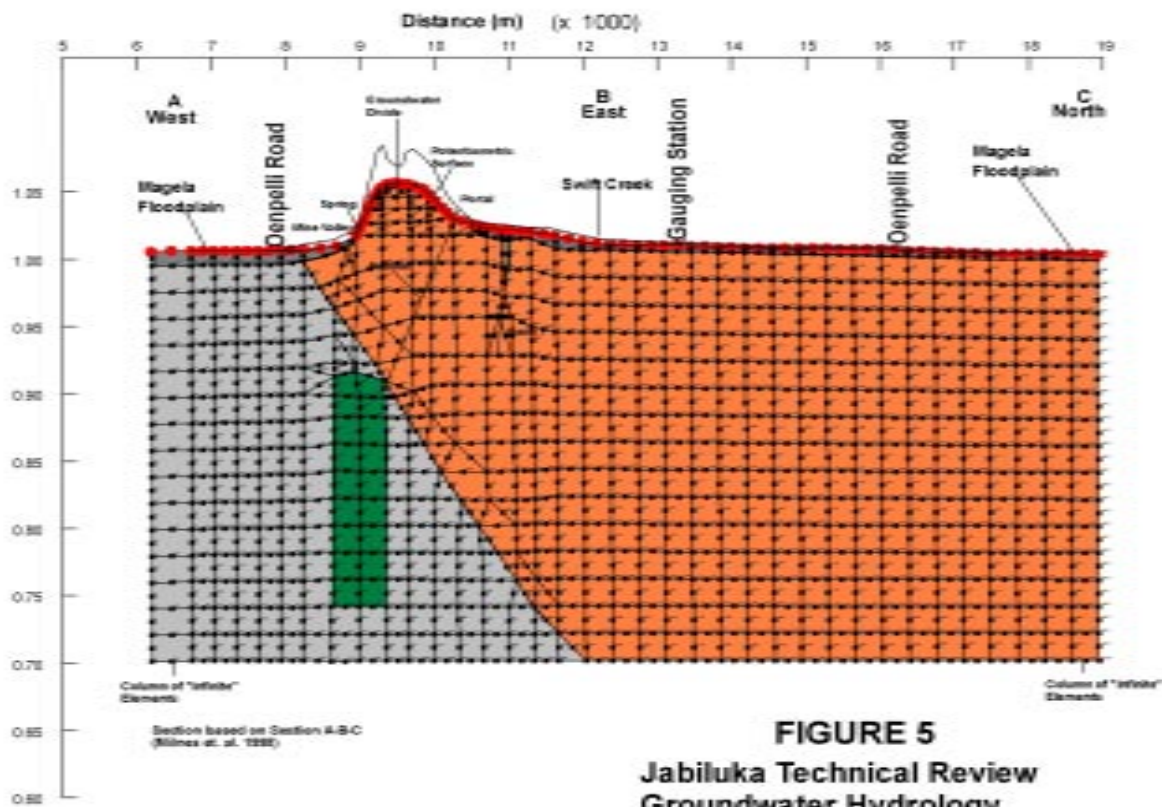


**FIGURE 5**  
**Jabiluka Technical Review**  
**Groundwater Hydrology**  
**Model Finite Element Mesh**  
**Section A-B-C and Boundary**  
**Conditions**

Kell and Associates Feb 99

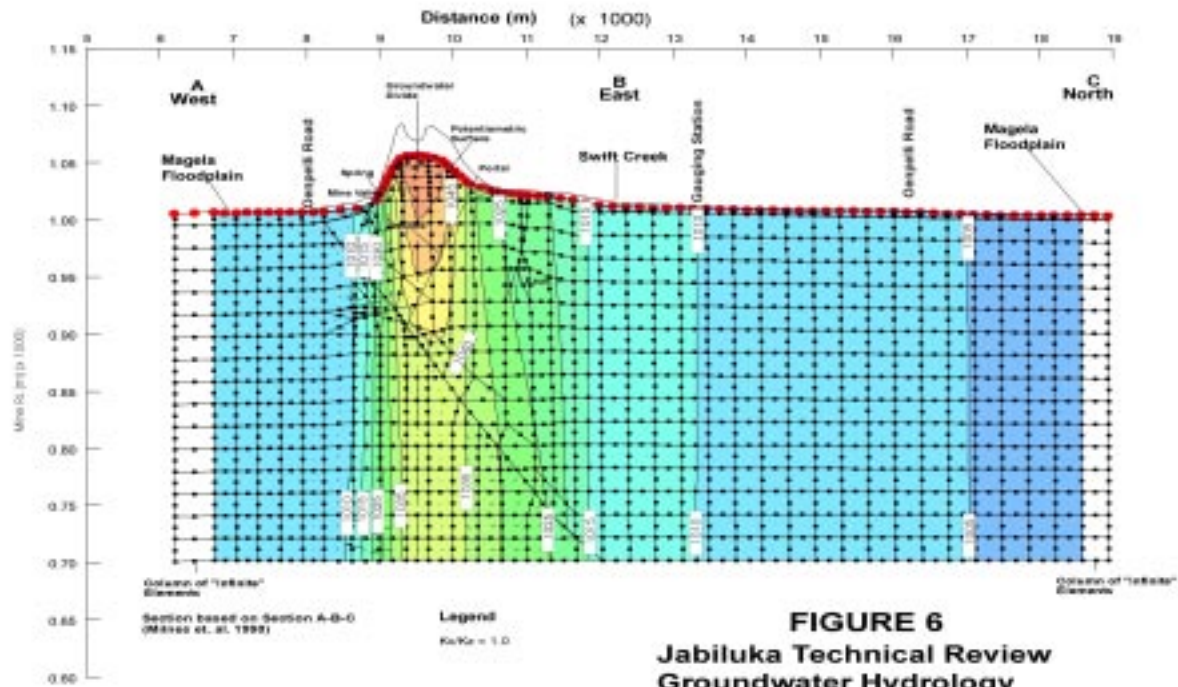
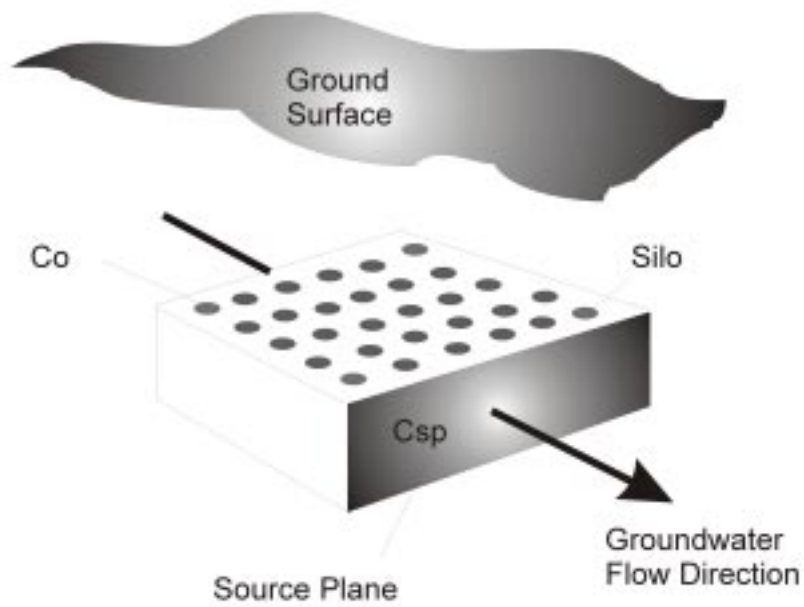


**FIGURE 6**  
**Jabiluka Technical Review**  
**Groundwater Hydrology**  
**Steady State Heads -Section A-B-C**

Kell and Associates Feb 93



$C_o$  - Silo Tailings Contaminant Concentration

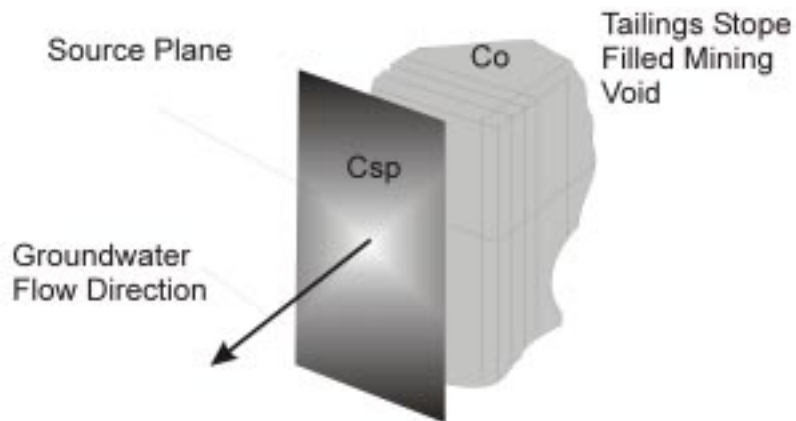
$C_{sp}$  - Source Plane Contaminant Concentration

## FIGURE 7

### Jabiluka Technical Review Groundwater Hydrology

#### Groundwater Flow Through Silo Bank and Assumed Source Plane

Koif and Associates Feb 99



Co - Stope Tailings Contaminant Concentration

Csp - Source Plane Contaminant Concentration

## FIGURE 8

**Jabiluka Technical Review  
Groundwater Hydrology**

**Groundwater Flow - Mine Void  
and Assumed Source Plane**

*Koif and Associates Feb 99*

**Figure 9a - Jabiluka Review - Groundwater Hydrology  
Non-Reactive Contaminant - Monte Carlo Simulations  
Relative Concentrations - Silo Bank - 255 realizations**

Time = 200 years

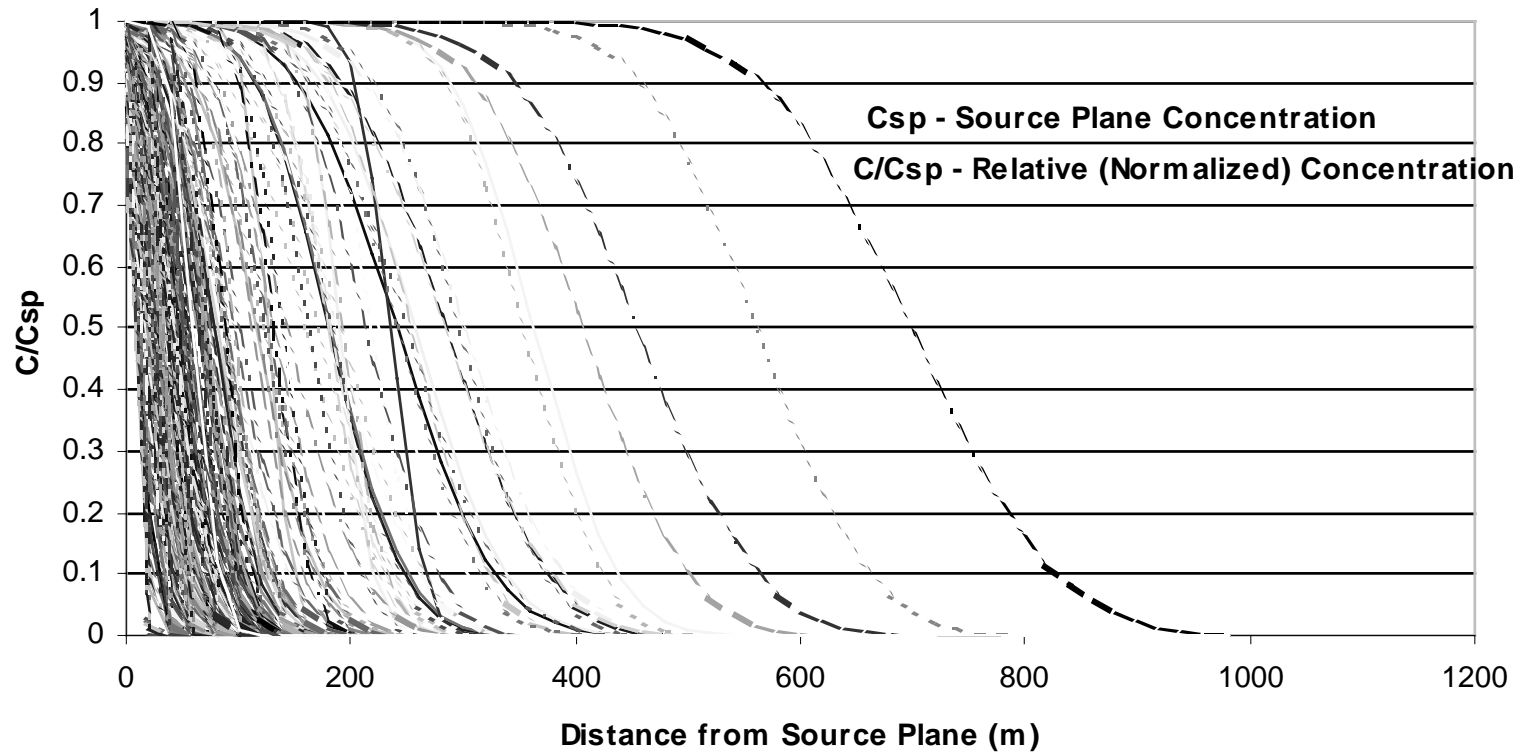


**Figure 9b-Jabiluka Review-Groundwater Hydrology  
Non-Reactive Contaminant -Monte Carlo Simulations  
Median Relative Concentration-Silo Bank - 255 Realizations**

Time 200 years

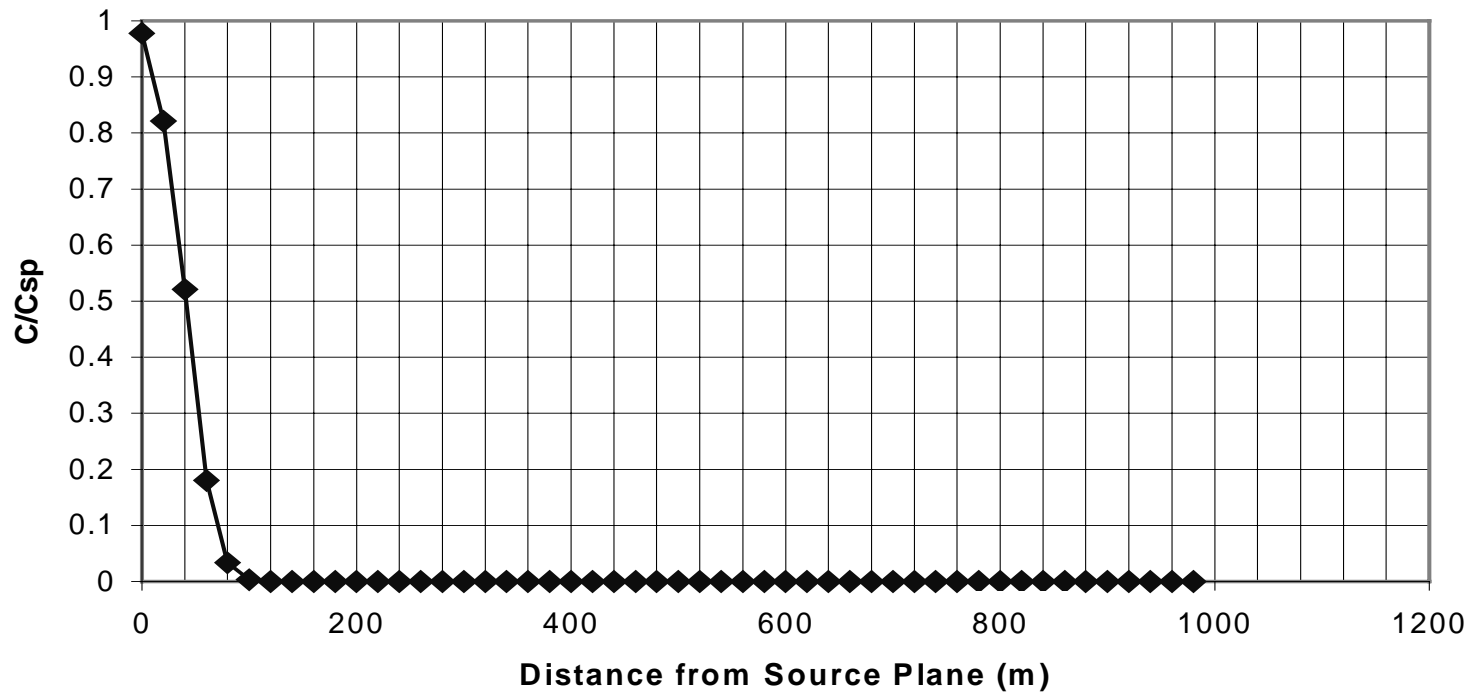


**Figure 9c Jabiluka Review - Groundwater Hydrology  
Non-Reactive Contaminant - Monte Carlo Simulations  
Median Relative Concentration - Silo Bank - 500 Realizations**

Time =200 years

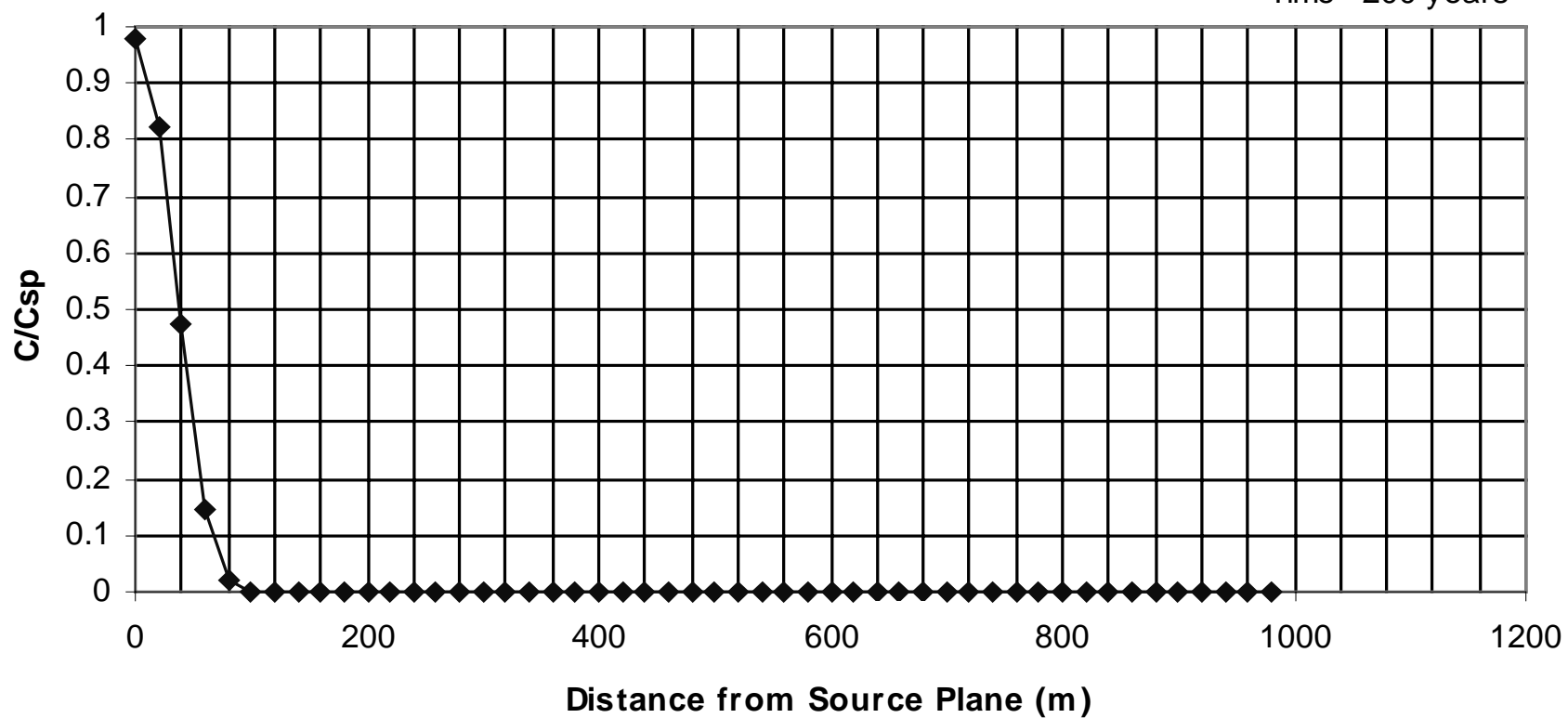


**Figure 9d Jabiluka Review - Groundwater Hydrology  
Non-Reactive Contaminant - Monte Carlo Simulations  
Median Relative Concentration - Silo Bank - 1000 Realizations**

Time = 200 years

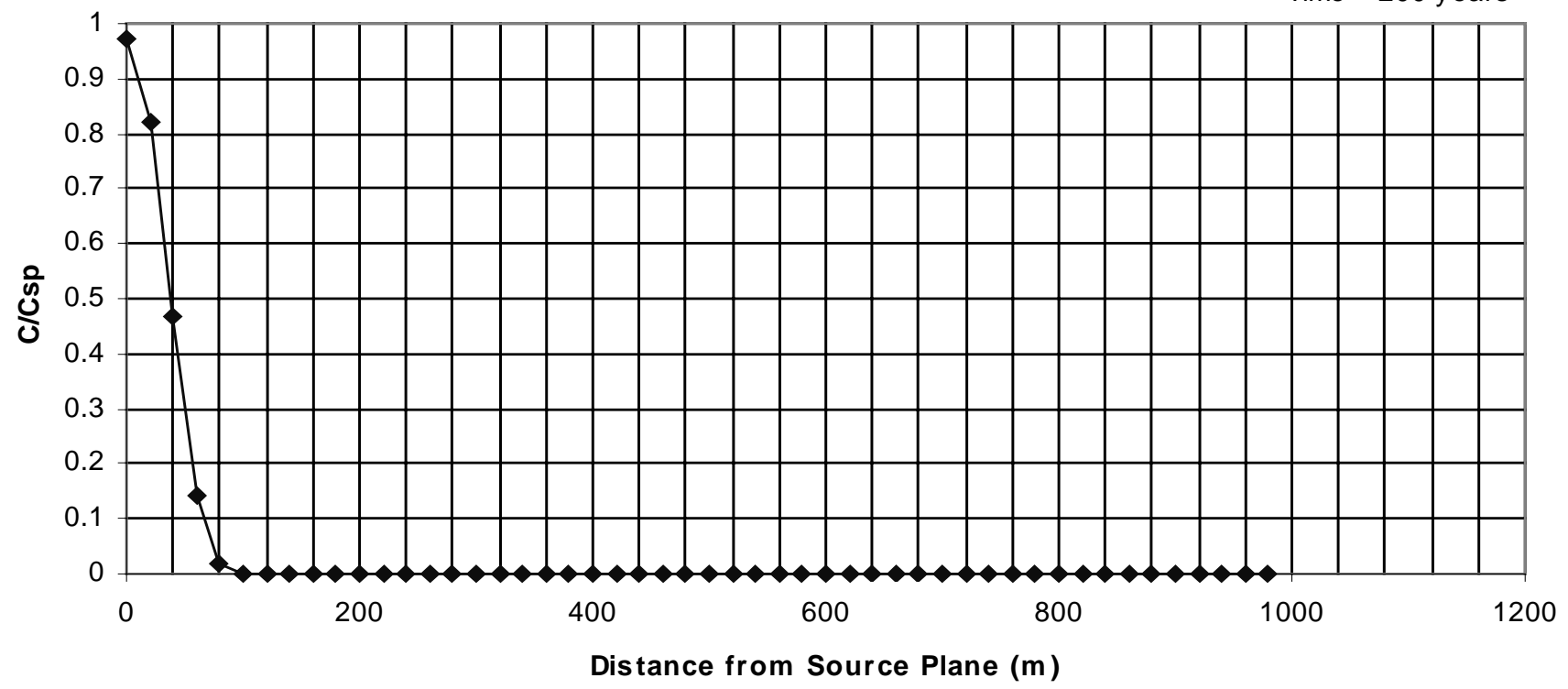


**Figure 10a Jabiluka Review - Groundwater Hydrology  
Uranium Monte Carlo Simulations Relative Concentrations  
Silo Bank - 255 Realizations**

Time = 1000 years

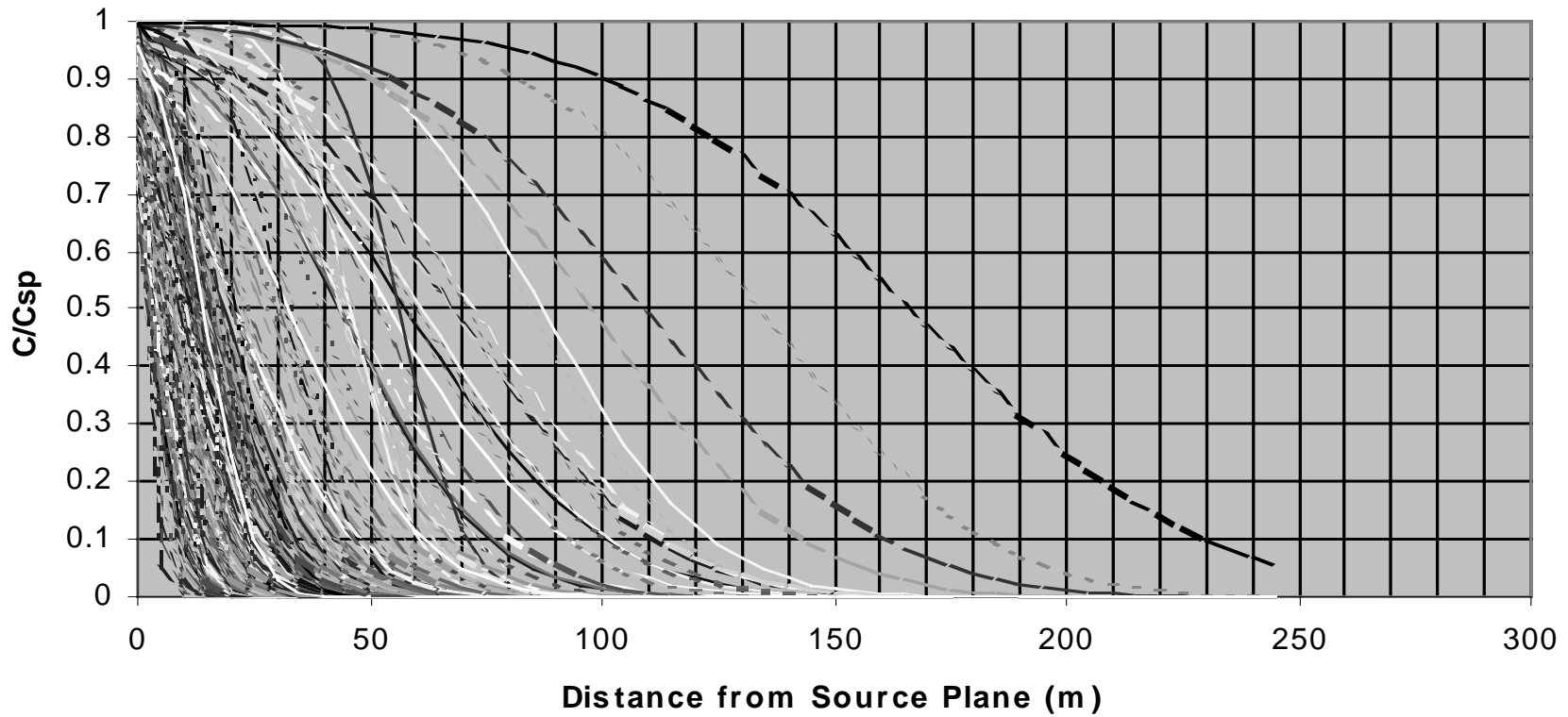


**Figure 10b Jabiluka Review - Groundwater Hydrology  
Uranium Monte Carlo Simulations  
Median Relative Concentrations -Silo Bank - 255 Realizations**

Time = 1000 years

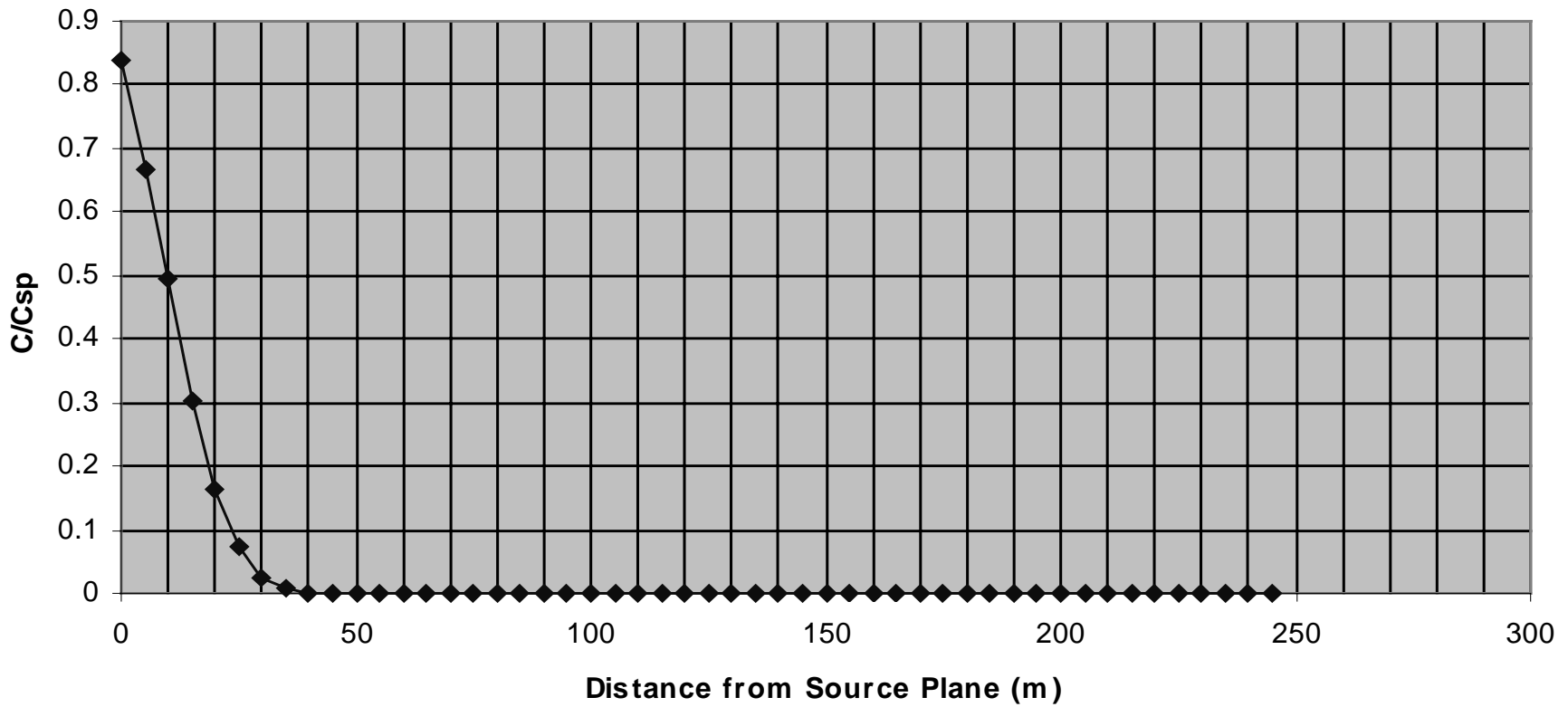


Figure 11a Jabiluka Review - Groundwater Hydrology  
Radium 226 Monte Carlo Simulations Relative Concentrations  
Silo Bank - 255 Realizations Time = 1000 years

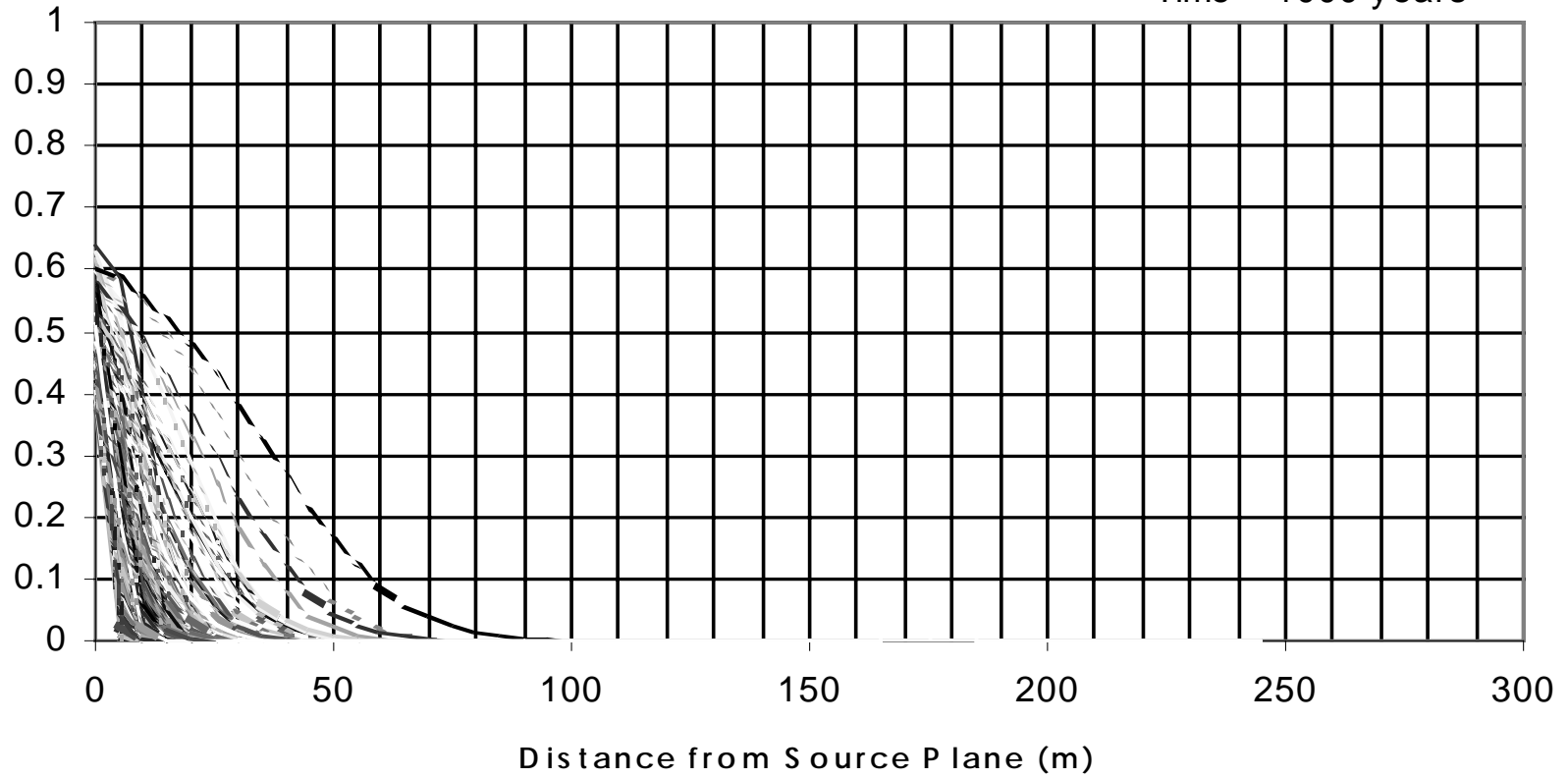
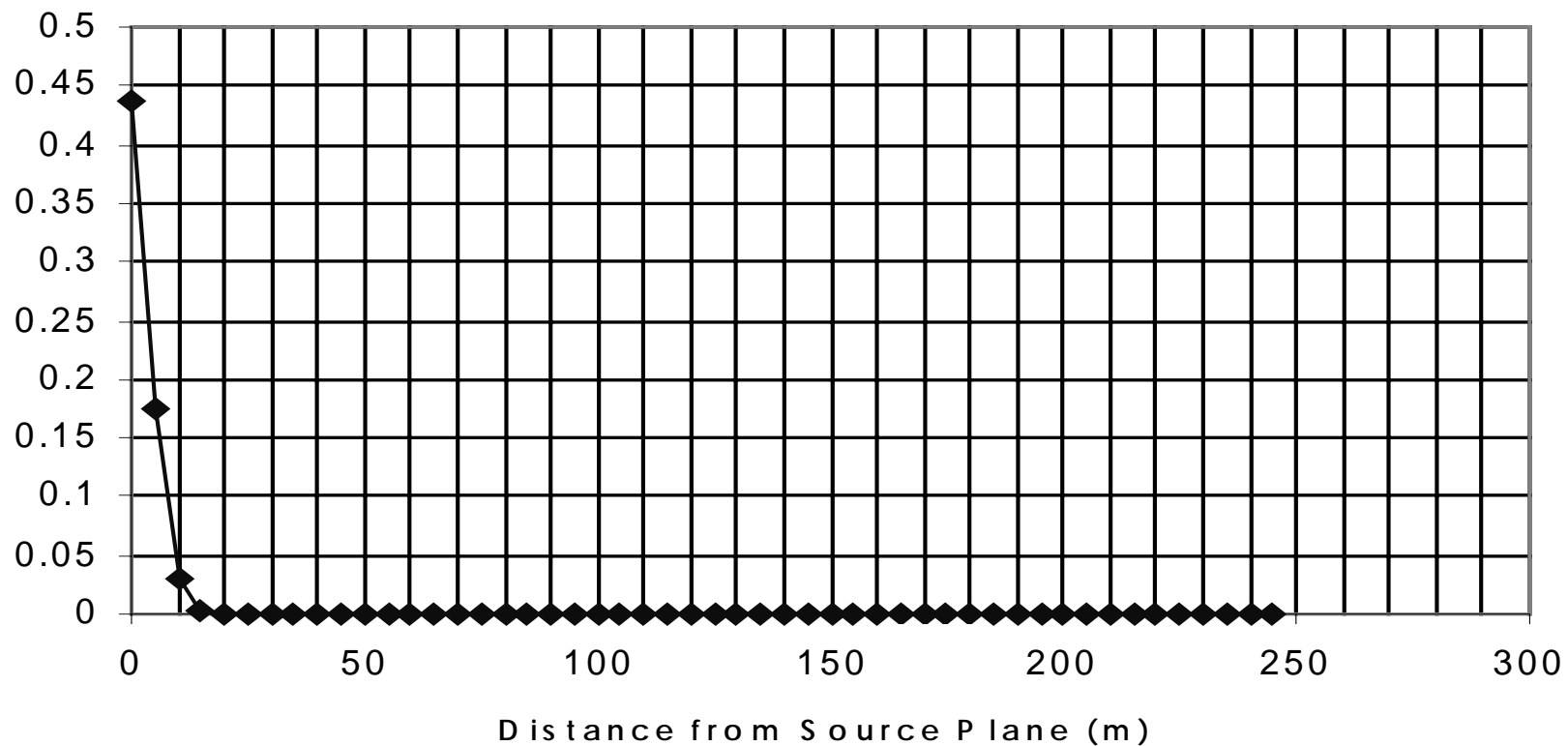


Figure 11b Jabiluka Review - Groundwater Hydrology  
Radium 226 Monte Carlo Simulations  
Median Relative Concentration - Silo Bank - 255 Realizations

Time = 1000 years



**Figure 11c Jabiluka Review - Groundwater Hydrology  
Radium 226 Monte Carlo Simulations Relative Concentrations  
Silo Bank - 255 Realizations - Constant Source Concentration**

Time = 1000 years

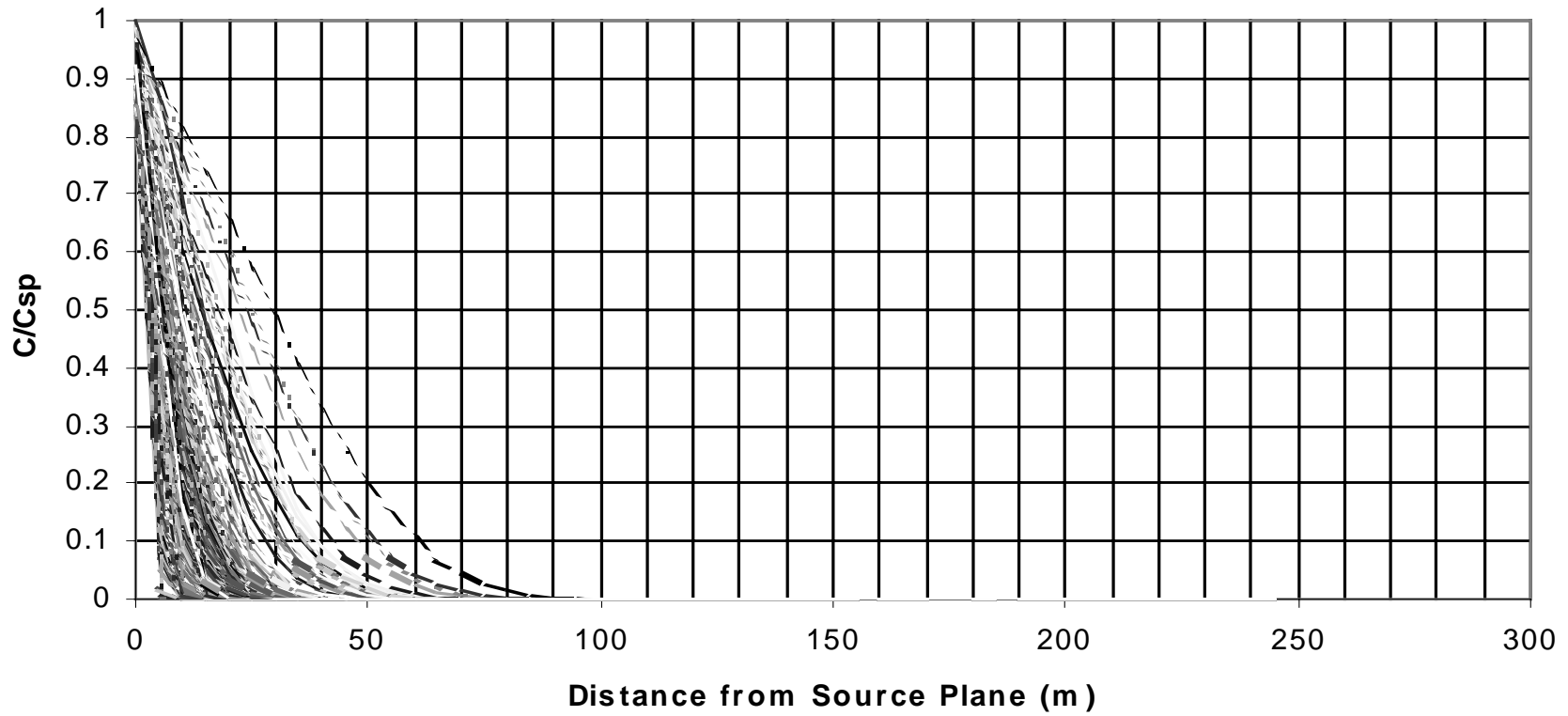


**Figure 11d Jabiluka Review - Groundwater Hydrology  
Radium 226 Monte Carlo Simulations  
Median Relative Concentration - Silo Bank - 255 Realizations  
- Constant Source Concentration**

Time = 1000 years

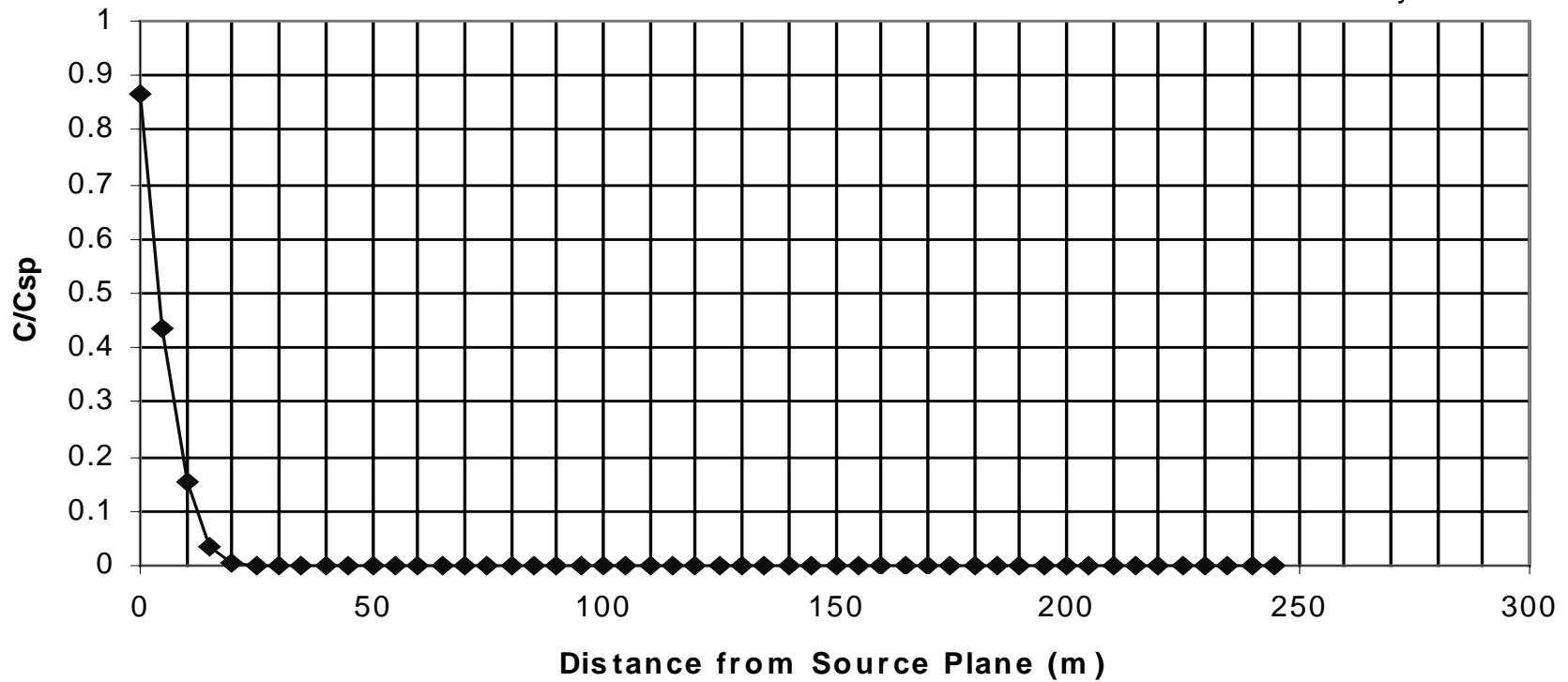


Figure 12a Jabiluka Review - Groundwater Hydrology  
Non-Reactive Contaminant - Monte Carlo Simulations  
Relative Concentrations - Mine Void Fill - 255 Realizations

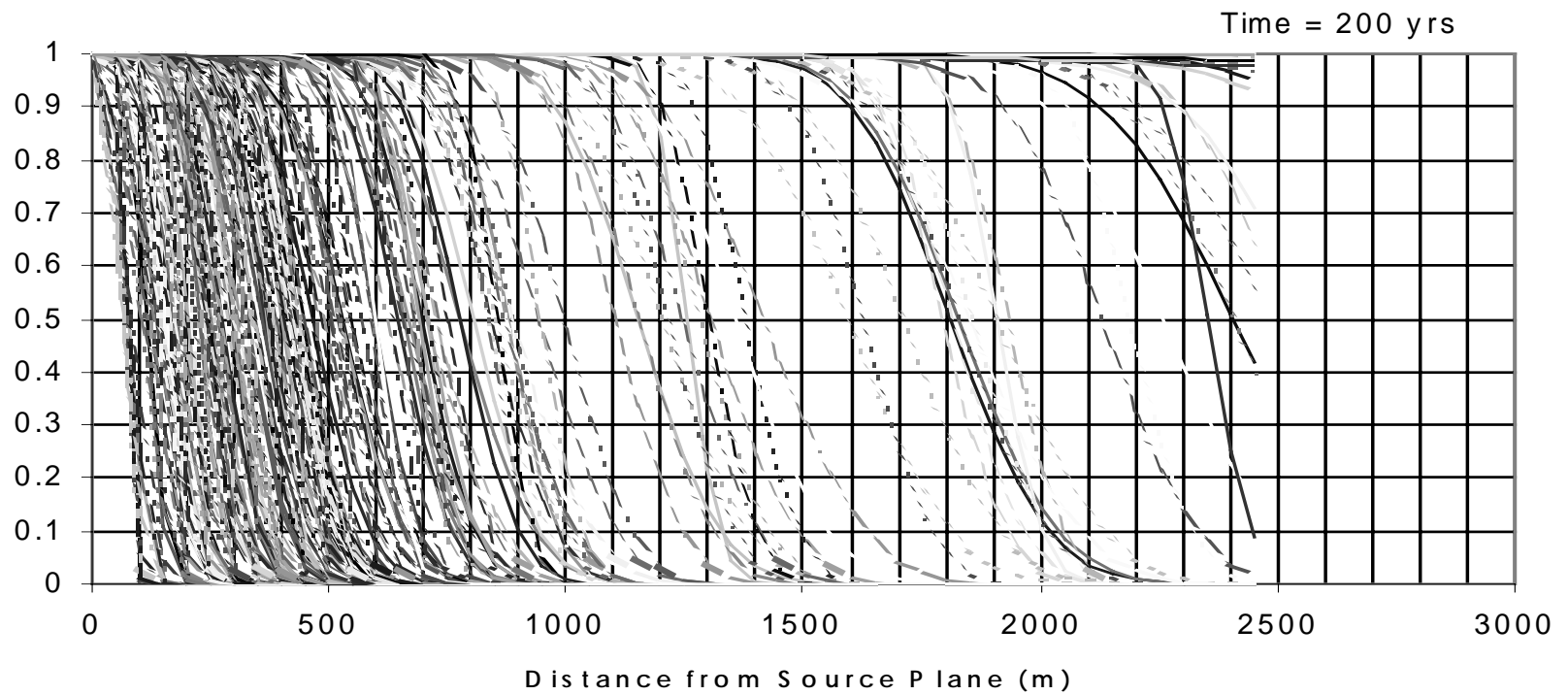


Figure 12b Jabiluka Review - Groundwater Hydrology  
Non-reactive Contaminant - Monte Carlo Simulations  
Median Relative Concentrations - Mine Void Fill - 255 realizations

Time = 200 yrs

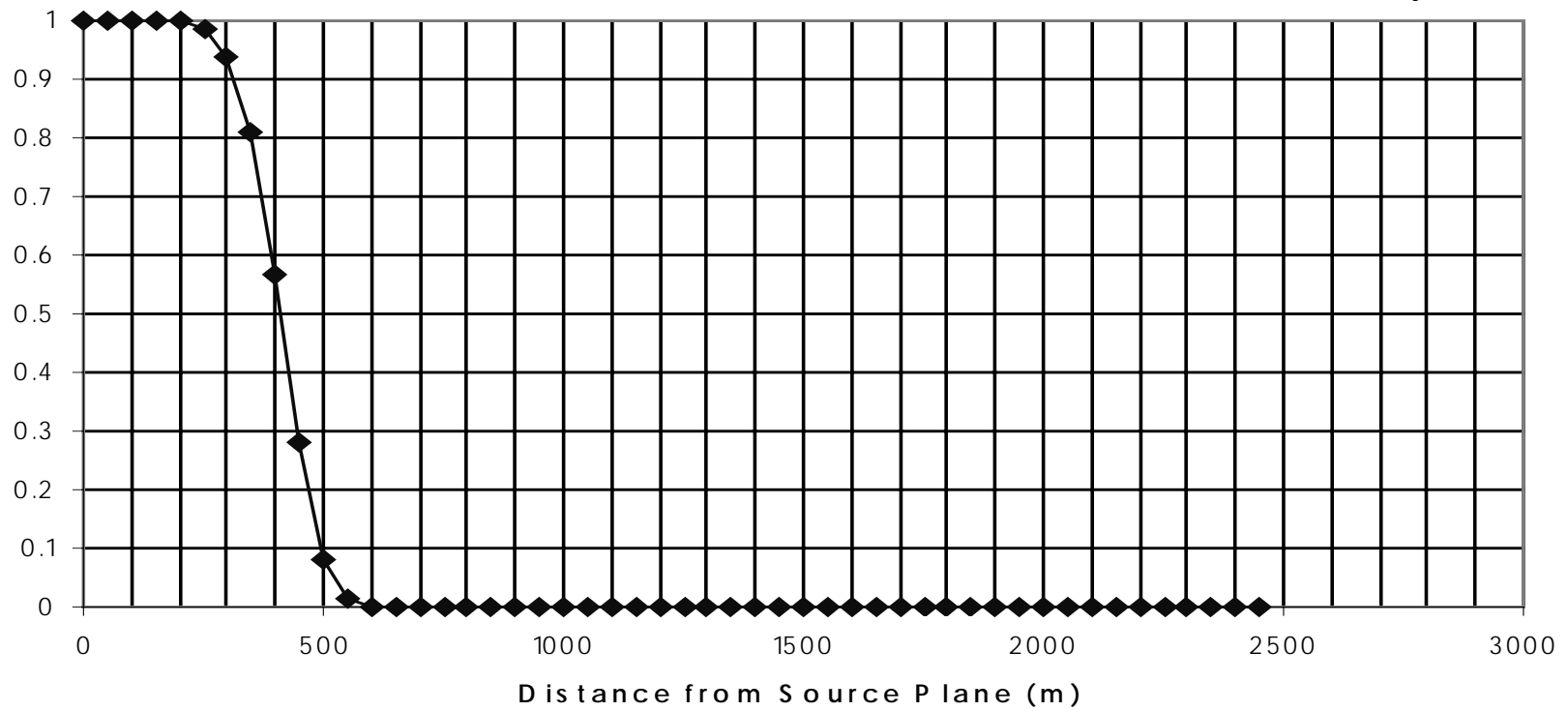


Figure 13a Jabiluka Review - Groundwater Hydrology  
Uranium Contaminant - Monte Carlo Simulations  
Relative Concentrations - Mine Void Fill - 255 Realizations

Time = 1000 yrs

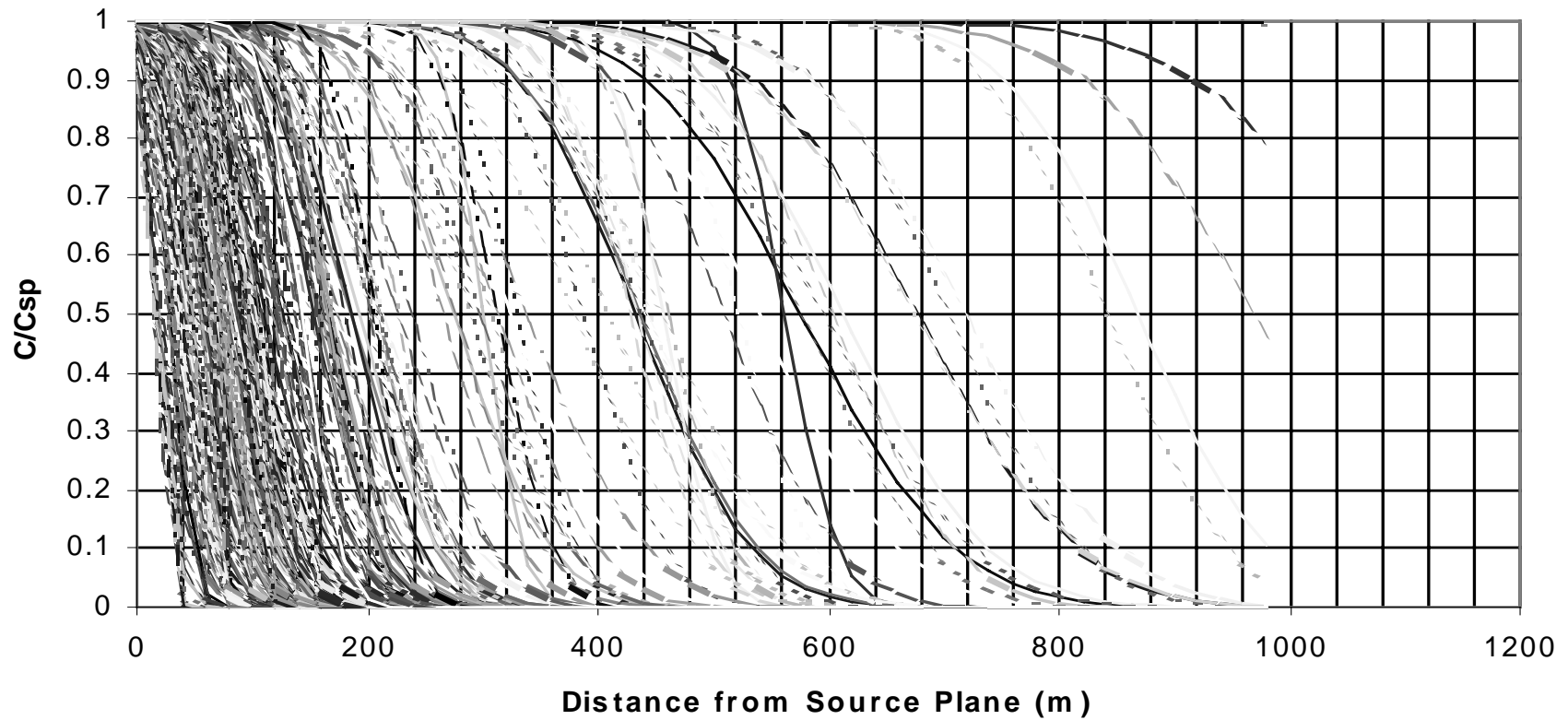


Figure 13b Jabiluka Review -Groundwater Hydrology  
Uranium Contaminant -M onte Carlo Simulations  
M edian R elative C oncentrations -M ine V oid F ill -255 R ealizations

Time =1000 yrs

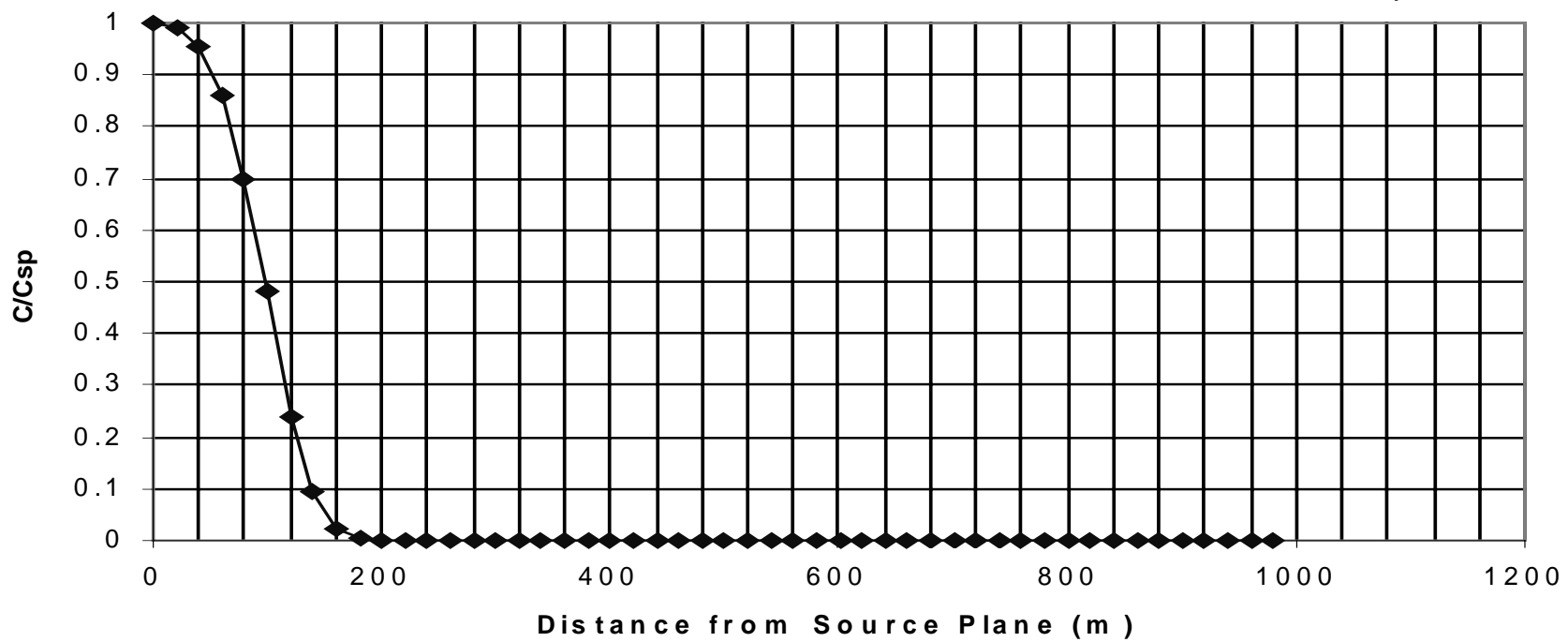


Figure 14a Jabiluka R review -Groundwater Hydrology  
Radium 226 Contaminant - Monte Carlo Simulations  
Relative Concentrations -Mine Void Fill - 255 Realizations

Time = 1000 years

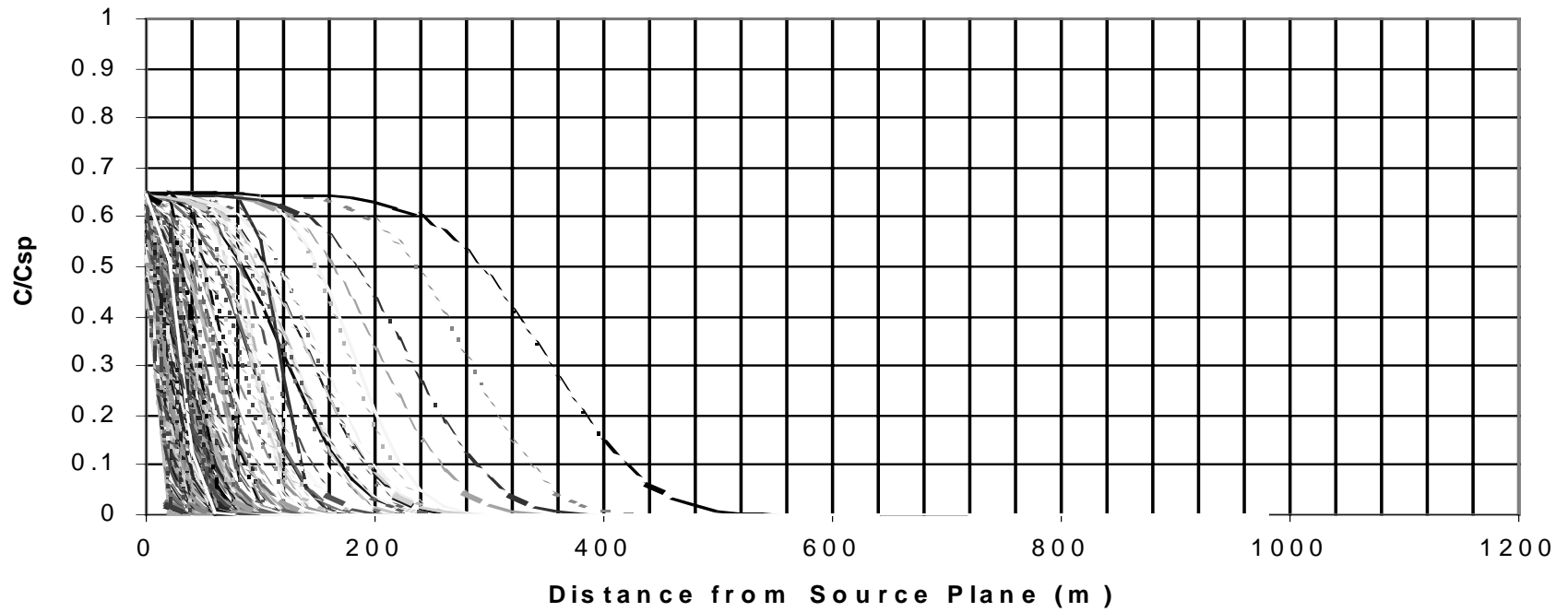
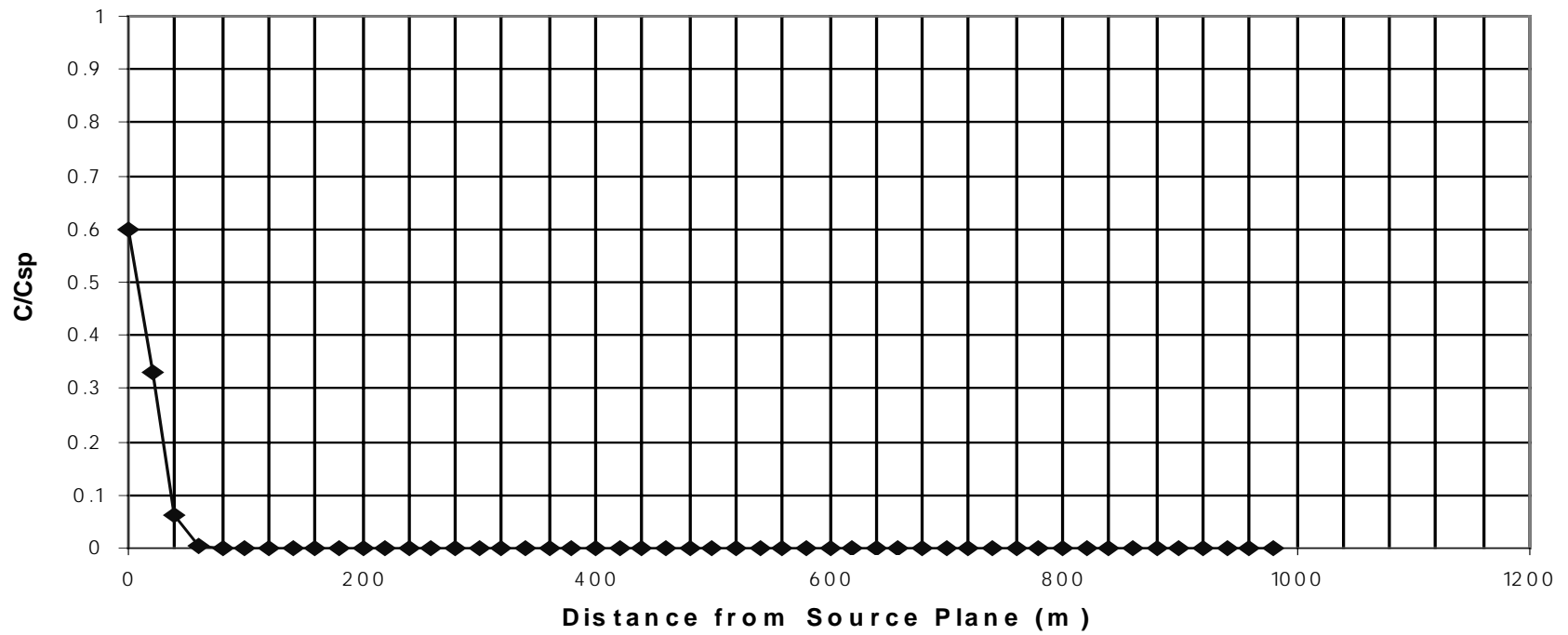
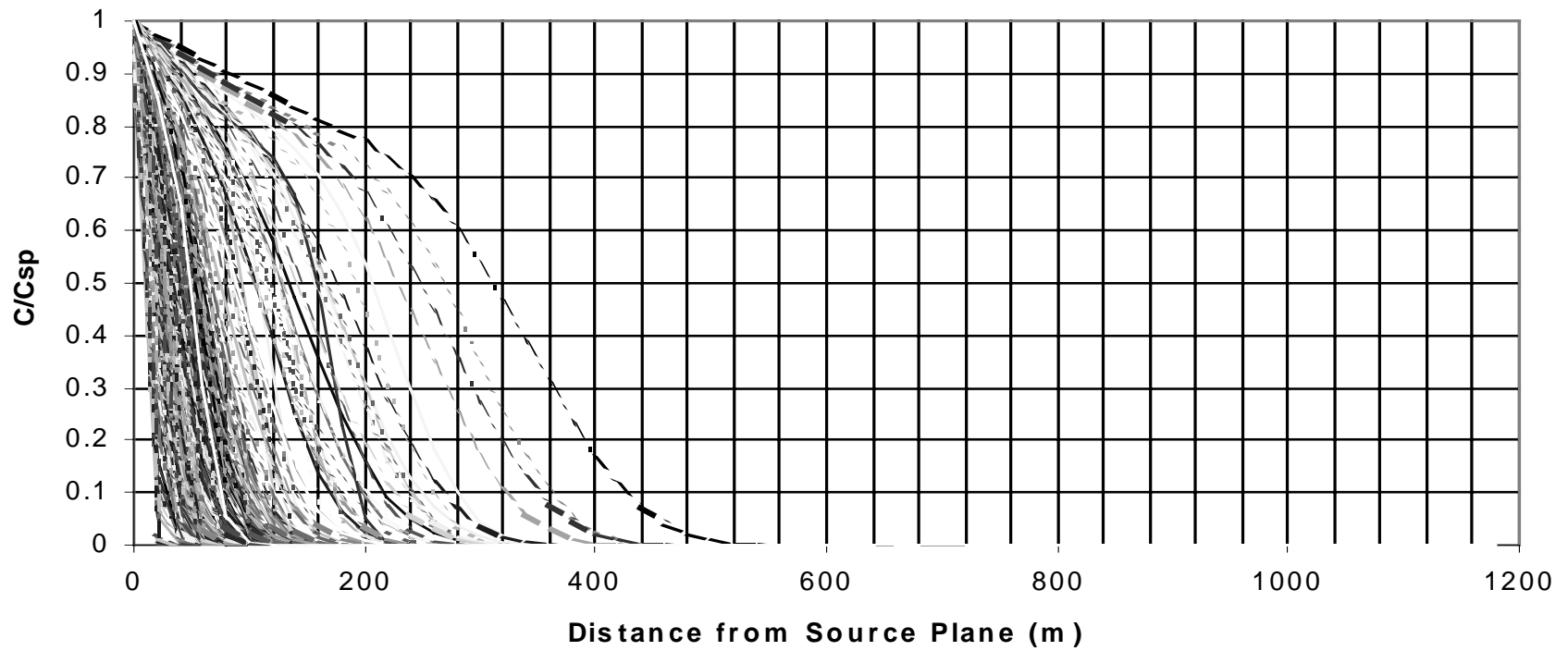


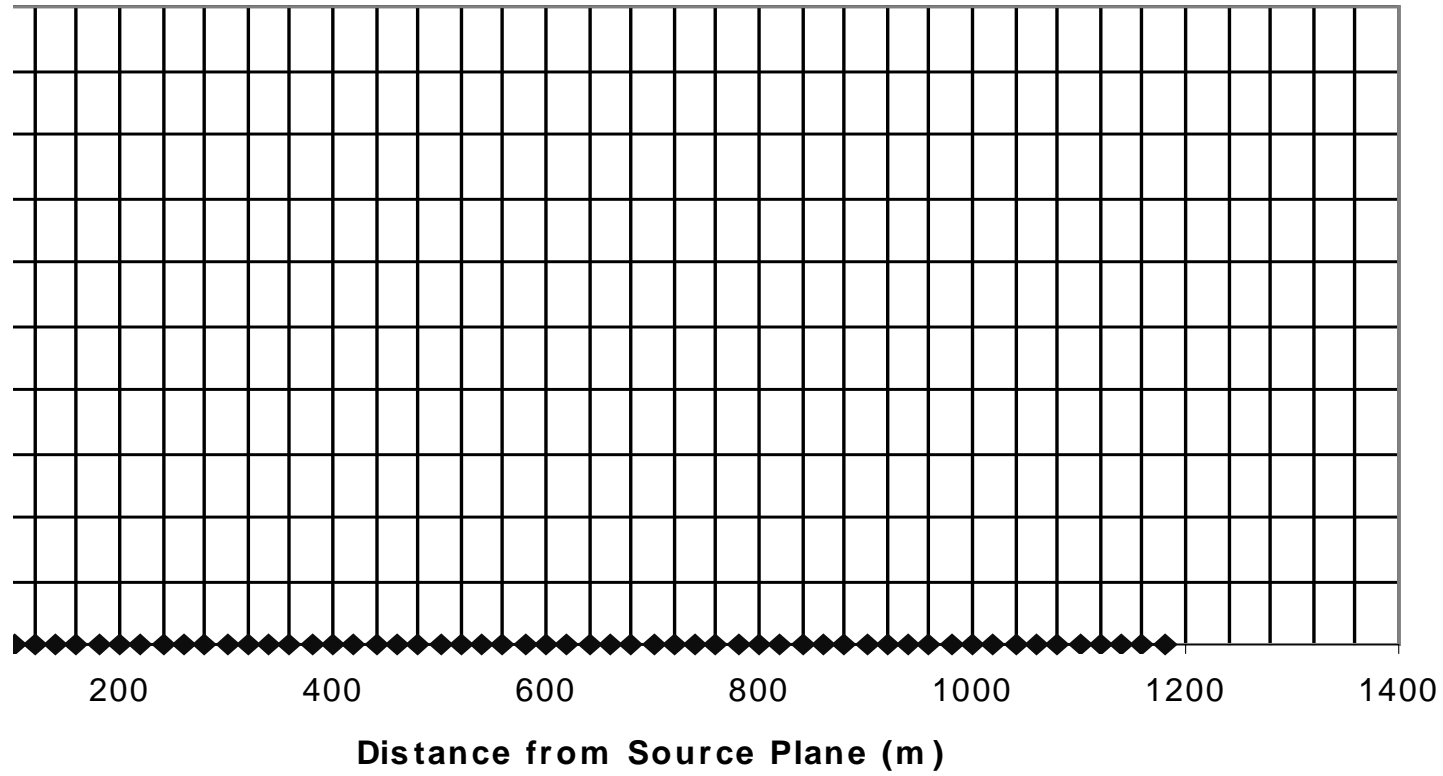
Figure 14b Jabiluka Review- Groundwater Hydrology  
Radium 226 Contaminant - Monte Carlo Simulations  
Median Relative Concentrations - Mine Void Fill - 255 Realizations



**Figure 14c Jabiluka Review -Groundwater Hydrology  
Radium 226 Monte Carlo Simulations Relative Concentrations  
Mine Void Fill - 255 Realizations- Constant Source Concentration**



**Figure 14d Jabiluka Review - Groundwater Hydrology**  
**um 226 - Monte Carlo Simulations - Median Relative Concentrations**  
**Mine Void Fill - 255 Realizations - Constant Source Concentration**



## Appendix A Domenico-Palciauskas-Robins Analytical Solute Transport Equation

This equation provides the concentration distribution in three co-ordinate directions within a groundwater flow system subject to: - advection in one co-ordinate direction, dispersion in three co-ordinate directions; retardation and radioactive decay (Domenico & Schwartz 1990).

$$C(x, y, z, t) = \left(\frac{C_0}{8}\right) * \exp\left\{\left(\frac{x}{2\alpha_x}\right)\left[1 - \left(1 + (4\lambda\alpha_x / v_c)\right)^{\frac{1}{2}}\right]\right\} * \operatorname{erfc}\left[\frac{x - v_c t (1 + (4\lambda\alpha_x / v_c))^{\frac{1}{2}}}{2(\alpha_x v_c t)^{\frac{1}{2}}}\right] * \left\{\operatorname{erf}\left[\frac{(y + Y/2)}{2(\alpha_y x)^{\frac{1}{2}}}\right] - \operatorname{erf}\left[\frac{(y - Y/2)}{2(\alpha_y x)^{\frac{1}{2}}}\right]\right\} * \left\{\operatorname{erf}\left[\frac{(z + Z/2)}{2(\alpha_z x)^{\frac{1}{2}}}\right] - \operatorname{erf}\left[\frac{(z - Z/2)}{2(\alpha_z x)^{\frac{1}{2}}}\right]\right\} \quad (1)$$

where the symbols above have the following meaning: (see also fig A-1)

$C(x,y,z,t)$	concentration at point (x,y,z) at time t. [M/L <sup>3</sup> ]
$C_0$	source concentration [M/L <sup>3</sup> ]
x,y,z	co-ordinate distances [L]
$\alpha_x$	dispersivity in x co-ordinate direction [L]
$\alpha_y$	dispersivity in y co-ordinate direction [L]
$\alpha_z$	dispersivity in z co-ordinate direction [L]
$v_c$	contaminant linear velocity in the x co-ordinate direction.[L/T]
t	time [T]
Y	width of source area[L]
Z	height of source area[L]
$\lambda$	radioactive decay constant [T <sup>-1</sup> ]

*erfc* and *erf* are the complimentary error and error function respectively and

$\lambda = \ln 2/t_{1/2}$  where  $t_{1/2}$  is the half life [T]

also  $v_c = v_D / (n R_f)$  where

$v_D$	Darcy velocity [L/T]
$n$	porosity of the water bearing formation (o)
$R_f$	retardation factor (o)

given by  $R_f = 1 + (1-n)\rho K_d/\theta$ .....

where

$\theta$	volumetric water content of the formation
----------	---

$K_d$	distribution co-efficient [ $L^3/M$ ]
$\rho$	mass density of the formation [ $M/L^3$ ]
$(1-n)\rho$	dry bulk density of the formation [ $M/L^3$ ]
$\theta = n$	under saturated conditions.

## Decrease of Source Concentration with Time

### Non-radioactive Component

For the case where the source concentration decreases due to leaching and the decrease is described by the equation:

$$C = C_0 e^{-\gamma t} \quad (2)$$

where  $\gamma$  is the source leaching decay constant ( $T^{-1}$ ), then equation (1) without radioactive decay is given by the following added modifications (Kalf 1999):

$$C(x, y, z, t) = \left(\frac{C_0}{8}\right) * \exp\left\{-\gamma t + \left(\frac{x}{2\alpha_x}\right)\left[1 - \left(1 - (4\gamma\alpha_x / v_c)\right)^{\frac{1}{2}}\right]\right\} * \\ \operatorname{erfc}\left[\frac{x - v_c t \left(1 - (4\gamma\alpha_x / v_c)\right)^{\frac{1}{2}}}{2(\alpha_x v_c t)^{\frac{1}{2}}}\right] * \left\{\operatorname{erf}\left[\frac{(y + Y/2)}{2(\alpha_y x)^{\frac{1}{2}}}\right] - \operatorname{erf}\left[\frac{(y - Y/2)}{2(\alpha_y x)^{\frac{1}{2}}}\right]\right\} * \\ \left\{\operatorname{erf}\left[\frac{(z + Z/2)}{2(\alpha_z x)^{\frac{1}{2}}}\right] - \operatorname{erf}\left[\frac{(z - Z/2)}{2(\alpha_z x)^{\frac{1}{2}}}\right]\right\} \quad (3)$$

### Radioactive Components

For 1<sup>st</sup> order decrease due to leaching and radioactive decay at the source, and where the source concentration is described by:

$$C = C_0 e^{-(\gamma + \lambda)t} \quad (4)$$

the added modifications to equation (1) are then (Kalf 1999):

$$C(x, y, z, t) = \left(\frac{C_0}{8}\right) * \exp\left\{-\left(\gamma + \lambda\right)t + \left(\frac{x}{2\alpha_x}\right)\left[1 - \left(1 - (4(\gamma + \lambda)\alpha_x / v_c) + (4\lambda\alpha_x / v_c)\right)^{\frac{1}{2}}\right]\right\} * \\ \operatorname{erfc}\left[\frac{x - v_c t \left(1 - (4(\gamma + \lambda)\alpha_x / v_c) + (4\lambda\alpha_x / v_c)\right)^{\frac{1}{2}}}{2(\alpha_x v_c t)^{\frac{1}{2}}}\right] * \left\{\operatorname{erf}\left[\frac{(y + Y/2)}{2(\alpha_y x)^{\frac{1}{2}}}\right] - \operatorname{erf}\left[\frac{(y - Y/2)}{2(\alpha_y x)^{\frac{1}{2}}}\right]\right\} * \\ \left\{\operatorname{erf}\left[\frac{(z + Z/2)}{2(\alpha_z x)^{\frac{1}{2}}}\right] - \operatorname{erf}\left[\frac{(z - Z/2)}{2(\alpha_z x)^{\frac{1}{2}}}\right]\right\} \quad (5)$$

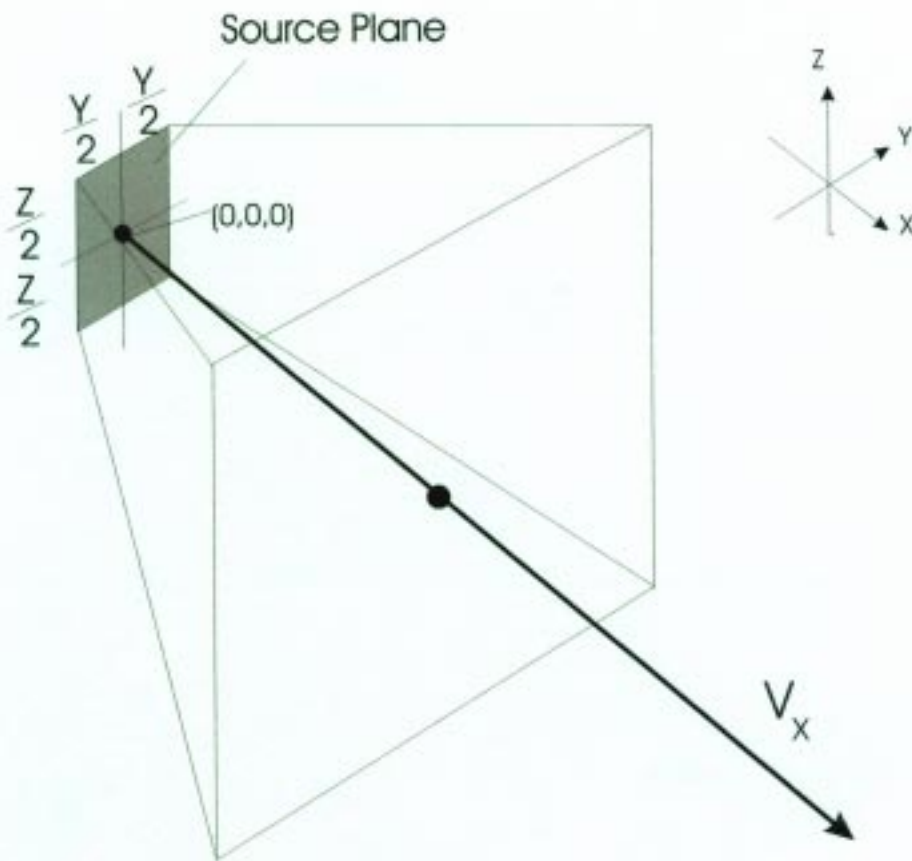


## FIGURE A1

Jabiluka Technical Review  
 Groundwater Hydrology  
 Analytical Model Migration  
 Geometry and Spreading Directions

Kalf and Associates Feb 99

## **Appendix B**

**Simulation of leaching of non-reactive and radionuclide contaminants from proposed Jabiluka silo banks**

# Appendix B

## Simulation of leaching of non-reactive and radionuclide contaminants from proposed Jabiluka silo banks

Groundwater flow through and past the proposed silos will be nearly horizontal, and to the east. The modelling described in this section was performed to provide estimates of local contaminant concentrations in groundwater near the silos. The results were then used in the regional contaminant transport model to predict the extent of movement of contaminants towards Swift Creek.

The regional Monte-Carlo analytical solute transport model is presented in Appendix A.

The model described here examines the interaction of groundwater flow between the silo tailings paste and the Kombolgie Formation fractured sandstone and determines the mobility of both non-reactive and reactive contaminants.

For these series of simulations a 3D saturated/unsaturated flow and solute transport model code MODFLOW-SURFACT (MS)<sup>1</sup> was used. MS is an enhanced and much advanced version of the standard USGS MODFLOW saturated groundwater flow code. MS uses a Total Variation Diminishing (TVD) van Leer flux limiting solution scheme for the solute transport equation producing very accurate mass balance results. MS includes linear and non-linear adsorption isotherms, 1<sup>st</sup> order decay processes (radioactive/biological) and multi-species contaminants with daughter decay simulation if required.

### Groundwater flow and a single silo

The MS code was set up to examine the leaching characteristics of a single silo repository. For these simulations a finite difference mesh of cells, each 1 m x 1 m in dimension were used representing a 2D one metre thick single horizontal layer through the silo. A steady state hydraulic gradient of 0.03 was used for all simulations under complete saturated flow conditions. For a single silo the model has dimensions 100 m x 50 m in the x and y directions respectively with the gradient in the x direction. Constant heads were applied at each end of the model to achieve the required gradient.

A gradient of 0.03 was selected as this is approximately the hydraulic gradient within the proposed silo bank area based on data provided by ERA.

Figures B1 and B2 present part of the hydraulic head contours and velocity vector magnitudes around a simulated single silo for ratios of aquifer permeability ( $K_a$ ) to silo tailings paste permeability ( $K_s$ ) of 10 and 1000. Note that the figures show only 36 m of the full 50 m model width.

Each contour in these figures represents a 0.1 m increment in the hydraulic head.

As would be expected, although some groundwater flow is directed into the silo, as the permeability ratio  $K_a/K_s$  increases flow around the edges of the silo<sup>2</sup> dominates.

---

<sup>1</sup> The program was developed by Hydrogeologic Ltd in the US, is internationally recognised and has been used to simulate high and low level radioactive waste sites in that country.

<sup>2</sup> The pattern of the flow is dimensionless in this case and depends only on the permeability ratios and not the absolute values of permeability of the aquifer or silo paste.

## Non-reactive contaminant movement

### Single silo

Under the groundwater flow conditions described above, two scenarios were examined: the first for an aquifer permeability  $K_a = 0.01$  m/day and paste permeability

$K_s = 10^{-4}$  m/day (ratio  $K_a/K_s = 100$ ); the second for  $K_a = 0.01$  m/day and  $K_s = 10^{-5}$  m/day (ratio  $K_a/K_s = 1000$ ).

Dispersivity values adopted in the fractured sandstone for all simulations were longitudinal dispersivity  $\alpha_L = 1.0$  m; transverse dispersivity  $\alpha_T = 0.1$  m and vertical dispersivity  $\alpha_V = 0$  m. For the tailings paste the values adopted were longitudinal dispersivity  $\alpha_L = 0.1$  m; transverse dispersivity  $\alpha_T = 0.01$  m and vertical dispersivity  $\alpha_V = 0$  m.

Porosity was set in the aquifer at a conservative 5% ( $P_a = 5\%$ ) and in the silo at 10% ( $P_s = 10\%$ ). Using 5% is conservative for the near field simulations since it will increase the source concentrations somewhat relative to simulations conducted at lower effective porosity values. Note however that porosity is not a sensitive parameter for concentrations near the source. Sensitivity runs indicate that a decrease of porosity from 0.05 to 0.01 will only decrease the concentrations near the source by about 10%.

The simulation was run over a period of 200 years.

The results are presented in figures B-3a, b, c and B-4a, b and c. In each case (a) is a plan view of percentage normalized contaminant concentrations  $C/C_o \times 100$ , (b) is a longitudinal profile through the center of the silo in the direction of flow showing the percentage normalized concentrations, and (c) is a profile at right angles to the flow direction 2 m from the down-gradient edge of the silo showing percentage normalized concentrations. Note that the plot minimum concentration (dark blue) was set at 0.1%.

In figures B-3a, b, c a plume emanates from the silo but the maximum concentration near to the source (2 m down-gradient from the edge of the silo) is less than 10% of the source concentration, decreasing to less than 5% at 100 m down gradient.

For figures B-4a, b, c with a paste permeability of  $10^{-5}$  m/day, the near source concentration is less than 2% of the source values.<sup>3</sup>

### Series of silos

In order to determine the effect of a series of silos on the concentration distribution, four silos<sup>4</sup> were examined using a model with adjacent boundaries taken along two longitudinal planes of flow symmetry. Silos were positioned with their centers 30 m apart<sup>5</sup>. This section would be representative of a 30 m wide part of the continuous double row of silos. For a group of silos the model dimensions are 100 m x 30 m in the x and y directions respectively with the gradient in the x direction.

The concentration distributions after a 200 year period for permeability ratios of 100 ( $K_a = 0.01$  m/d,  $K_s = 10^{-4}$  m/day) and 1000 ( $K_a = 0.01$  m/day,  $K_s = 10^{-5}$  m/day) are shown in figures B-5a, b, c and B-6a, b, c respectively.

---

<sup>3</sup> As an hypothetical example in this case: if the source were sulphate at 20 000 mg/L then at 2 m the concentration would be 2% of 20 000 mg/L or 400 mg/L.

<sup>4</sup> The scope, budget and timing for the current report does not permit simulation of the entire series of silos proposed.

<sup>5</sup> Data provided by ERA Jan 1999

In these cases concentrations in a longitudinal profile along one of the symmetry planes through the center of the silos (top or bottom profiles yield the same values) were plotted. They were also plotted for a section at right angles, two metres down-gradient from the edges of the silos.

For the first case, the downstream concentrations reach a maximum of 12% of the source concentrations whilst in the second case they reach a maximum of 3%.

## **Reactive contaminant movement**

### **Series of silos**

#### *Uranium*

Uranium movement was simulated near field (2 m down-gradient from silos) over a 1000 year period, using a distribution co-efficient  $K_d$  of 1 mL/g (conservative retardation factor of 21) and a permeability ratio between tailings paste and aquifer permeability of 100 ( $K_a = 0.01$  m/day and  $K_s = 0.0001$  m/day). The results are presented in figures B-7a, b and c. Note that the same retardation was applied to the tailings paste.

The results indicate maximum concentrations of 18% near the source.

#### *Radium 226*

Figures B-8a, b, c present the concentration distribution near field results for Radium 226 after 1000 years for a permeability ratio of 100 ( $K_a = 0.01$  m/day and  $K_s = 10^{-4}$  m/day and a distribution co-efficient of 5 mL/g (conservative retardation factor 101).

The results show effective immobilisation for the permeabilities and retardation factor considered. The plot of concentrations through the silos show a decrease in the maximum concentration due to decay of radium 226 during the 1000 year period (radium 226 half life 1600 yrs) and about 5% concentration at 2 m from source.

Also simulated was the case where the source radium 226 concentration stays constant as a result of thorium decay. That is, it was assumed that the radium 226 derived from thorium 230 decay would be sufficient to replace the decayed radium at the source over 1000 years. These results showed only a relatively small increase in the maximum concentration 2 m down gradient from the source from the previous 5% to a value of 6%.

## **Effect of single major fault/fracture system**

The effect of a single fault /fracture system within the aquifer between two silos (but not through them) was also examined. Note that it can be assumed that in the case of discovery of a geological feature of this type running through a proposed silo site, the site would not be utilised or the fissure would be grouted to prevent groundwater flow along it.

The fault is assumed to be 2 m wide (1 m each side of the plane of symmetry) and to have a permeability of 0.5 m/day (fig 9). Two cases were simulated. The first is a repeat of the case of a non-reactive contaminant given in figures B-3a, b, c, but with included fault, over a period of 200 years, and the second of the case given in figures B-7a, b, c for uranium, but with a fault included, over a period of 1000 years.

Parameters for these cases are those used previously except that the fault zone was also assigned a longitudinal dispersivity of 1 m and a transverse value of 0.1 m and vertical 0 m.

The results for each of these cases are shown in figures B-10a, b, c and figures B-11a, b, c respectively.

For the 200-year simulation comparison made between the cases with and without a fault zone indicate that the concentrations are less with the fault zone than without it in the near field. It would appear that higher velocities in the fault zone remove solute mass more rapidly, but because silo mass flux is rate-limited (ie the silo cannot supply sufficient mass) the concentration is lower in the fault zone in this case.

For the 1000 year simulation the effect of the fault is to cause increased leaching which reduces the concentrations in the silos to less than 5–10% with very low concentrations in a down gradient direction after this time.

### **Leaching rate – non-reactive contaminant**

The source leaching rate for a non-reactive contaminant was determined using the case depicted in figure B-5a over a period of 1000 years. To determine this rate, concentrations were calculated 2 m down-gradient from the set of silos and a curve fitted to the numerical model data.

The results indicate a leaching decay constant  $\gamma$  of  $4 \times 10^{-6} \text{ day}^{-1}$ . Thus the source decay by leaching is given by:

$$C = C_0 e^{-0.000004 t}$$

where C is the concentration at the ‘source’<sup>6</sup>;  $C_0$  the initial concentration at the ‘source’, and t the time in days. This constant has been used in the analytical model described in Appendix A.

Note that this constant only applies to the assumed hydrogeological conditions at the site.

### **Non-reactive contaminant movement – higher paste permeability**

The final simulation examines the case presented in figures B-3a ,b, c but with a tailings paste permeability of  $10^{-3} \text{ m/day}$ . The results are presented in figures B-12a, b and c and indicate severe leaching of the contaminant over the 200-year period.

### **Mine void fill**

The mine void fill tailings paste will respond in a similar manner to the single silo, but at a larger scale. Estimates made of the likely relative concentrations immediately down-gradient of the fill for a non-reactive contaminant are given in table B-1.

It is recommended that a more complete numerical simulation of the mine void fill be set up to reproduce as far as possible the actual site conditions to verify the above estimates.

---

<sup>6</sup> The ‘source’ in this instance is the concentration at 2 m, not the concentration in the silo.

**Table B-1** Tailings paste permeability and immediate down-gradient  
Relative Concentration % Non-Reactive Contaminant in Mine Fill Void

<b>Tailings Paste Permeability m/day</b>	<b>Relative Concentration %</b>
$10^{-5}$	<5
$10^{-4}$	<30
$10^{-3}$	80-90

## Appendix B Figures

**Note:**

All grid dimensions in the figures which show plan views of the finite difference grid used in the silo leaching model (fig B-1a, B2a,...B12a) are in metres. Each grid square is 1 m x 1 m.

# FIGURE B-1

## Jabiluka Review - Groundwater Hydrology

Silo/Aquifer Head and Velocity Vectors

$K_s = 0.001(m/d)$ ;  $K_a=0.01 (m/d)$  - Gradient 0.03 -Steady State

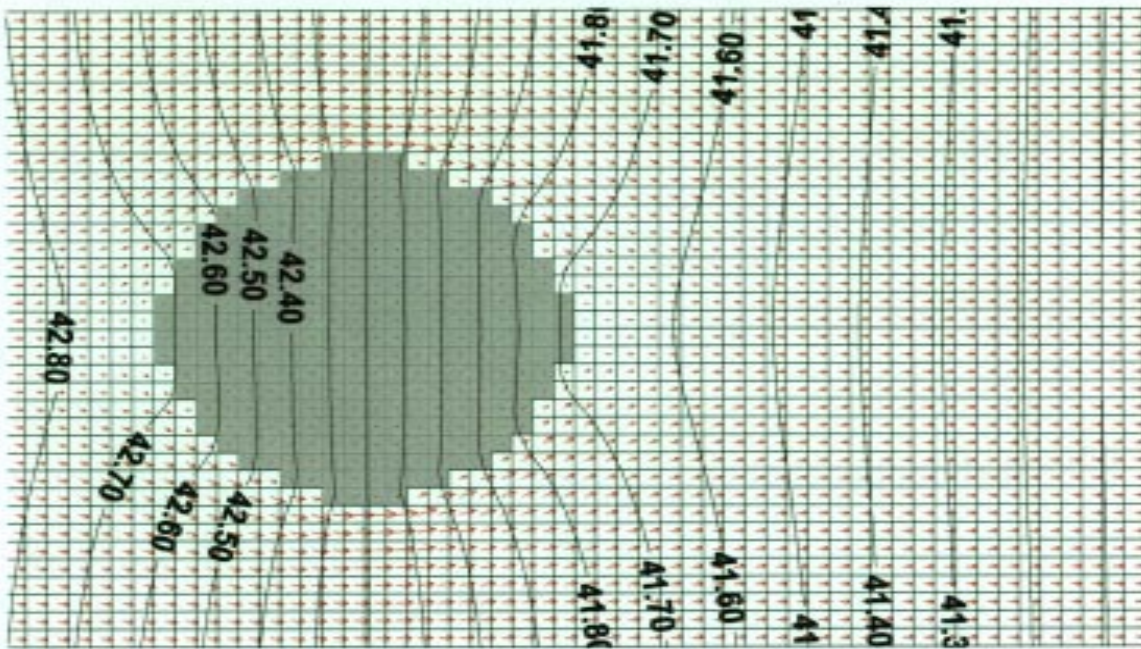




## FIGURE B-3a

### Jabiluka Review - Groundwater Hydrology

Silo/Aquifer Concentration % - non-reactive contaminant

$K_s = 1e-4$  (m/d);  $K_a=0.01$  (m/d) - Gradient 0.03 -  $P_a=5\%$ ;  $P_s=10\%$ ; 200 yrs

---

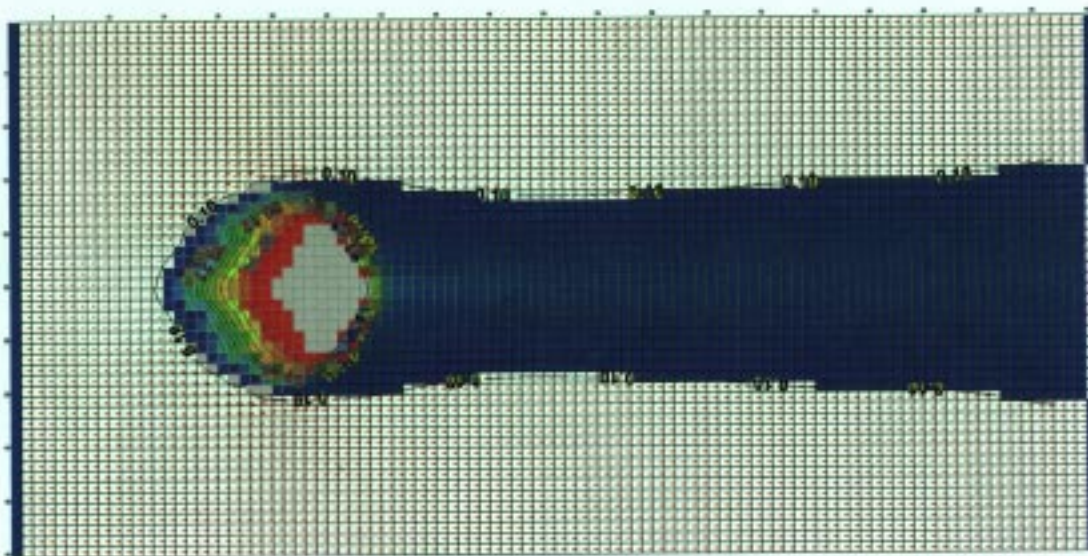


Figure B-3b - Concentration % Profile - Row 25 - non-reactive - 200 yrs

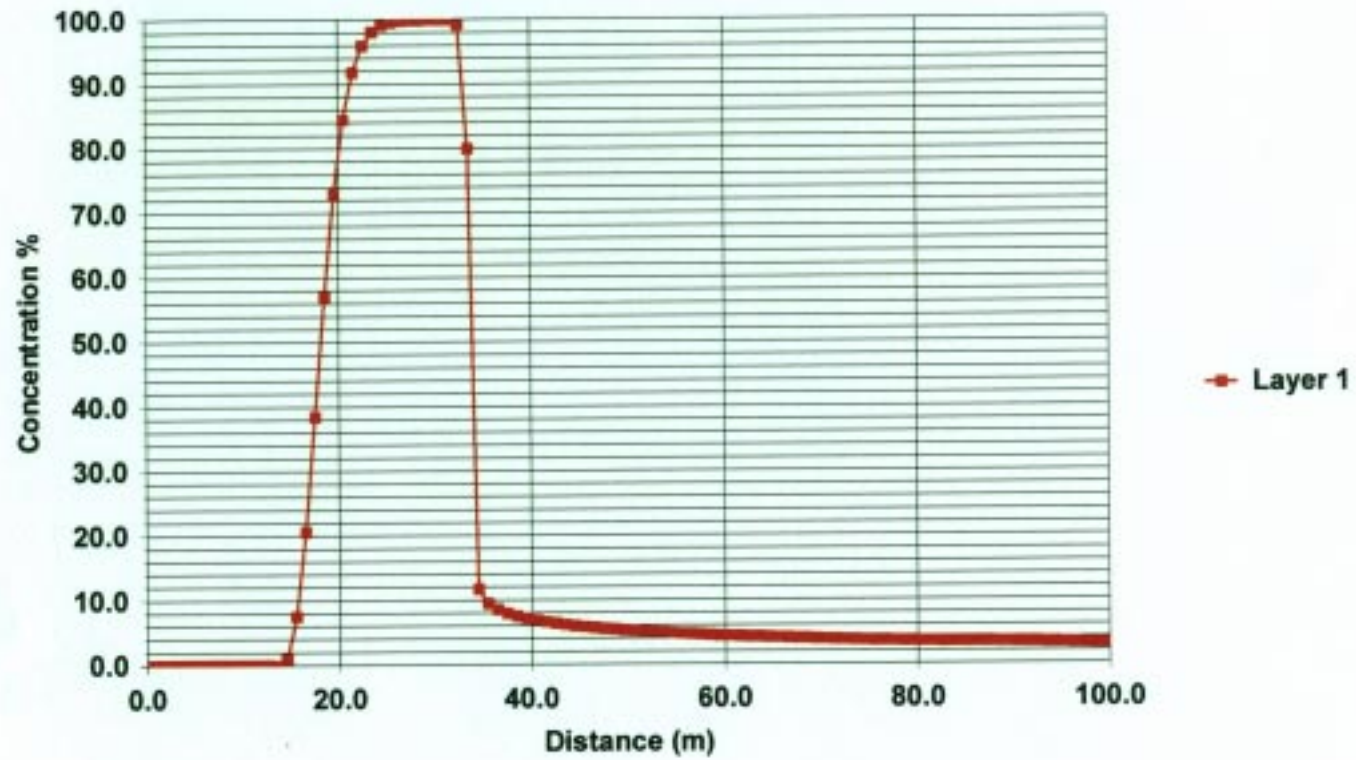
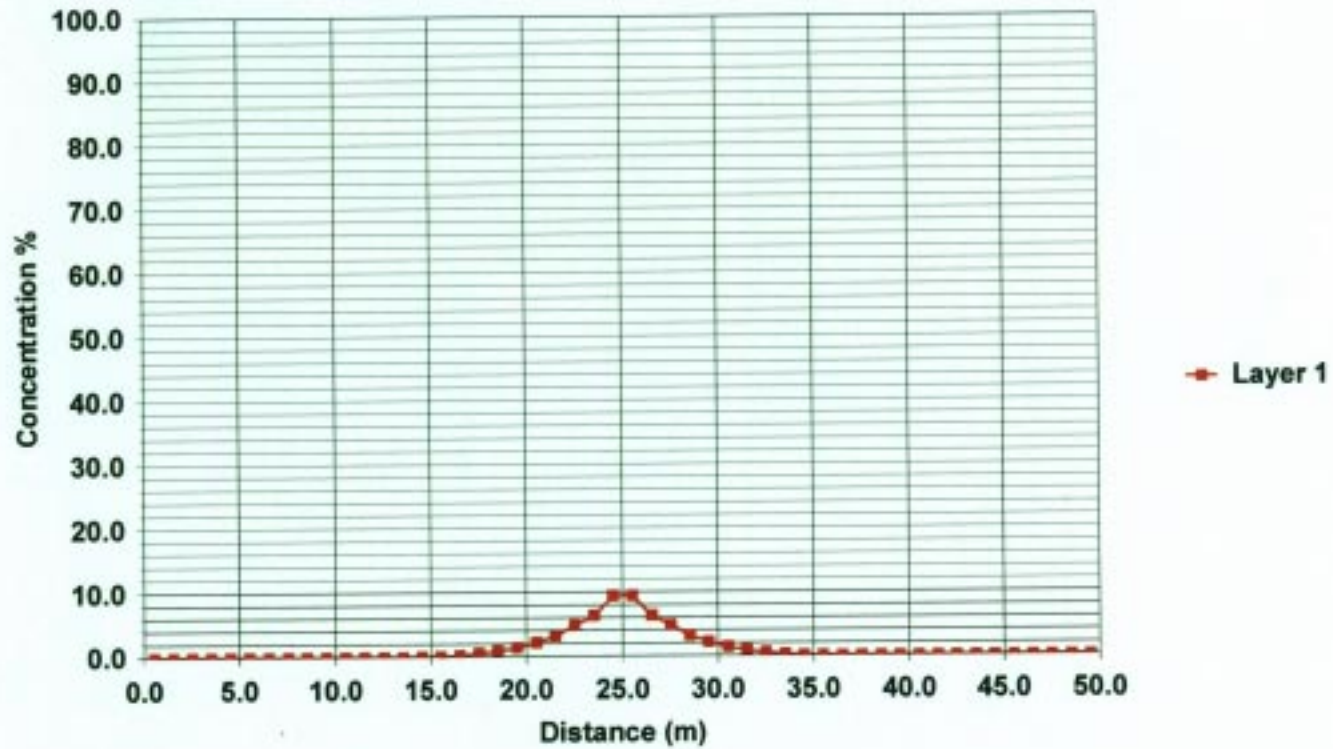


Figure B-3c - Concentration % Profile - Col 36 - non-reactive - 200 yrs



## FIGURE B-4a

### Jabiluka Tech Review - Groundwater Hydrology

Silo/Aquifer Concentration % -non-reactive contaminant

$K_s = 1e-5$  (m/d);  $K_a=0.01$  (m/d) - Gradient 0.03 - $P_a=5\%$ ;  $P_s=10\%$ ; 200 yrs

---

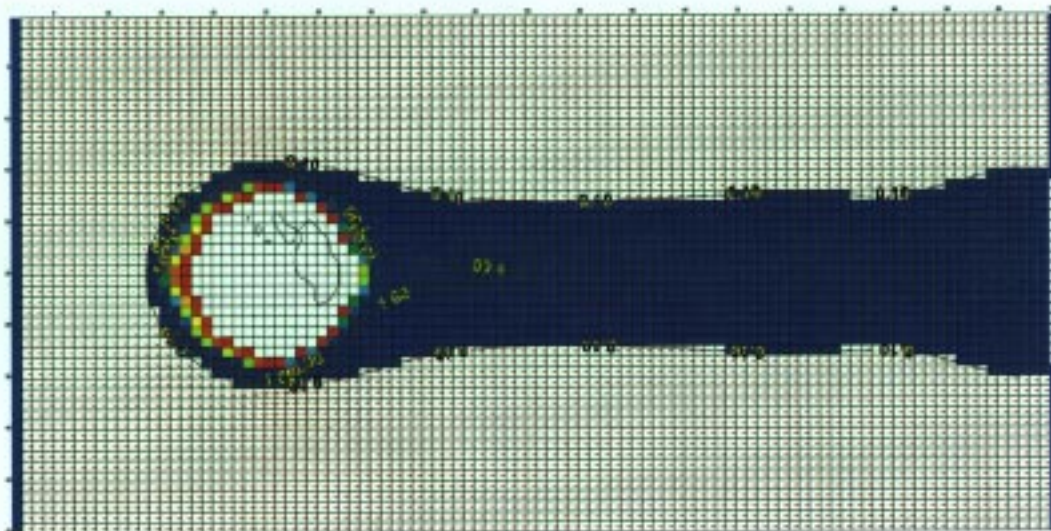
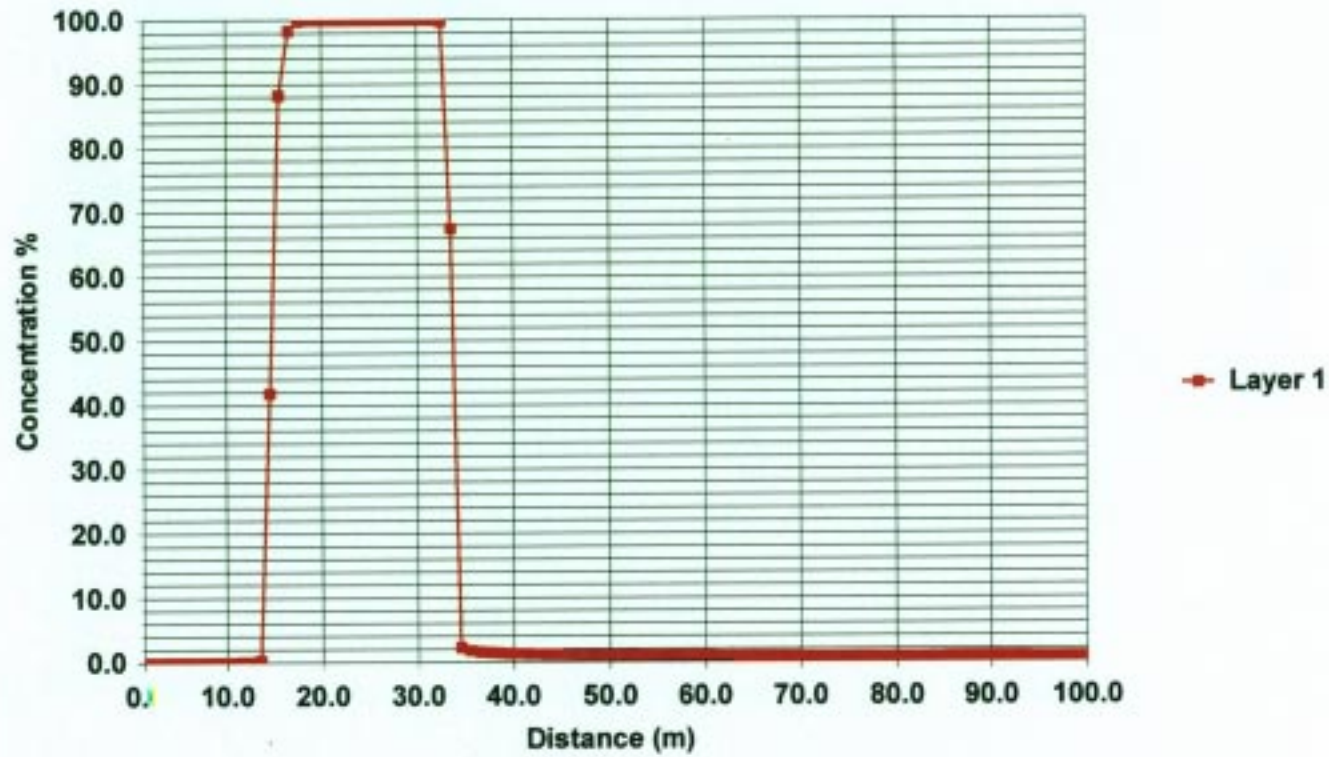
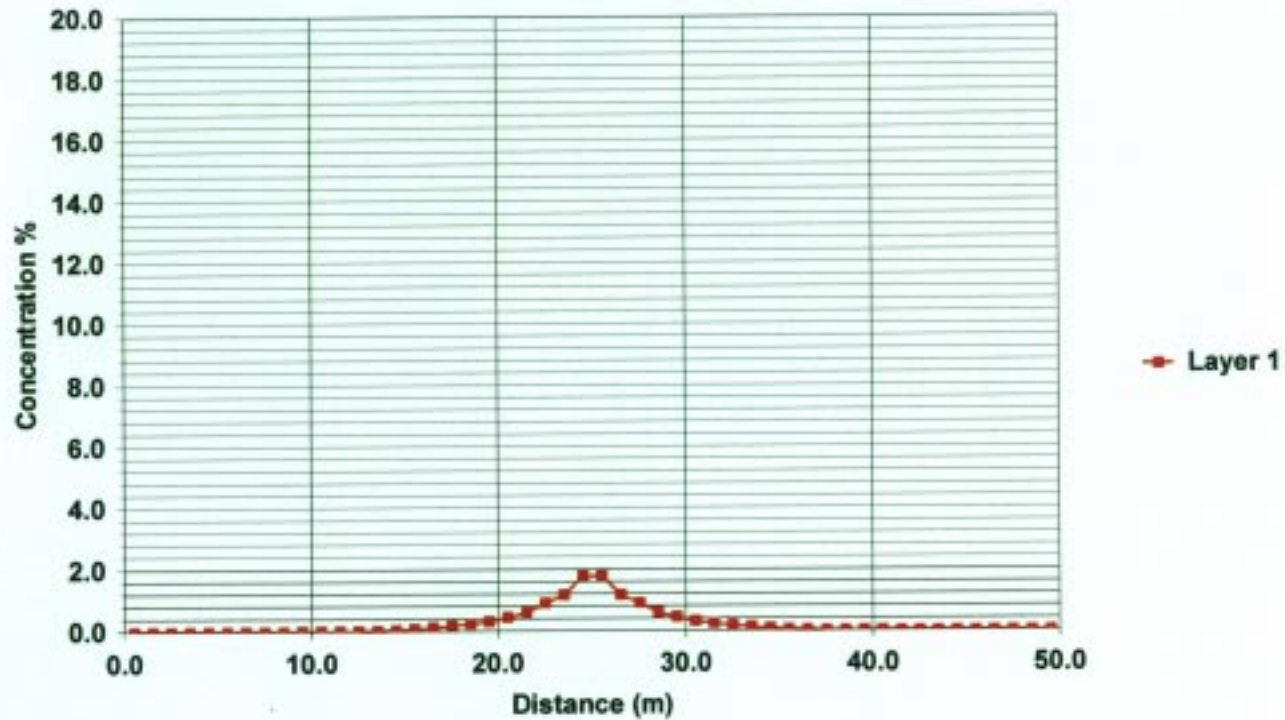


Figure B-4b Concentration % Profile -Row 25 - non-reactive -200 yrs



Kalf and Associates 99

Figure B-4c Concentration % Profile - Col 36 - non-reactive - 200 yrs



## FIGURE B-5a

### Jabiluka Review - Groundwater Hydrology

Silo/Aquifer Concentration % - non-reactive contaminant

$K_s = 1e-4$  (m/d);  $K_a = 0.01$  (m/d) - Gradient 0.03- $P_a=5\%$ ;  $P_s=10\%$ -200 Years

---

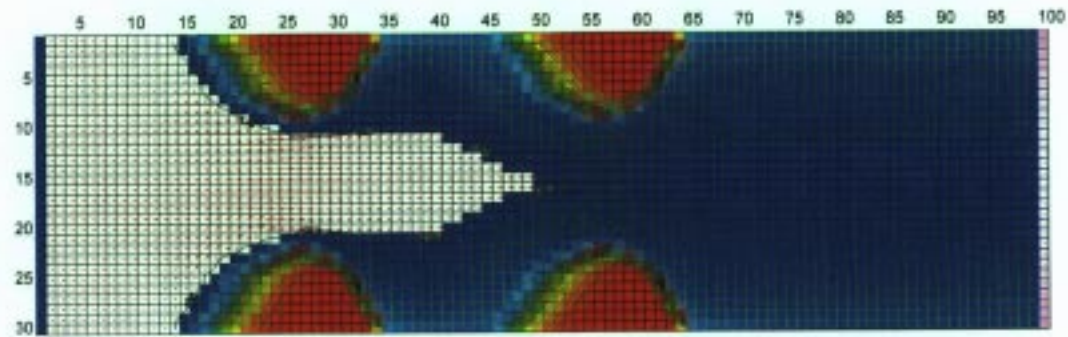


Figure B-5b Concentration % Profile - Row 1 -non-reactive - 200 yrs

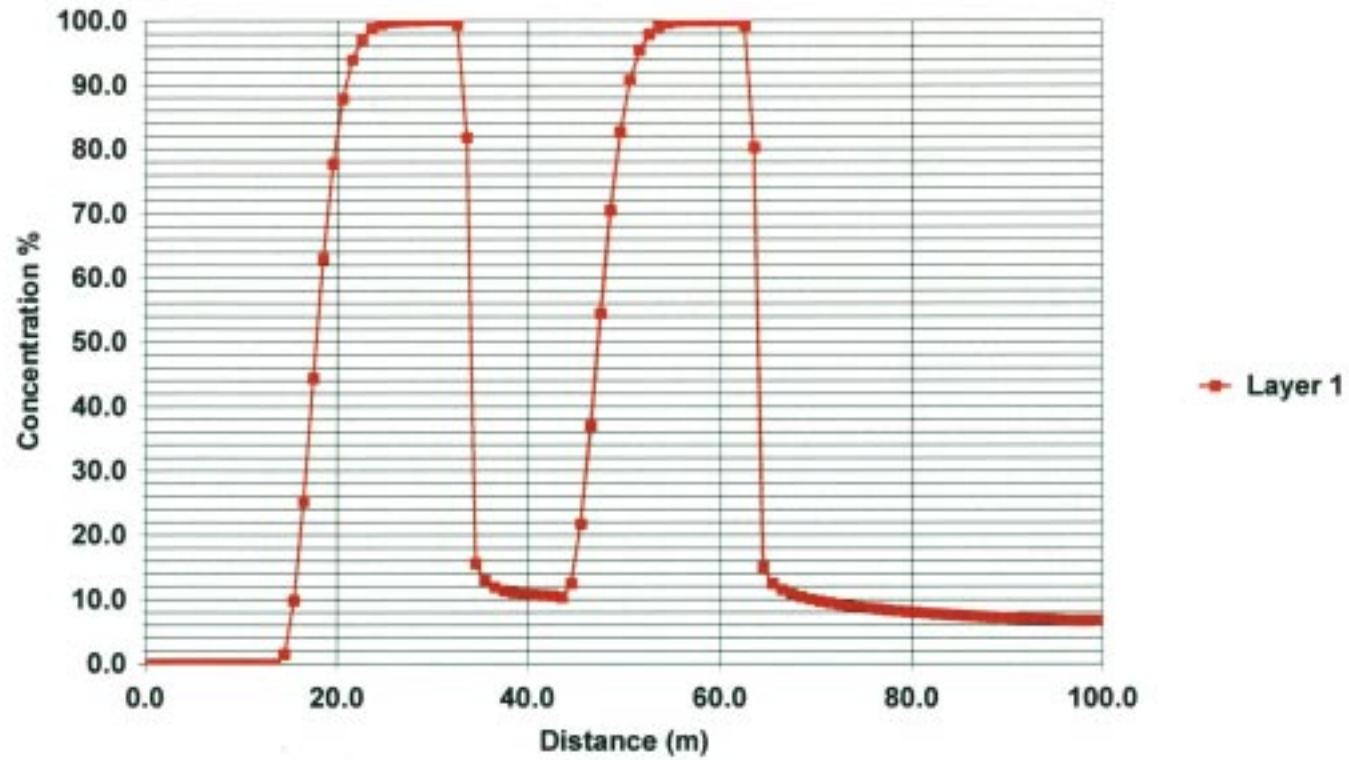
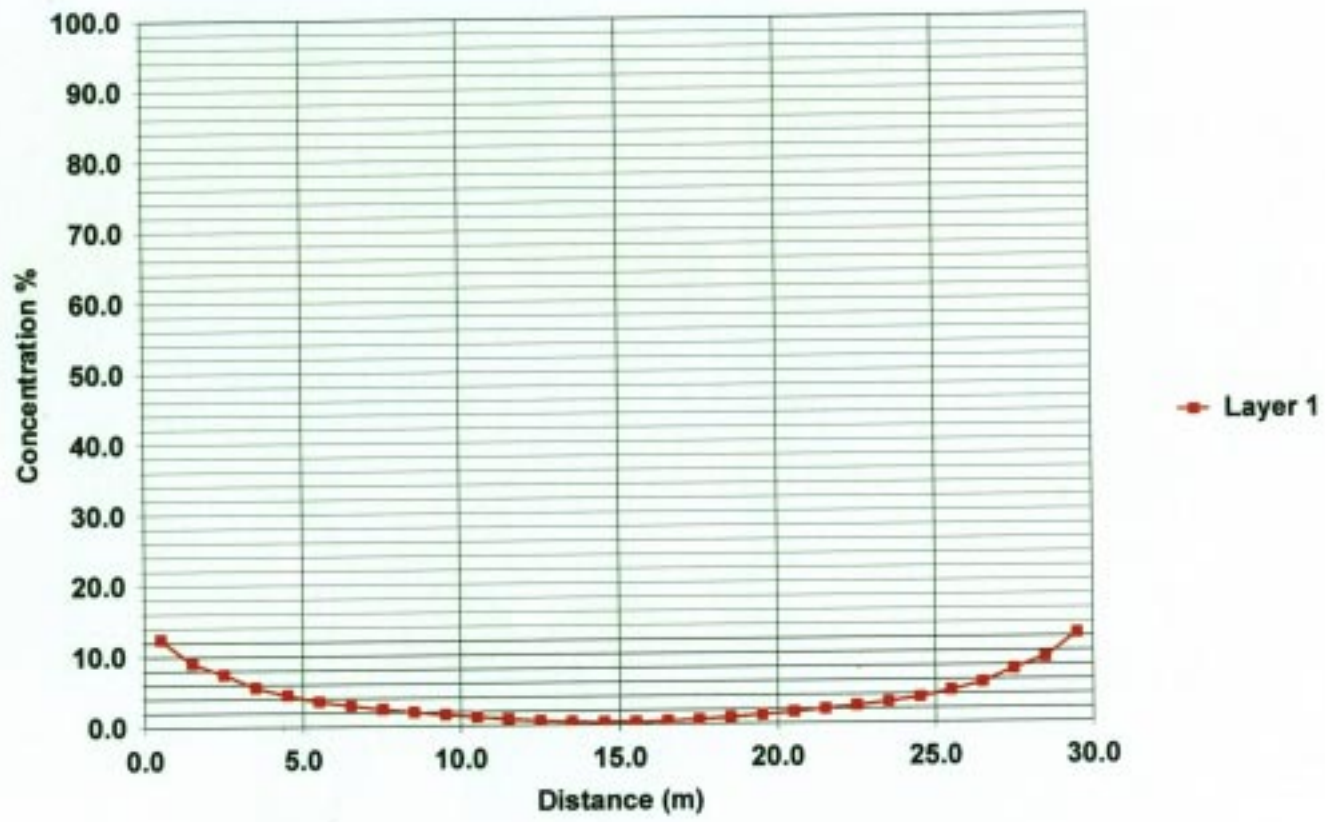


Figure B-5c Concentration % Profile - non-reactive - Col 66- 200 yrs



## FIGURE B-6a

### Jabiluka Review - Groundwater Hydrology

Silo/Aquifer Concentration % - non-reactive contaminant

$K_s = 1e-5$  (m/d);  $K_a = 0.01$  (m/d) - Gradient 0.03 -  $P_a = 5\%$ ;  $P_s = 10\%$  - 200 Years

---

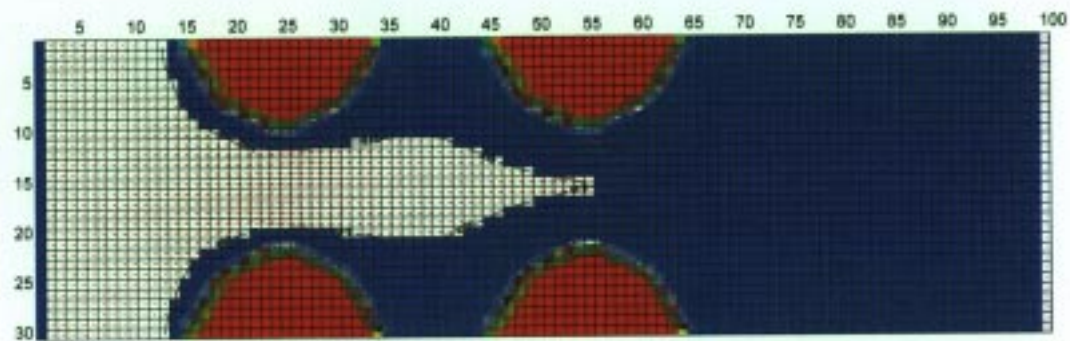


Figure B-6b Concentration % Profile - Row 1 - non-reactive - 200 yrs

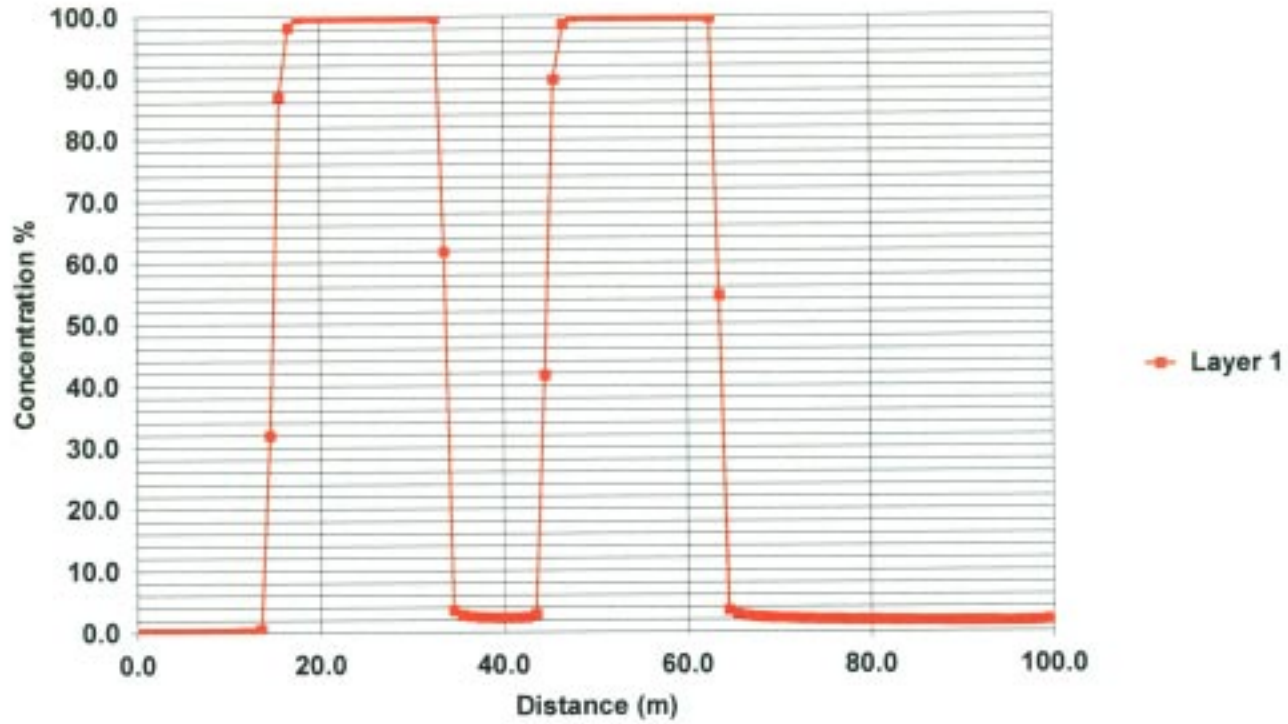
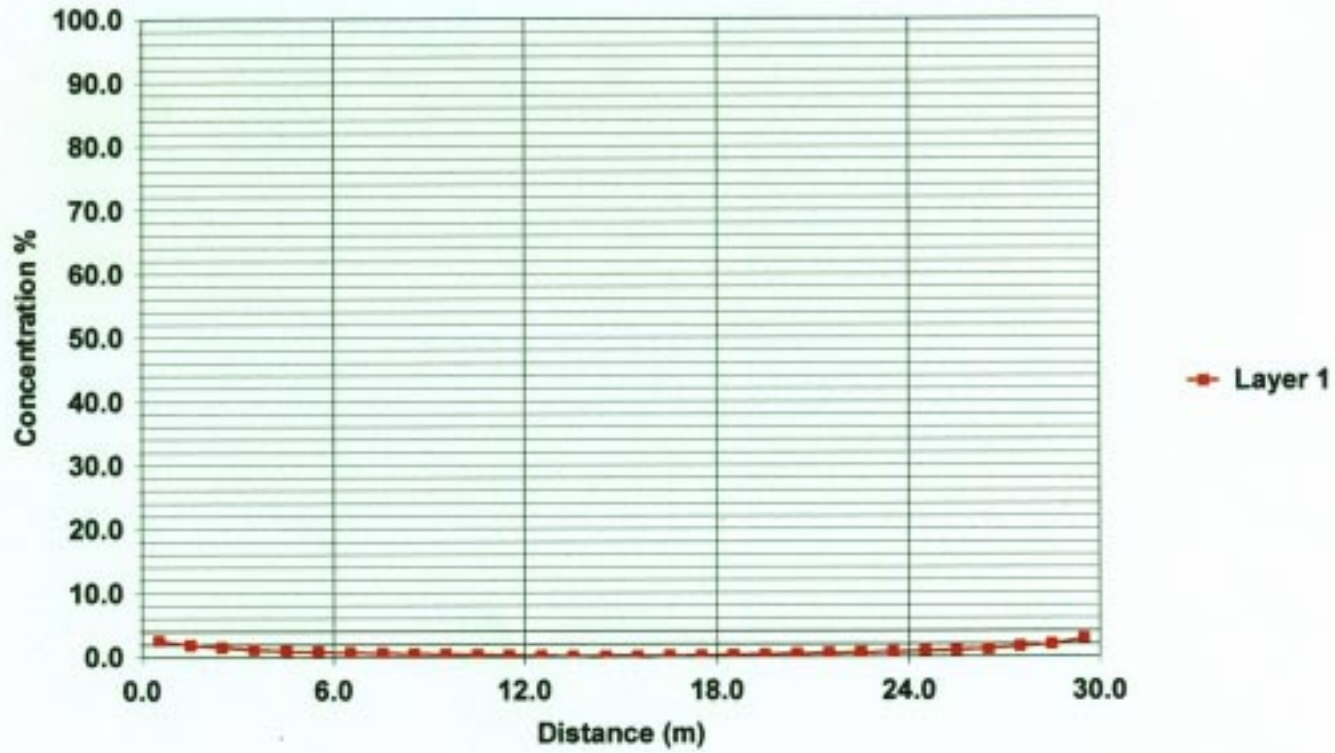


Figure B-6c Concentration % Profile - Col 66 - non-reactive - 200 yrs



# FIGURE B-7a

## Jabiluka Review - Groundwater Hydrology

Silo/Aquifer Concentration % - Uranium

$K_s = 1e-4$  ( m/d);  $K_a=0.01$  (m/d) - Gradient 0.03 -  $P_a=5\%$ ;  $P_s=10\%$  - 1000 Yrs;  $R_f=21$

---

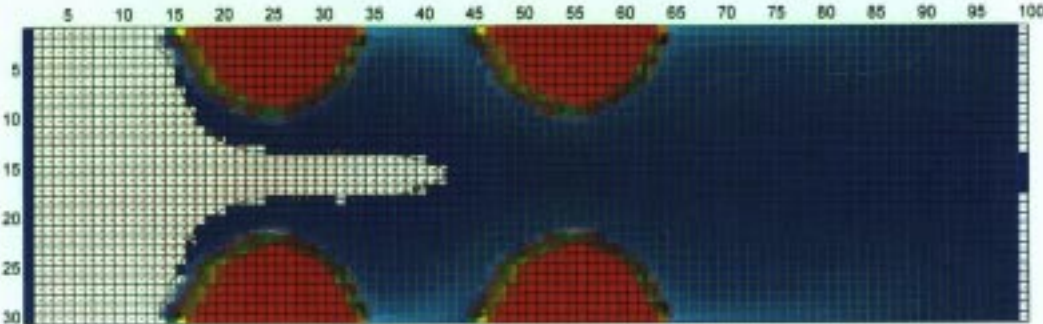


Figure B-7b Concentration % Profile - Row 1 - Uranium - 1000 yrs- Rf=21

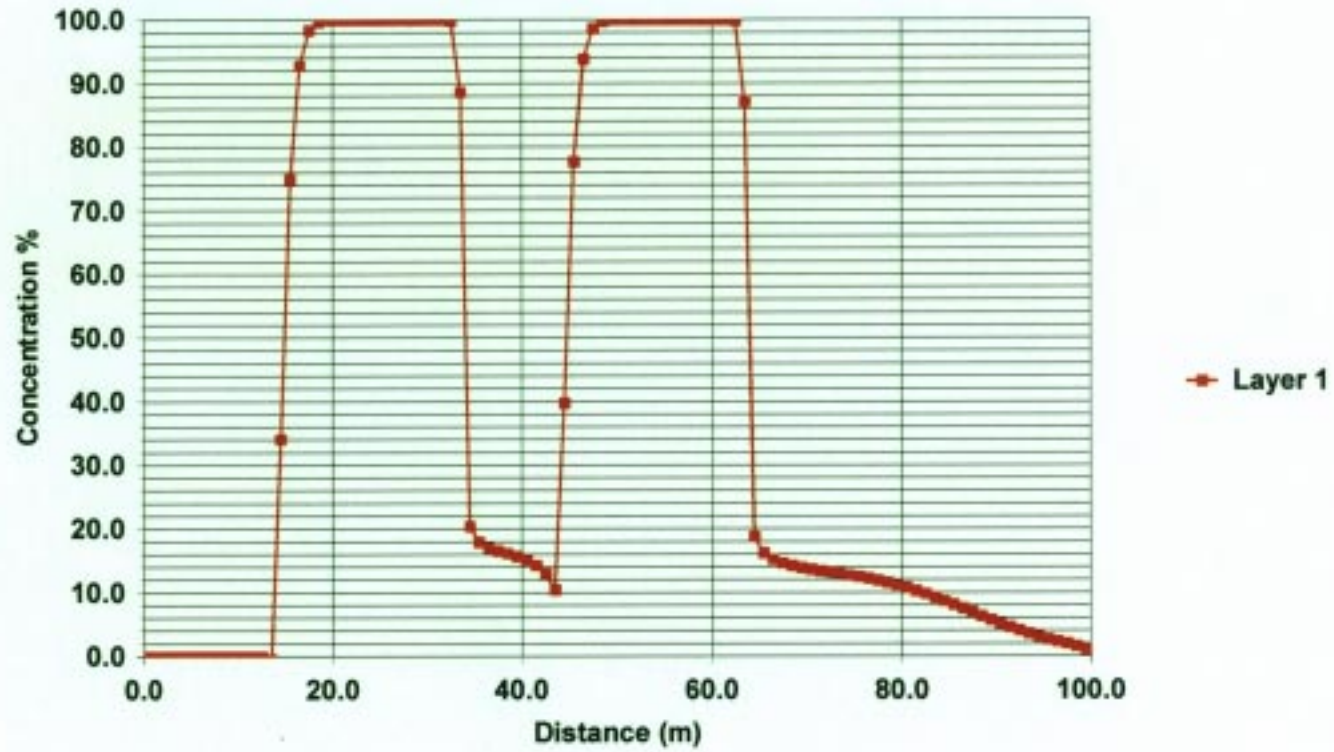
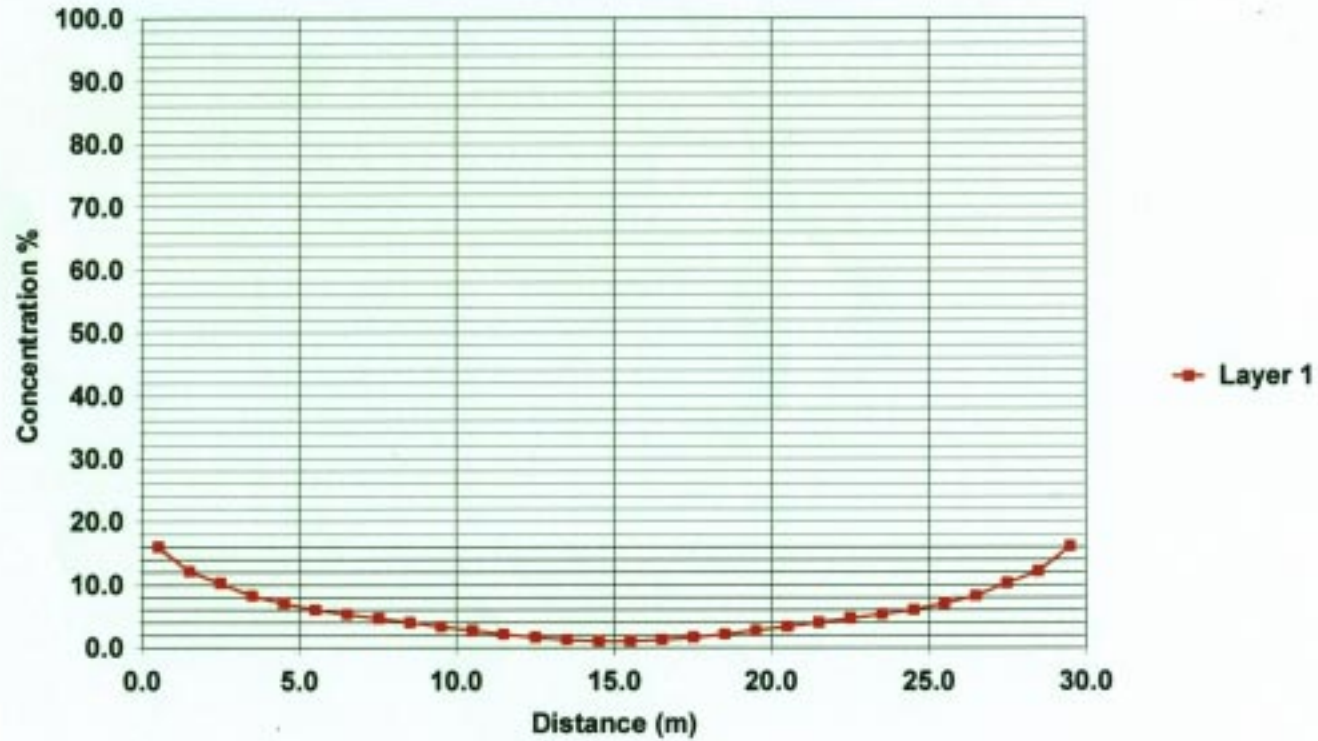


Figure B-7c Concentration % Profile - Column 66 -Uranium -1000 yrs - Rf=21



## FIGURE B-8a

### Jabiluka Review - Groundwater Hydrology

Silo/Aquifer Concentration % - Radium 226

$K_s = 1e-4$  ( m/d);  $K_a=0.01$  (m/d) - Gradient 0.03 -  $P_a=5\%$ ;  $P_s=10\%$  - 1000 Yrs;  $R_f=200a$ ; 100s

---

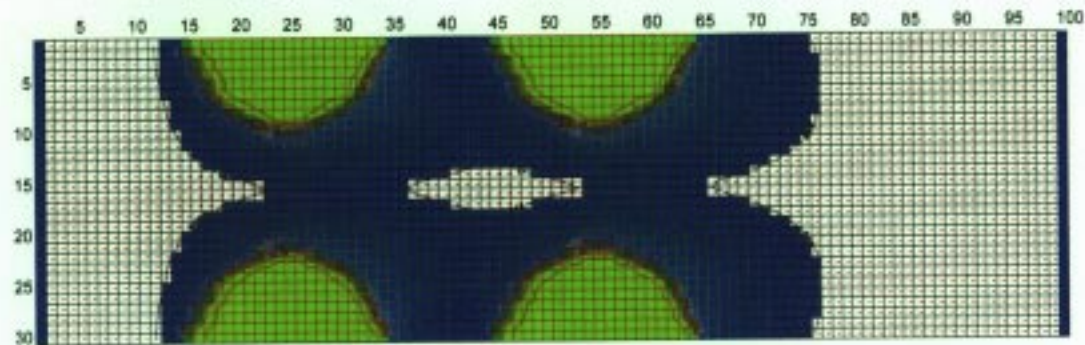


Figure B-8b Concentration % Profile - Row 1 -Radium 226-1000 yrs;Rf=201a,101s

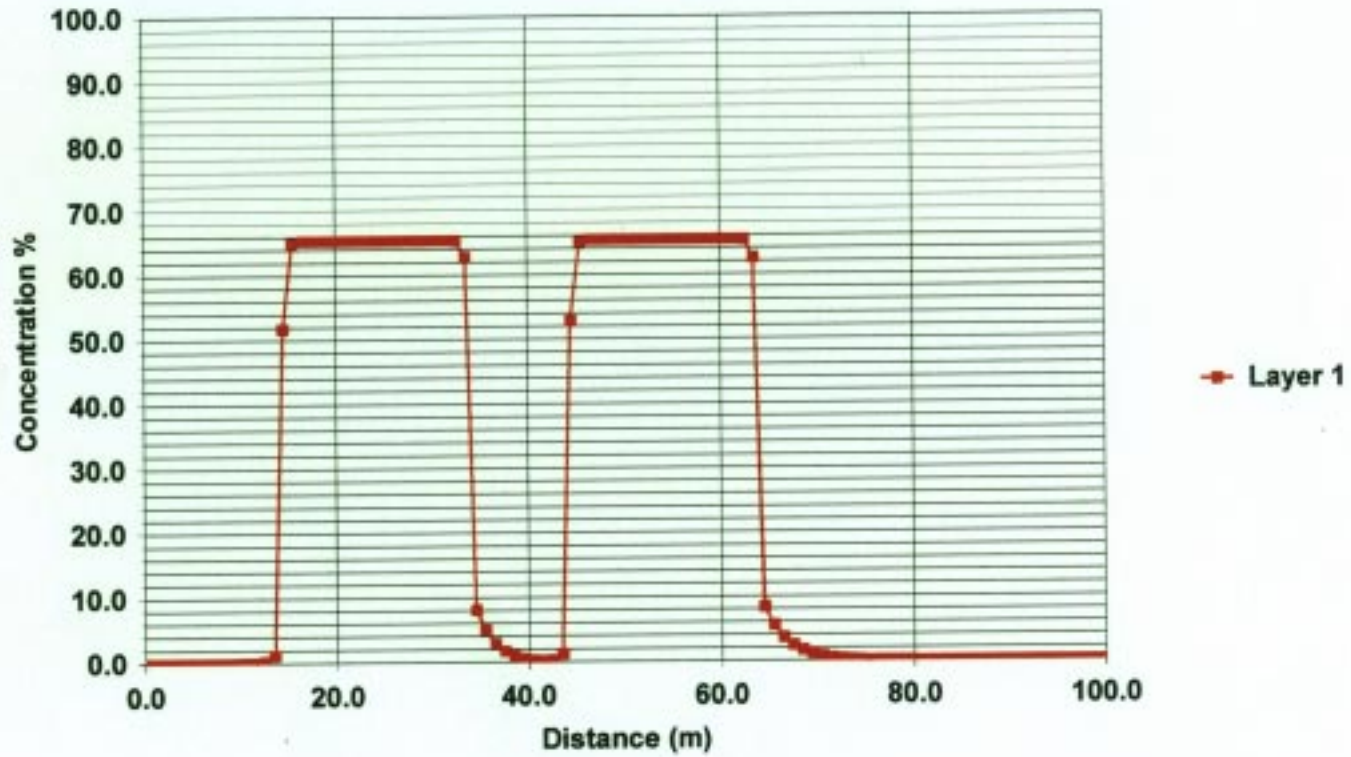
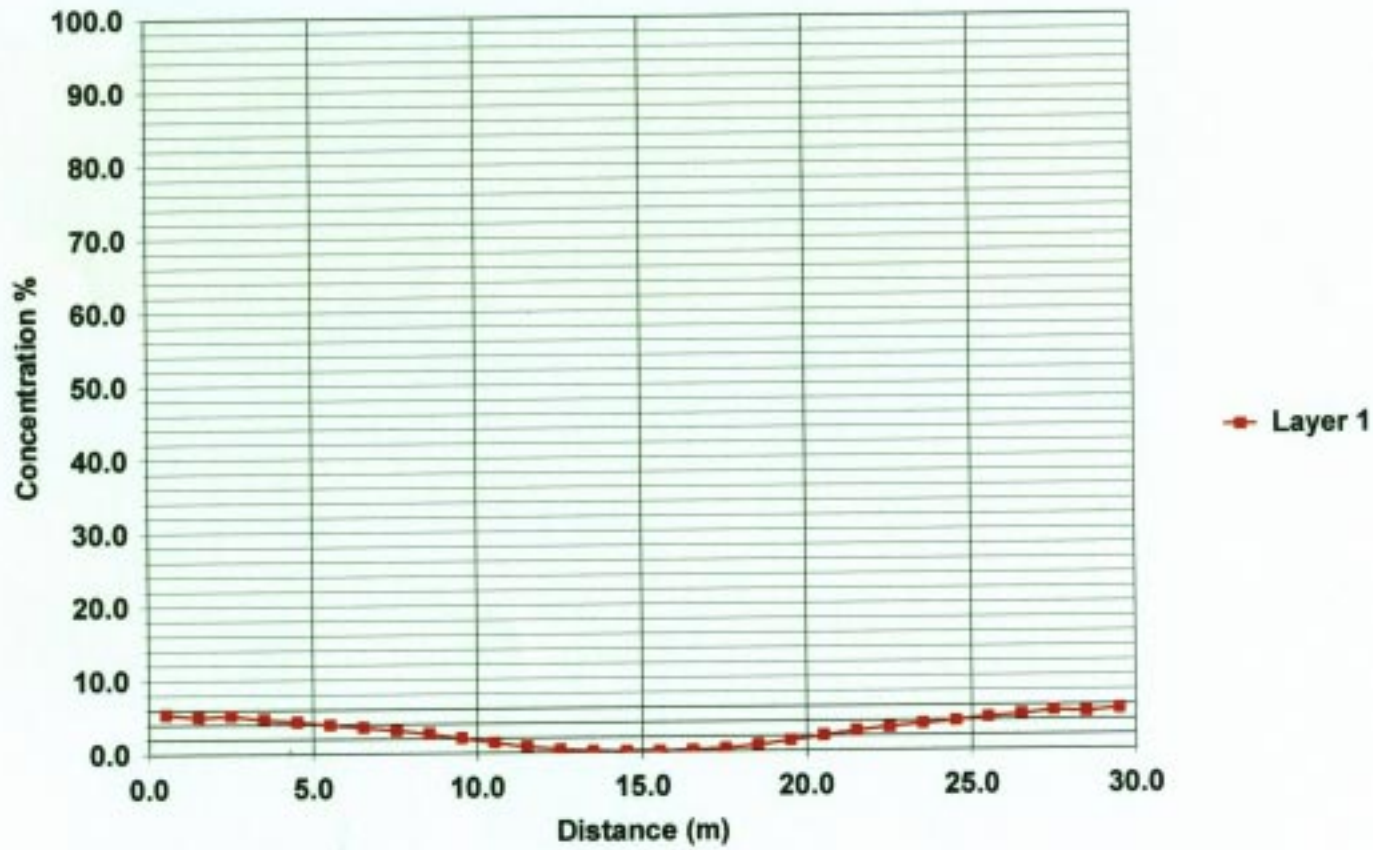
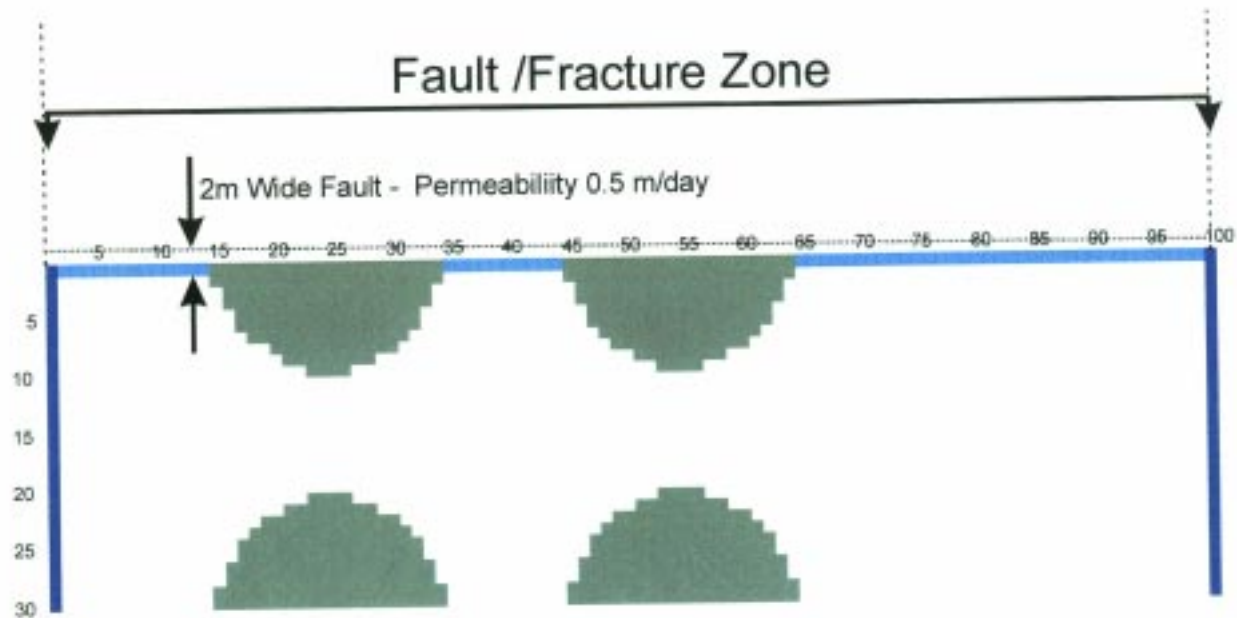


Figure B-8c Concentration % Profile - Col 66 - Radium 226 - 1000 yrs-Rf=201a,101s





**FIGURE B-9**  
**Jabiluka Technical Review**  
**Groundwater Hydrology**  
 Assumed Fault/Fracture Zone

Kaif and Associates 99

## FIGURE B-10a

### Jabiluka Review - Groundwater Hydrology

Silo/Aquifer Concentration % -non-reactive contaminant

$K_s = 1e-4$  ( m/d):  $K_a=0.01$  (m/d) - Gradient 0.03 -  $P_a=5\%$ ;  $P_s=10\%$  - 200 Yrs-Fault  $K_f=0.5$  m/day

---

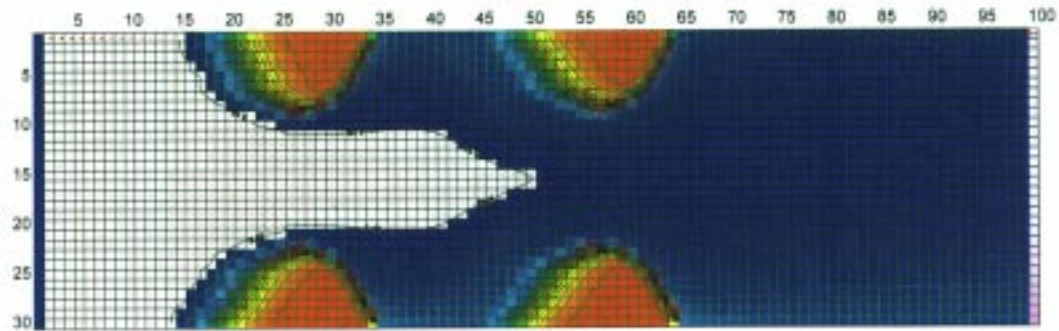


Figure B-10b Concentration % Profile - Row 1- non-reactive-200 yrs with Fault

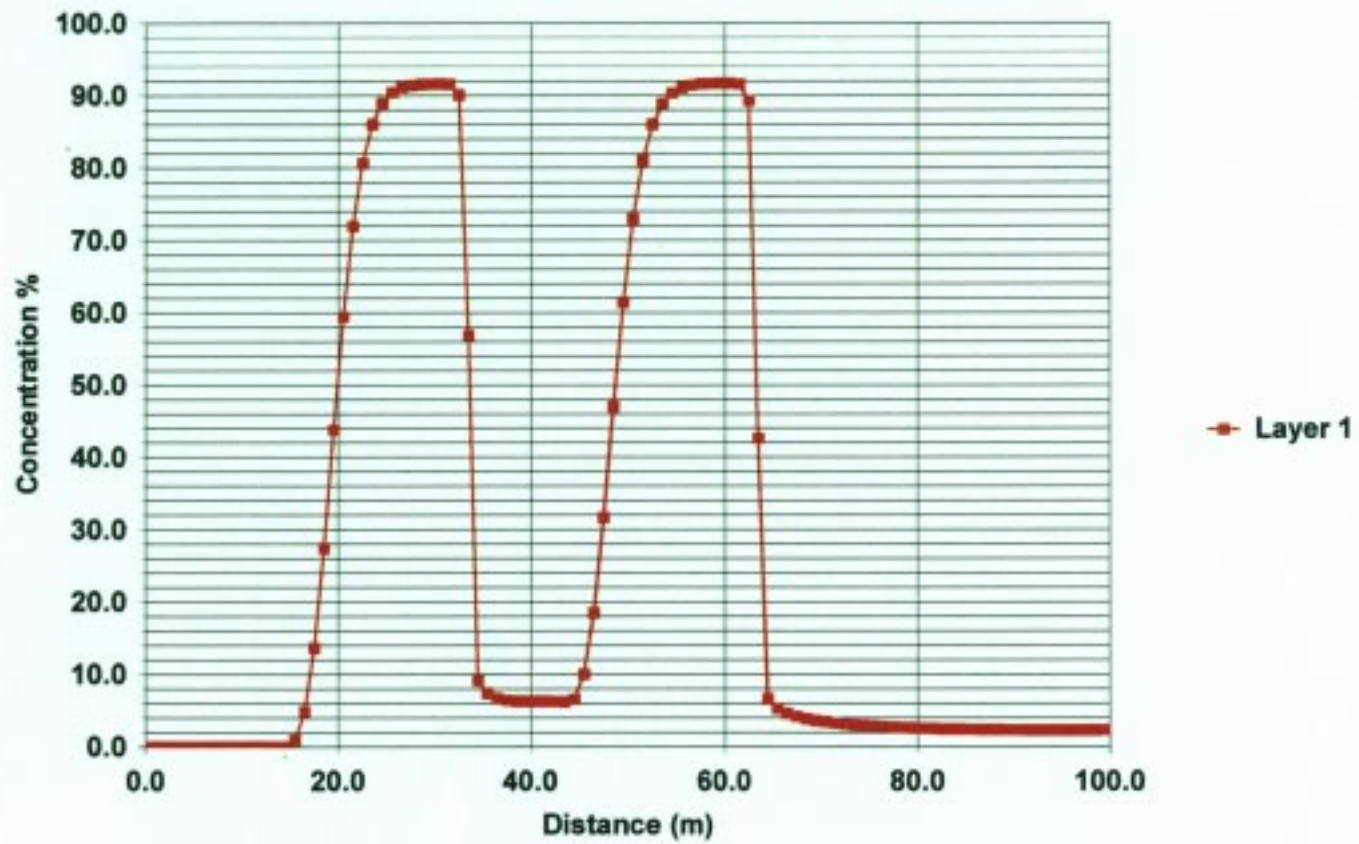


Figure B-10c Concentration % Profile - Col 66- non-reactive-200 yrs with Fault

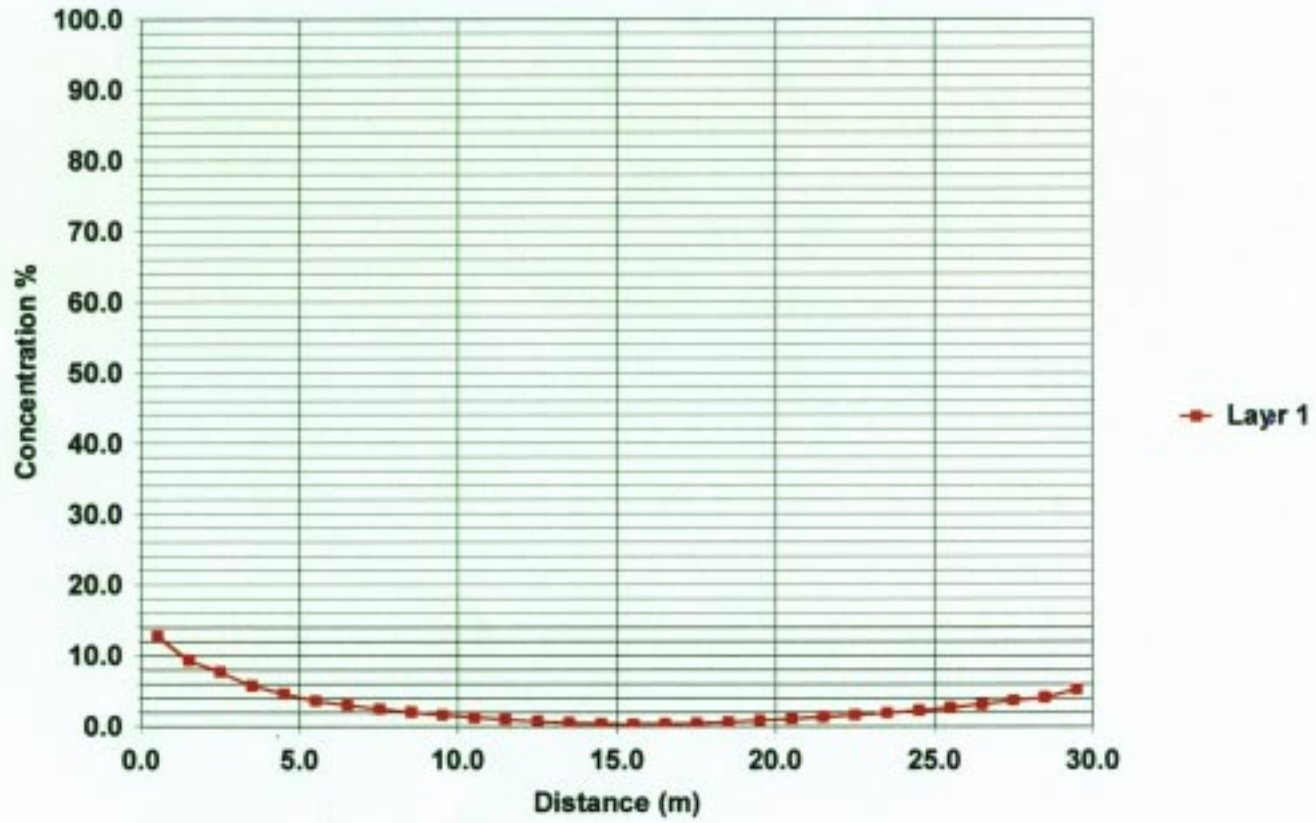
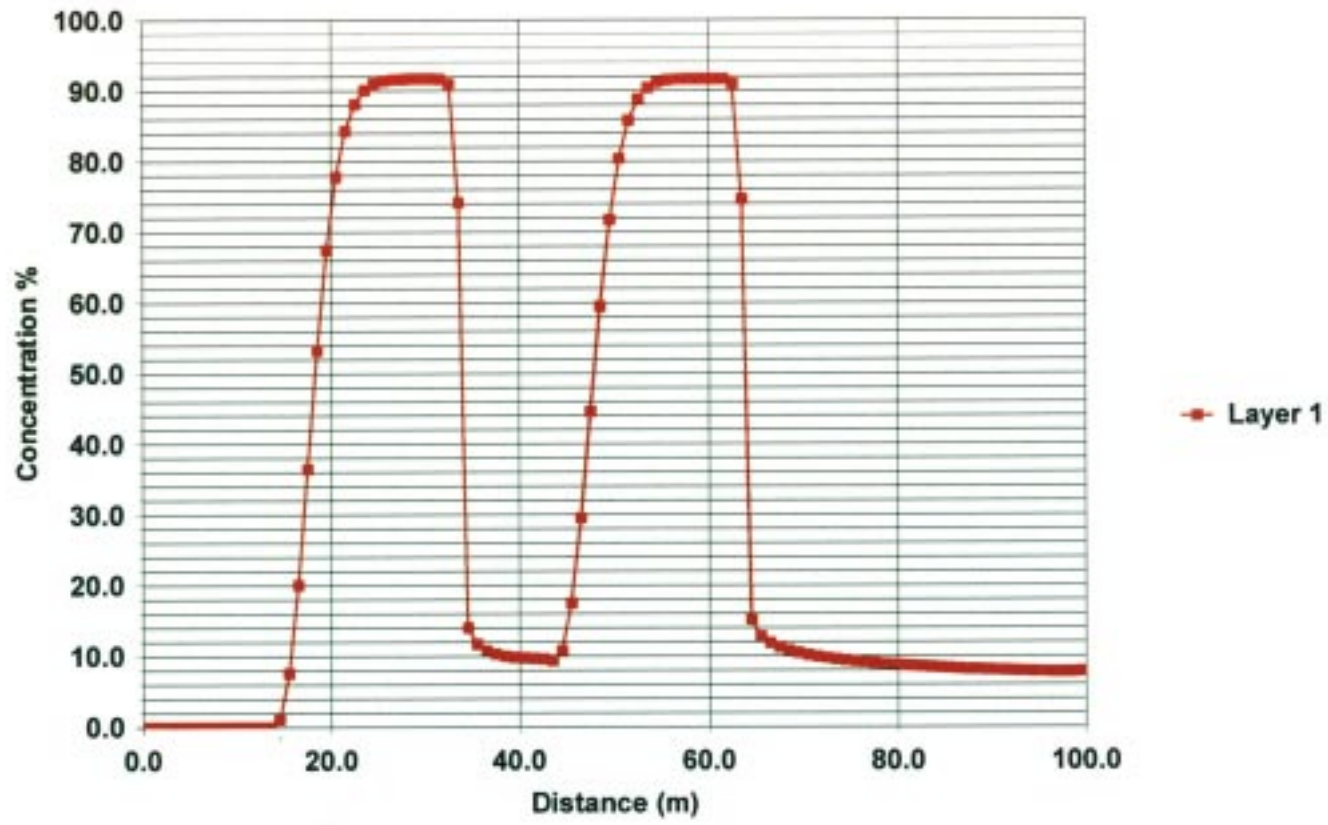


Figure B-10d Concentration % Profile - Row 30 -non-reactive-200 yrs fault opposite



## FIGURE B-11a

### Jabiluka Review - Groundwater Hydrology

Silo/Aquifer Concentration % -Uranium

$K_s = 1e-4$  ( m/d);  $K_a=0.01$  (m/d) - Gradient 0.03 -  $P_a=5\%$ ;  $P_s=10\%$  - 1000 Yrs-Fault  $K_f=0.5$  m/day;  $R_f=21$

---

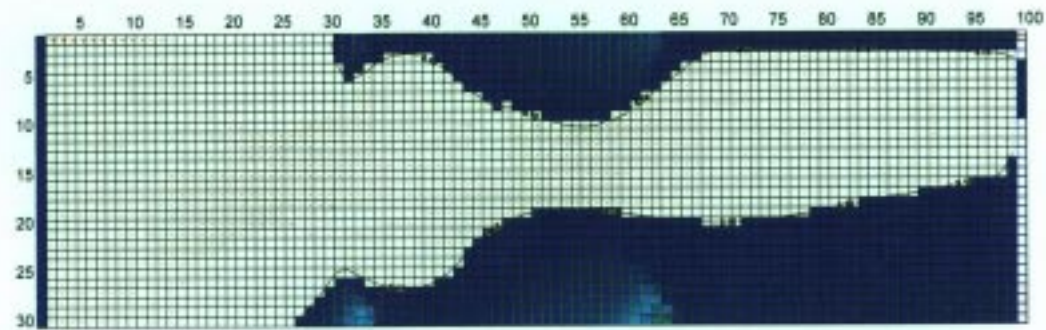


Figure B-11b Concentration % Profile - Row 1 - Uranium - 1000 yrs with Fault

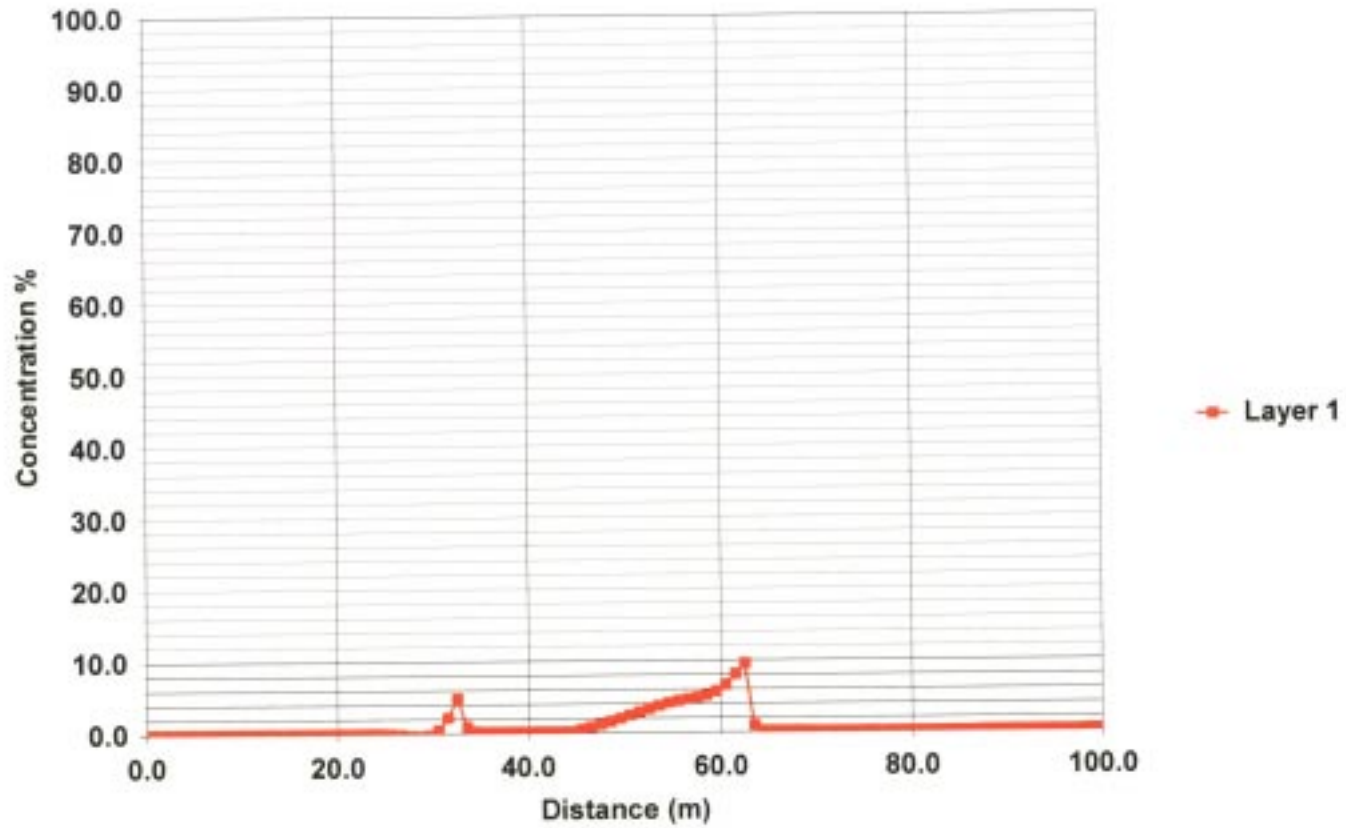


Figure B-11c Concentration % Profile - Col 66 -Uranium-1000 yrs with fault

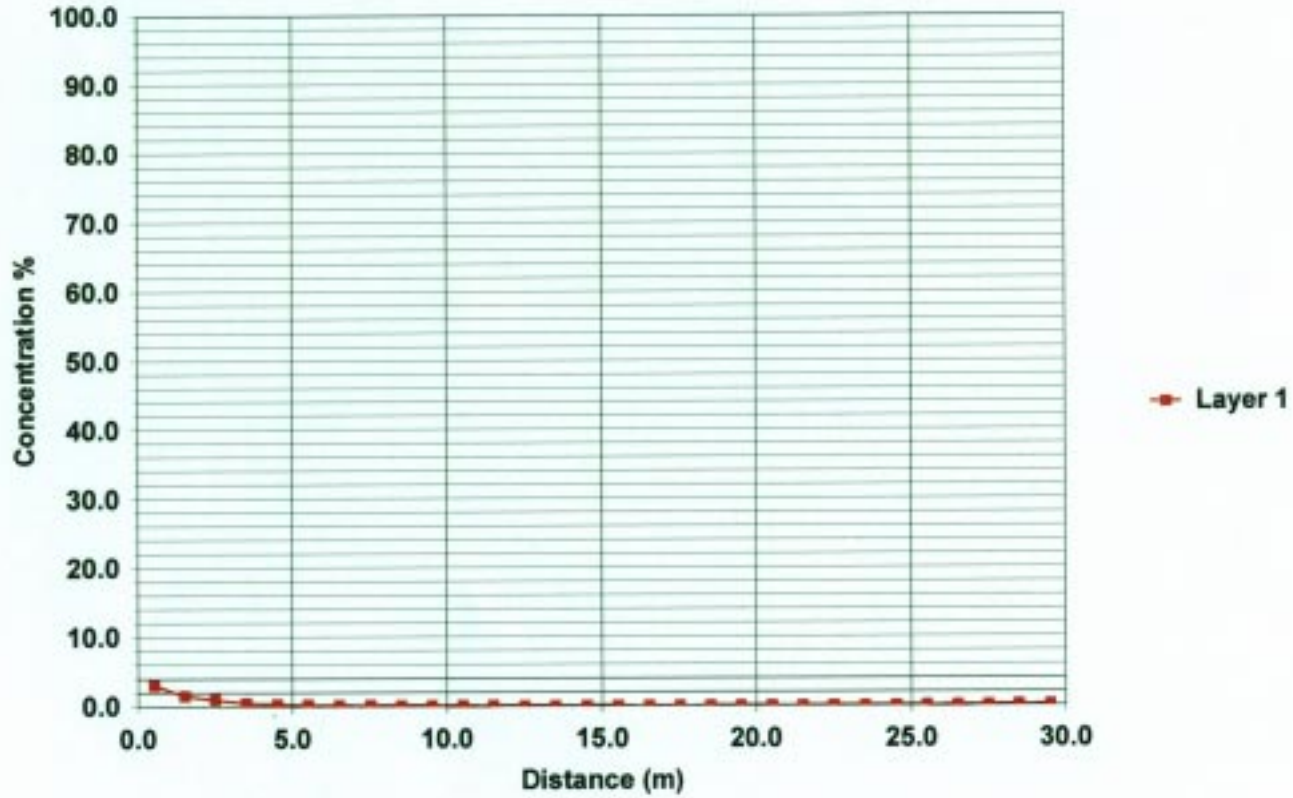
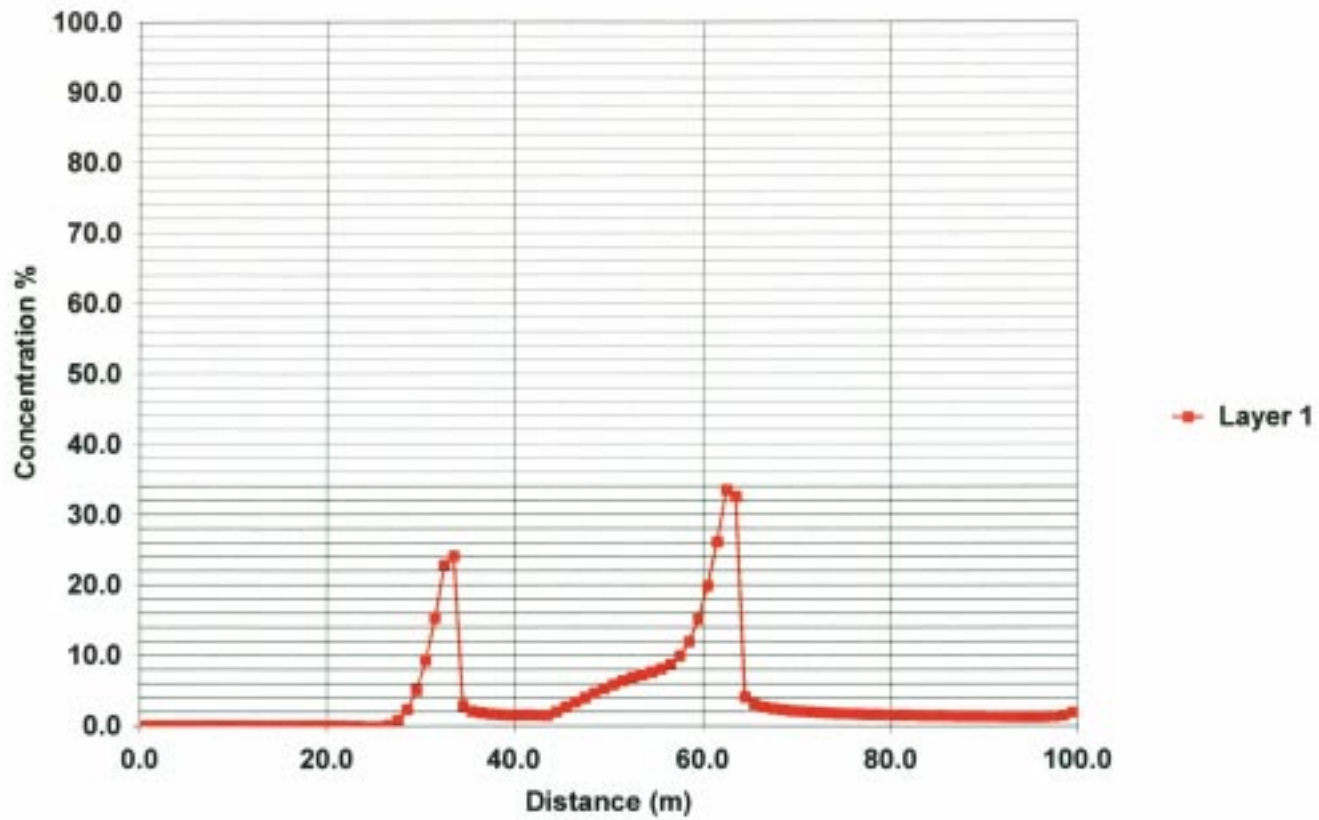


Figure B-11d Concentration % Profile - Row 30 - Uranium - 1000yrs with Fault



## FIGURE B-12a

### Jabiluka Review - Groundwater Hydrology

Silo/Aquifer Concentration % - non-reactive contaminant

$K_s = 1e-3$  ( m/d);  $K_a=0.01$  (m/d) - Gradient 0.03- $P_a=5\%$ ;  $P_s=10\%$ -200 Years

---

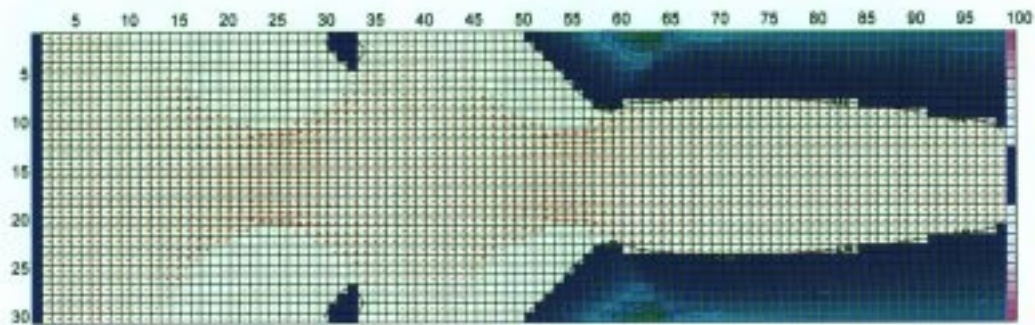


Figure B-12b Concentration % Profile - Row 1 - non-reactive -200 yrs

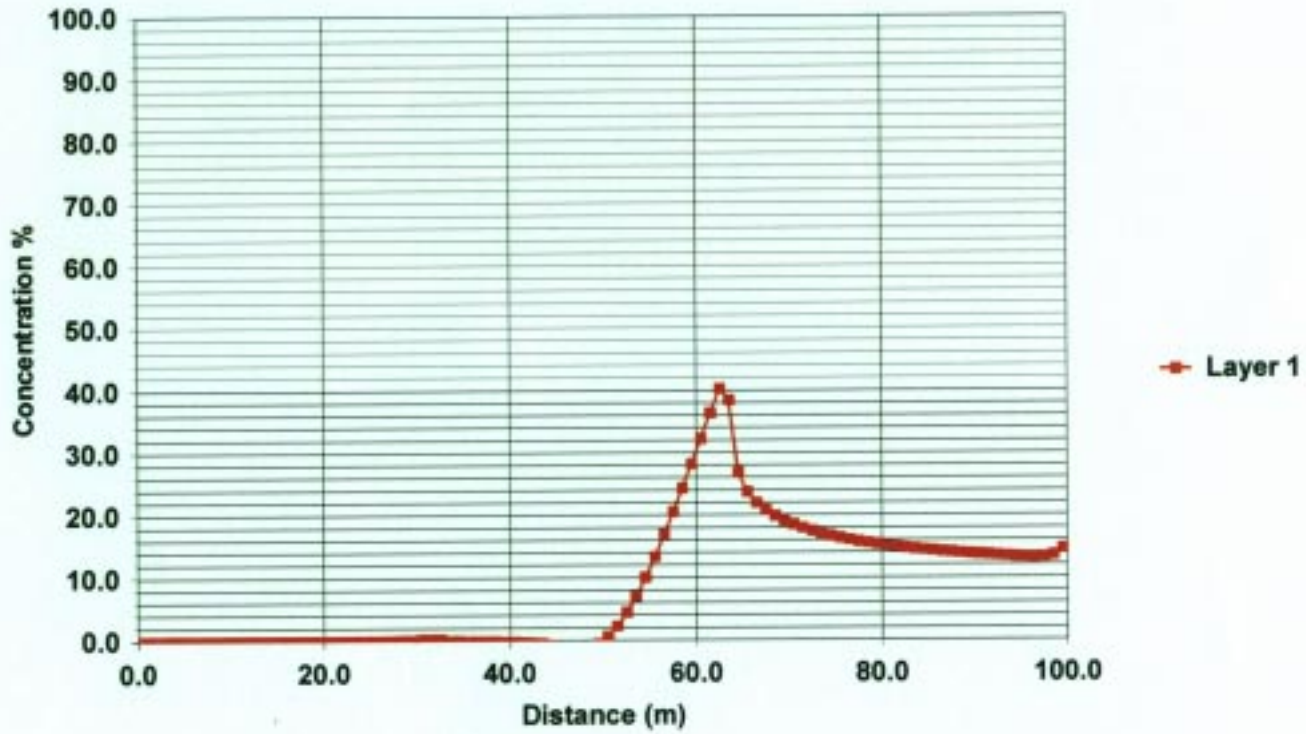
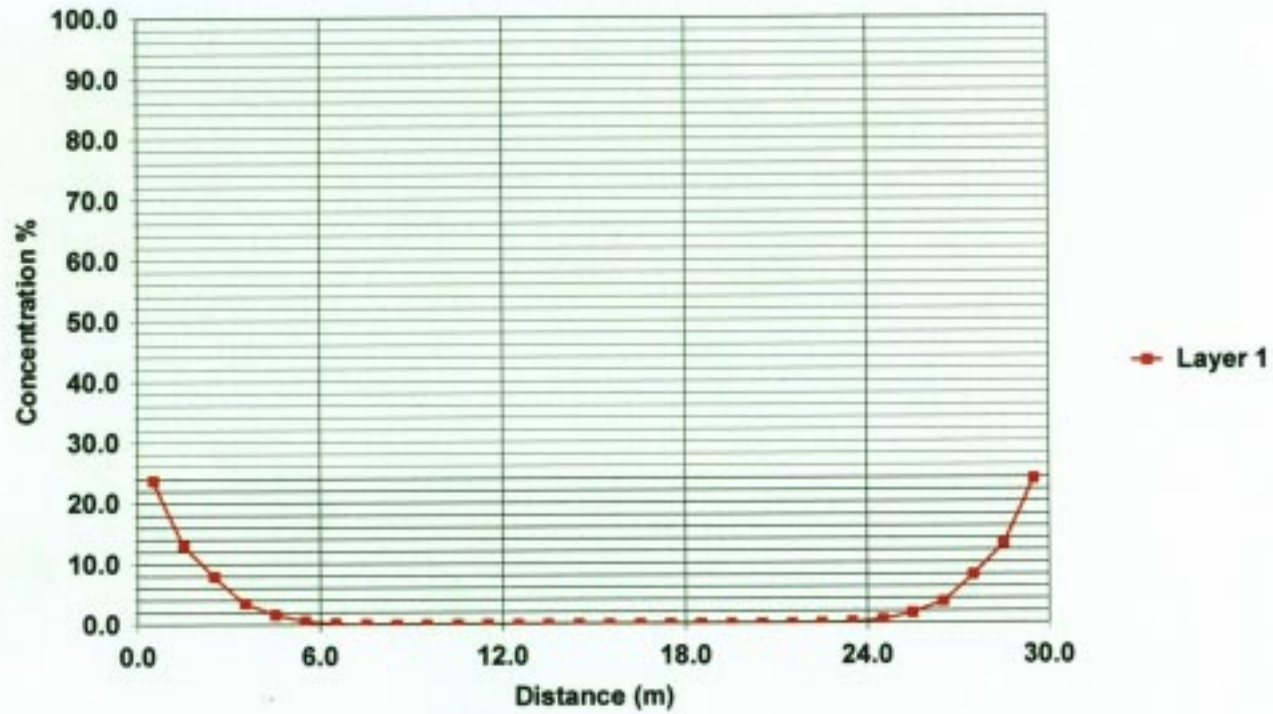


Figure B-12c Concentration % Profile - Col 66 - non-reactive - 200 yrs



Kalf and Associates 99